

**Effects of Palmitoylethanolamide Against the Toxicity of Paclitaxel on  
Primary Dorsal Root Ganglion Neuronal and Non-Neuronal Cells**

Thesis

to obtain the academic degree of  
Doctor rerum medicarum (Dr. rer. medic.)  
in the field of Medical Physiology and Pathophysiology

submitted to the Faculty of Medicine of  
Martin Luther University Halle-Wittenberg

by Amira Abdelgleal Mohamed Elfarnawany

Supervisor:

Prof. Dr. Faramarz Dehghani

Reviewers:

1. PD Dr. med. Torsten Kraya, Leipzig, Germany
2. Prof. Dr. Kirsten Haastert-Talini, Hannover, Germany

Date of defense: 03.06.2024

# Abstract

Chemotherapy-induced peripheral neuropathy (CIPN) is a common side effect of several chemotherapeutic agents such as Paclitaxel. The main symptoms of CIPN are pain and numbness in the hands and feet which disrupts the quality of patients' life. Paclitaxel is believed to accumulate in the dorsal root ganglia (DRG). Primary DRGs were used as a model to investigate the potential protective effects of the endocannabinoid-like substance, palmitoylethanolamide (PEA) against toxicity of paclitaxel on DRG neuronal and non-neuronal cells. DRGs of 6-8 weeks Wistar rats were isolated, and DRG neuronal and non-neuronal cell populations were separated using the density gradient centrifugation method. The effects on different endpoints including cell viability, cell death, cell proliferation, and morphological changes were addressed using multiple techniques. The results showed that paclitaxel treatment exhibited a set of toxicological effects on primary DRG neuronal cells including a reduction in viability, a strong reduction in neurite length, and an increase in the size of neuronal cells at all investigated time windows. In addition, paclitaxel showed adverse effects on primary DRG non-neuronal cells including suppression in cell viability, an increase in cell death, a decrease in cell proliferation rate, as well as morphological changes. The effects of paclitaxel on both primary DRG neuronal and non-neuronal cells were concentration- and time-dependent. Furthermore, PEA demonstrated neuroprotective effects by reducing paclitaxel toxicity by increasing viability, neurite outgrowth, and decreasing swelling of neuronal soma. Furthermore, PEA at various concentrations protects DRG non-neuronal cells from the adverse effects of paclitaxel, including increased cell survival and accelerated cell proliferation. PEA also revealed synergistic anticancer effects with paclitaxel against human breast cancer cells. Taken together, PEA might be used as a therapeutic option to mitigate paclitaxel-induced peripheral neuropathy in breast cancer patients suffering from CIPN.

Elfarnawany, Amira: Effects of Palmitoylethanolamide Against the Toxicity of Paclitaxel on Primary Dorsal Root Ganglion Neuronal and Non-Neuronal Cells, Halle (Saale), Univ., Med. Fac., Diss., 75 Pages, 2024.

# Referat

Chemotherapie-induzierte periphere Neuropathie (CIPN) ist eine häufige Nebenwirkung mehrerer Chemotherapeutika wie Paclitaxel. Die Hauptsymptome von CIPN sind Schmerzen und Taubheitsgefühle in Händen und Füßen, welche die Lebensqualität der Patienten beeinträchtigen. Es wird angenommen, dass sich Paclitaxel in den Spinalganglien (DRG) anreichert. Für die vorgelegte Arbeit wurden primäre Spinalganglien als Modell verwendet, um die potenziellen Schutzwirkungen der endocannabinoid-ähnlichen Substanz Palmitoylethanolamide (PEA) gegen die Toxizität von Paclitaxel auf neuronale und nicht-neuronale DRG-Zellen zu untersuchen. Zu diesem Zweck wurden DRGs von 6–8 Wochen alten Wistar-Ratten isoliert und neuronale und nicht-neuronale DRG-Zell Populationen mithilfe der Dichtegradientenzentrifugation getrennt. Die Auswirkungen verschiedener Konzentrationen von Paclitaxel (0.01  $\mu\text{M}$ –10  $\mu\text{M}$ ) oder/und PEA (0.1  $\mu\text{M}$ –10  $\mu\text{M}$ ) wurden 24 Stunden, 48 Stunden und 72 Stunden nach der Behandlung analysiert. Die Auswirkungen auf verschiedene Endpunkte, einschließlich Zelllebensfähigkeit, Zelltod, Zellproliferation und morphologische Veränderungen, wurden mithilfe mehrerer Techniken untersucht. Die Ergebnisse zeigten, dass die Behandlung mit Paclitaxel eine Reihe toxischer Auswirkungen auf primäre neuronale und nicht-neuronale DRG-Zellen hatte, darunter eine Verringerung der Lebensfähigkeit, eine starke Verringerung der Länge Neuriten und eine Zunahme der Größe neuronaler Zellen in allen untersuchten Zeitfenstern. Paclitaxel zeigte nachteilige Auswirkungen auf primäre nicht-neuronale DRG-Zellen, darunter eine Minderung der Zell Vitalität, eine Zunahme des Zelltods, eine Abnahme der Zellproliferationsrate sowie morphologische Veränderungen. Die Wirkung von Paclitaxel auf primäre neuronale und nicht-neuronale DRG-Zellen war konzentrations- und zeitabhängig. PEA zeigte neuroprotektive Wirkungen, indem es die Toxizität von Paclitaxel durch eine Steigerung der Lebensfähigkeit, des Neuritenwachstums und eine Verringerung der Schwellung der neuronalen Somata abschwächte. Des Weiteren übt PEA in verschiedenen Konzentrationen eine schützende Wirkung gegen die nachteiligen Auswirkungen von Paclitaxel auf nicht-neuronale DRG-Zellen aus, einschließlich einer Verbesserung des Zellüberlebens sowie einer Beschleunigung der Zellproliferationsrate. PEA wies synergistische Antikrebseffekte mit Paclitaxel gegen humane Mammakarzinom Zelllinien (HBCCs) auf. Insgesamt könnte PEA neben Paclitaxel als Therapieoption für Brustkrebspatientinnen eingesetzt werden, die an einer CIPN leiden.

Elfarnawany, Amira: Effects of Palmitoylethanolamide Against the Toxicity of Paclitaxel on Primary Dorsal Root Ganglion Neuronal and Non-Neuronal Cells, Halle (Saale), Univ., Med. Fac., Diss., 75 Pages, 2024.

# Table of Contents

Table of Contents.....	i
List of Abbreviations.....	ii
<b>1. Introduction and Objectives.....</b>	<b>1</b>
1.1. Chemotherapy-induced peripheral neuropathy.....	1
1.2. Taxanes (Paclitaxel) .....	2
1.3. Dorsal root ganglion (DRG) .....	4
1.4. Endocannabinoids (Palmitoylethanolamide) .....	6
1.5. Objectives.....	9
<b>2. Discussion.....</b>	<b>9</b>
2.1. Effects of Paclitaxel on DRG neuronal and non-neuronal cells.....	9
2.2. Effects of PEA against paclitaxel toxicity on DRG neuronal and non-neuronal cells .....	10
2.3. Conclusions.....	16
<b>3. References.....</b>	<b>17</b>
<b>4. Theses.....</b>	<b>26</b>
<b>Publications.....</b>	<b>27</b>
<b>Declarations of independence.....</b>	<b>I</b>
<b>Declarations of previous dissertation attempts .....</b>	<b>II</b>
<b>Acknowledgments.....</b>	<b>III</b>
<b>Appendix.....</b>	<b>IV</b>
Publication 1.....	IV
Publication 2.....	V
Supplementary videos.....	VI
Copyrights permission.....	VII

# List of Abbreviations

AEA	Anandamide
BAX	Bcl-2-associated X protein
Bcl-2	B-cell Leukemia 2
BrdU	Bromodeoxyuridine
BSA	Bovine Serum Albumin
CB1	Cannabinoid receptor type 1
CB2	Cannabinoid receptor type 2
CIPN	Chemotherapy-induced peripheral neuropathy
DAPI	4',6-diamidino-2-phenylindole
DRG	Dorsal Root Ganglion
ECs	Endocannabinoid system
FAAH	Fatty acid amide hydrolase
FBS	Fetal Bovine serum
GPCRs	G-Coupled Protein Receptors
GPR55	G protein-coupled receptor 55
HBCCs	Human breast cancer cells
LDH	Lactate dehydrogenase
MTAs	Microtubules Target Agents
MTs	Microtubules
MMP	Mitochondrial membrane potential
MTT	3-(4,5-dimethylthiazol-2-yl) -2,5-diphenyltetrazolium bromide
NAAA	N-acylethanolamine-hydrolyzing acid amidase
NAPE	N-acylphosphatidylethanolamine
NAPE-PLD	N-acyl-phosphatidyl-ethanolamine-selective phospholipase D
NAT	N-acyl-transferase
OEA	N-oleoylethanolamine
PEA	Palmitoylethanolamide
PI	Propidium iodide
PN	Peripheral neuropathy
PPAR- $\alpha$	Peroxisome proliferator-activated alpha
SCs	Schwann cells
SGCs	Satellite glial cells
TRPV1	Transient Receptor Potential Vanilloid 1
TTUB3	Beta- Tubulin-3
2-AG	2-arachidonoylglycerol

# 1. Introduction and Objectives

## 1.1. Chemotherapy-induced peripheral neuropathy

Systemic chemotherapy is a cornerstone in the treatment of many cancer entities. Recent advances in chemotherapeutic regimens have resulted in significant improvements in cancer patients' long-term survival [1,2]. Unfortunately, chemotherapeutic agents cause numerous changes in cellular structure and function, resulting in progressive, ongoing, and often irreversible toxic side effects. Chemotherapy-induced peripheral neuropathy (CIPN) is a common side effect of many first-line chemotherapeutic agents [3,4], affecting several million patients worldwide each year. The most common symptoms of CIPN are two types of sensory abnormalities. The first mode manifests as tingling and burning sensations, while the second manifests as numbness and diminished touch sensations. CIPN alters sensations in the hands and feet in both modes, which is commonly referred to as a "glove and stocking" distribution (**Figure 1**) [5,6]. Typically, pain symptoms appear early in treatment cycles, while numbness and tingling appear later and can last for years after the treatment discontinuation [6]. Acute or chronic symptoms can occur; nearly 90% of patients develop at least one symptom of acute neuropathy during the first treatment cycle [7]. The incidence of chronic CIPN is high ranging from 13% to 70% depending on the type and dose of chemotherapy used [8–10]. According to data, once pain transitions from acute to chronic, it is more likely to be persistent [11]. These neurological changes, which are associated with pain, loss of sensation, and motor functionality, result in a lower quality of life. Economically, CIPN places a strain on both patients and the healthcare system because it is very frequently the main reason for job loss [12]. Despite receiving a cancer cure, patients still experience chronic, incapacitating neuropathy brought on by their cancer treatment.

There are currently no biomarkers available to assess and diagnose CIPN, or to predict the susceptibility or severity of neuropathy symptoms based on chemotherapy duration or dosage. However, the application of both clinical and web-based techniques yielded promising results. [13]. Further development of these measures will allow for earlier detection and will improve medical decisions about whether to continue or discontinue chemotherapy [10]. CIPN may develop because of treatment with different chemotherapy agents, including platinum compounds (cisplatin, carboplatin, oxaliplatin), taxanes (paclitaxel, docetaxel), vinca alkaloids (vincristine, vinblastine), thalidomide, and bortezomib.

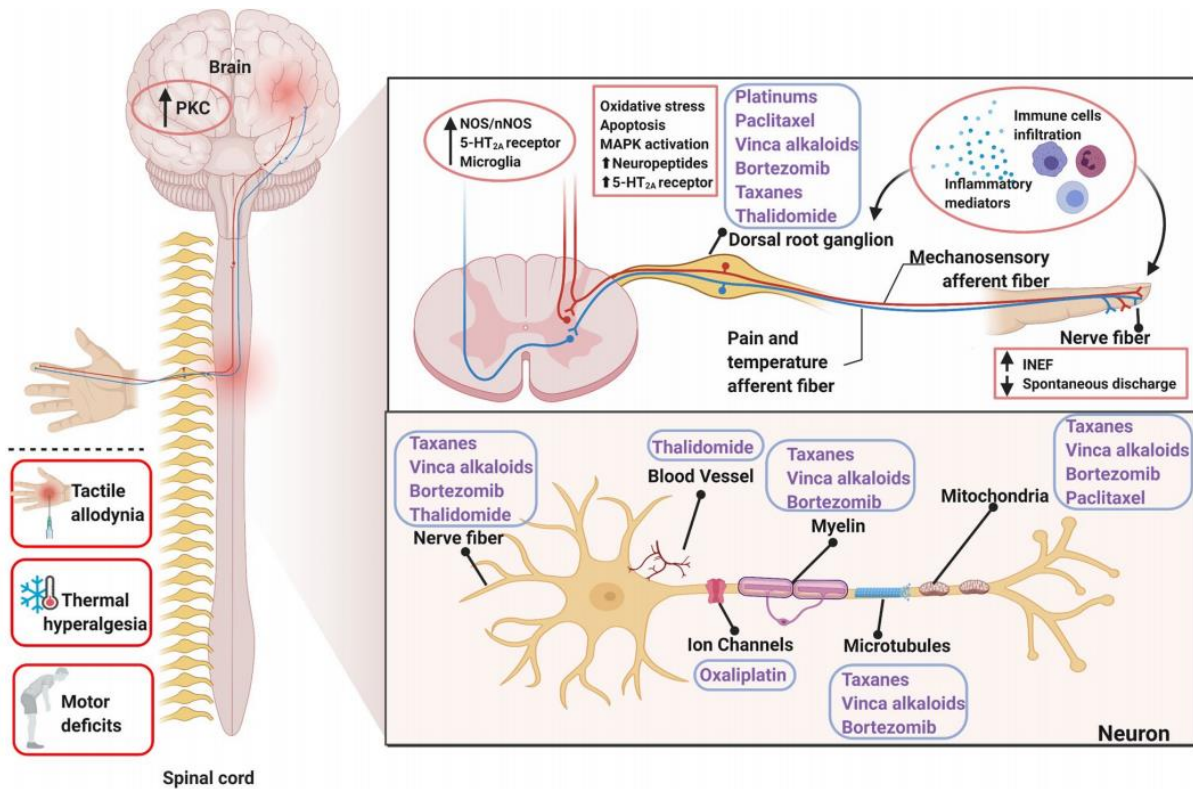


**Figure 1.** Sketch-map of the mechanism of chemotherapy-induced peripheral neuropathy (CIPN). Depiction of the typical symptoms and targets for CIPN toxicity in the peripheral nervous system depicted from the distal nerve terminals to axonal components (myelin, microtubules, mitochondria, ion channels, and vascular network), the dorsal root ganglion (DRG), and the central nervous system (CNS). CIPN was initiated and progressed by chemotherapeutic-agents through intraepidermal nerve fibers impairment, abnormal spontaneous discharge, activation of ion channels, up-regulation of neuro-immune system, oxidative stress, and the abnormal kinase activation in DRG and CNS. Contents in the blue boxes refer to different chemotherapy agents. Solid dots refer to the target of relative chemotherapeutic agents. Contents in the pink boxes refer to the pathological progress in peripheral and central nerve systems underlying CIPN (used with permission from [14]).

## 1.2. Taxanes (Paclitaxel)

Taxanes are widely used to treat a variety of cancers, including breast, ovarian, prostate, gastric, and head-and-neck cancers, as well as non-small cell lung cancer [15–17]. Even though cancer therapy research has been continuously emerging, taxanes and especially paclitaxel were described as the first-line therapy for breast cancer and remain one of the most commonly used types of chemotherapy for other types of cancer [16, 18]. Paclitaxel was originally extracted from the bark of the yew tree (*Taxus brevifolia*) in the Western region of the United States [18]. It belongs to a group of chemotherapy agents defined as “microtubule stabilizing agents” [19].

It targets the cytoskeleton and spindle apparatus of tumor cells by binding to the microtubules (MTs), which are fibrillary polymers of  $\alpha$ - and  $\beta$ -tubulin monomers. Paclitaxel promotes MT assembly by preventing  $\beta$ -tubulin polymerization into bundles. This action causes mitotic spindles to be disrupted and the cell cycle to be arrested in the G0/G1 and G2/M phases, resulting in apoptosis in dividing cells [20,21]. This action alters the natural dynamics of MTs, prevents proper spindle formation, blocks mitosis, and induces apoptosis and eventually cell death [22] (**Figure 2**). In addition, paclitaxel induces a down-regulation in the expression of the anti-apoptotic protein B-cell Leukemia 2 (Bcl-2) and an over-expression of the pro-apoptotic protein Bcl-2-associated X protein (BAX) [23,24]. These alterations are responsible for the triggering of mitochondrial apoptosis through disruption of the mitochondrial membrane potential (MMP) and the consequent release of cytochrome C from mitochondria into the cytoplasm and cleavage of the caspase-3 protein (**Figure 2**) [25,26]. However, it is unclear whether an increase in ROS directly induces mitochondrial apoptosis [23].

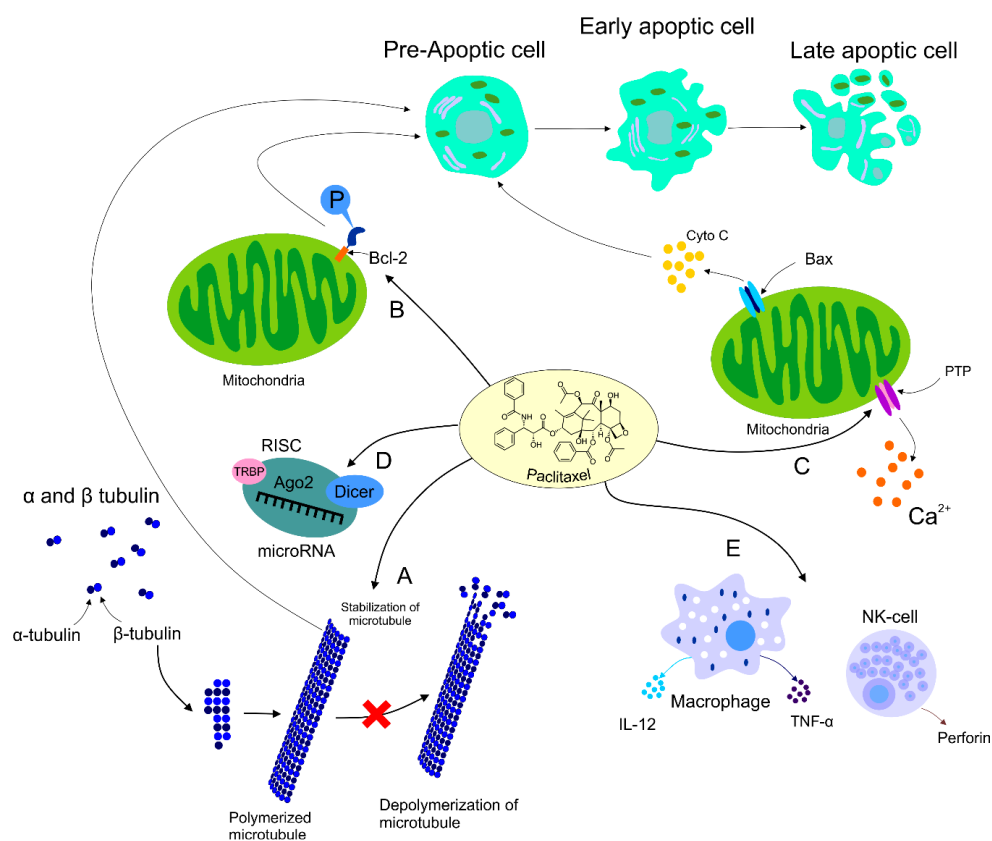


**Figure 2.** Mechanism of action of paclitaxel. Anti-tumor mechanism of action of paclitaxel leading to stabilization of microtubule, cell arrest, and subsequent apoptosis (**A**). Paclitaxel also causes activation of the immune response contributing to tumor eradication (**B**). The ability of paclitaxel to inactivate Bcl-2 via phosphorylation of the anti-apoptotic protein resulting in apoptosis (**C**). Participation of paclitaxel in the regulation of certain miRNAs associated with



the modulation of tumor progression (**D**). Regulation of calcium signaling by paclitaxel results in paclitaxel-induced release of cytochrome C from the mitochondria and programmed cell death. The immunomodulatory effects of paclitaxel via stimulation of macrophages leading to cytokine secretion including TNF- $\alpha$  or IL-12 that induce activation of natural killer cells (NK), dendritic cells (DC), and cytotoxic T lymphocytes resulting in the eradication of tumor cells (**E**) (used with permission from [27]).

The exact pathophysiologic mechanism of paclitaxel-induced PN is not well understood [28]. The inhibition of tubulin depolymerization and consequent MTs dysfunction appears to be the most widely accepted mechanism associated with the neurotoxic profile of paclitaxel [29,30]. Intact MTs are required for both anterograde and retrograde axonal transport, and neuronal survival and function are dependent on these transport processes. Increased axonal MTs stability or polar reconfiguration [31], secondary paclitaxel might alter the retrograde axonal transport of growth factors, or other substances resulting in abnormal nerve physiology, and altered mitochondrial supply, leading to a loss of axonal integrity, or axonal degeneration in more severe cases. This phenomenon starts in the most vulnerable part of the nerve, the distal nerve endings of the longest nerves, where transport problems may manifest most quickly, and after this, it spreads centrally, similar to other ‘dying back’-type peripheral neuropathies (**Figure 1**) [29,32] .

Despite paclitaxel’s efficacy as a chemotherapeutic agent, it promotes the formation of abnormal bundles of microtubules within the cytoplasm, leading to the disruption of normal cell function and proliferation. In patients, this results in the desired effect on the tumor, however, this is not without toxicity to normal tissue [33]. Paclitaxel does not cross the blood-brain barrier, and its accumulation in the soma of sensory neurons in the dorsal root ganglia (DRG) is likely due to a more permeable blood-nerve barrier as well as strong vascularization due to fenestrated capillaries in DRG[32].

### **1.3. Dorsal root ganglion (DRG)**

Chemotherapeutic drugs cause toxicity in myelin sheaths (myelopathy), sensory cell bodies (neuronopathy), and axonal compartments (axonopathy) in the DRG by affecting ion channels, microtubules, mitochondria, and associated capillaries [34,35]. DRG explants have thus been shown to be a good, simple, and well-accepted model for studying antineoplastic agent-induced PN [36–38]. MTs impairment in the soma of the sensory neurons have been noted [32,33]. Additionally, recent studies have linked the onset of paclitaxel-induced neuropathy to changes in the gene expression of some neuronal ion channels and increased excitability of primary

sensory neurons in animal models [39]. The ability of DRG explants to outgrow neurites *in vitro*, as well as their response to toxic substances with neurite shortening, makes them a reliable model for evaluating drug neurotoxicity [36,40–42].

Primary DRG cultures consist of a diverse population of cells, including differentiated sensory post-mitotic neuronal cells (neurons) and proliferative non-neuronal cells [43]. DRG neurons are subdivided to three different subpopulations according to the size of their somata (small,  $\leq 599 \mu\text{m}^2$ ; medium,  $600\text{--}1199 \mu\text{m}^2$  and large,  $1200\text{--}1300 \mu\text{m}^2$ ), which represented 67%, 31%, and 2% of neurons in culture, respectively [44] while DRG non-neuronal cells consist of (Satellite glial cells (SGCs), Schwann cells (SCs), and other glial cells) (**Figure 3**) [45–48]. In addition to the importance of neurons, DRG non-neuronal cells are increasingly being recognized as being important in the development and maintenance of neuropathic pain [49,50].

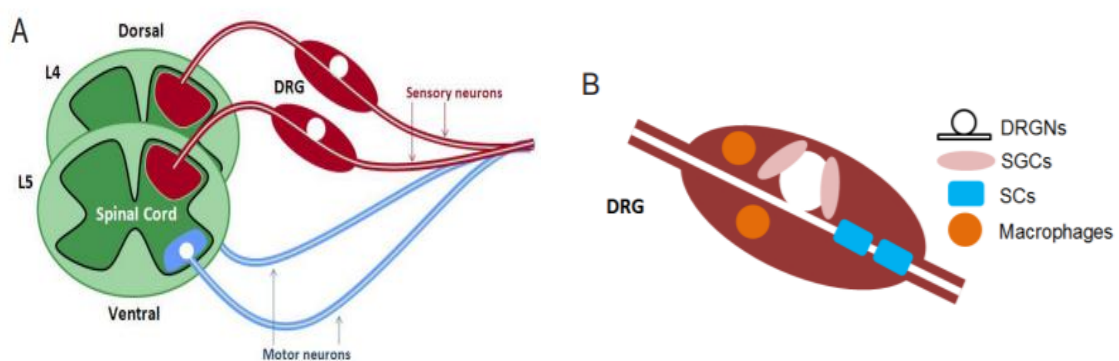


**Figure 3.** Schematic diagram of DRG structure and cell types of composition. (A) A diagram of a DRG. The sensory neurons cell body is located within the DRG, with central and peripheral axon extensions. The motor neurons project out from the ventral horn of the spinal cord and combine with the peripheral sensory neurons to form the sciatic nerve. (B) An illustration of the prominent cells within the DRG. The SGCs surround the neuronal cell bodies, whilst SCs ensheath and myelinate single or multiple axon fibers, and finally the macrophages are present for the immune response (used with permission from [43]).

Paclitaxel-induced neuropathy is most likely caused by dysfunctional MTs in DRGs, axons, and SCs [51,52]. *In vivo* studies have shown that direct injection of paclitaxel into the rat sciatic nerve causes the formation of unusual MT aggregates resulting in demyelination and loss of axoplasmic transport [51,52]. Although paclitaxel affected SCs in *in vitro* studies, it is unclear whether this effect is only due to a demyelinating process. In conclusion, it is likely that paclitaxel causes both sensory axonopathy and a ganglio-neuropathy, the latter occurring with higher single and cumulative doses, or when combined with cisplatin [53]. Subsequent studies

revealed that paclitaxel administration inhibits the normal regenerative response of axons and SCs to nerve crush injuries in rodent models [54].

Paclitaxel showed neurotoxic effects on DRG neurons, including a significant reduction in neurite length in rat DRG neurons, as previously reported [44]. Furthermore, Paclitaxel's effects on neuronal survival and neurite length in the DRG were dose- and time-dependent [44,55].

Paclitaxel reduced cell viability and changed the phenotype of SCs isolated from the sciatic nerve at 24 h and 48 h [56]. A recent study looked at the effect of paclitaxel on the viability and proliferation of SGCs and discovered that it had no effect on viability but had a negative effect on cell proliferation [57]. More research is needed, however, to fully understand the mechanisms of paclitaxel toxicity on non-neuronal cells (SCs, SGCs, and other glial cells). These effects may have adverse functional consequences on DRG sensory neurons and should be considered in the management of PN. As a result, it is critical to discover novel therapeutic agents capable of mitigating or preventing PN caused by paclitaxel treatment. It is critical to find ways to manage the neurological complications of chemotherapy treatment. When symptoms of CIPN first appear in many patients, dose reduction or discontinuation of treatment is implemented, a strategy that may ultimately have a negative impact on overall survival. Symptoms persist in more than half of all patients long after treatment has been discontinued [58]. Even more difficult, there are no cures for the tingling and numbness that up to 70% of CIPN patients experience as side effects, and the therapeutics available for neuropathy are typically ineffective [59,60]. Despite the lack of data from prospective placebo-controlled trials, physicians typically recommend topical analgesics, antidepressants, and anticonvulsants, cannabinoids, opioids, and non-opioid analgesics. Until now, evidence of their effectiveness has been scant or negative [61,62].

#### **1.4. Endocannabinoids (Palmitoylethanolamide)**

The Endocannabinoid system (ECS) is a complex molecular/biological system [63], plays critical roles in multiple physiological processes such as homeostasis, anxiety, emotional behavior, depression, nervous functions, neurogenesis, neuroprotection, learning, memory, pain sensation, fertility, pregnancy, and pre-and post-natal development [64]. The role of the ECS in health and disease processes has drawn more attention in recent years and its components have been implicated as an emerging target of pharmacotherapy for a wide range of diseases including general pain, headache, migraine, glaucoma, mood and anxiety disorders, obesity/metabolic syndrome, neuromotor, neuropsychological and neurodegenerative diseases,

respiratory diseases such as asthma, cardiovascular diseases such as atherosclerosis, myocardial infarction, metabolic disorders, and hypertension [65,66].

The ECS includes receptors, their ligands, and enzymes responsible for their biosynthesis and degradation/deactivation, and they are widely distributed throughout mammalian tissues and cells [67]. The three main receptor classes of ECS involves (i) G-Coupled Protein Receptors (GPCRs) such as CB1, CB2 [68], (ii) Ligand-sensitive ion channels (e.g., Transient Receptor Potential Vanilloid 1-TRPV1) which is also activated by chemical agents, physical stimuli, capsaicin, and ions, and (iii) Nuclear receptors (e.g., PPARs) [69]. The endogenous ligands N-arachidonoyl ethanolamine (AEA, anadamide), N-palmitoylethanolamine (PEA), and N-oleoylethanolamine (OEA) are synthesized from membrane N-acylphosphatidylethanolamine (NAPE) precursors either directly through a NAPE-selective phospholipase D or through the serial action of lipases (phospholipase C and then a phosphatase or phospholipase A2 and then lysophospholipase D) and 2-arachidonoylglycerol (2-AG), and the endocannabinoid metabolic enzymes responsible for endocannabinoid synthesis and degradation such as diacylglycerol lipase isozymes  $\alpha$  and  $\beta$ , fatty acid amide hydrolase (FAAH), monoacylglycerol lipase, and N-acylphosphatidylethanolamine-selective phospholipase [70].

Palmitoylethanolamide (PEA) is a non-endocannabinoid lipid mediator belonging to the class of the *N*-acylethanolamine phospholipids that was first isolated from soy lecithin, egg yolk, and peanut meal [71]. Both preclinical and clinical studies indicate that PEA is potentially useful in a wide range of therapeutic areas, including eczema, pain, and neurodegeneration reviewed in [71]. PEA is commonly used in humans for its analgesic and anti-inflammatory properties, and it has been shown to be extremely safe and tolerable. Several preclinical *in vitro* and *in vivo* studies have demonstrated that PEA can cause biological effects by acting on a variety of molecular targets in both the central and peripheral nervous systems [71].

PEA interacts with a wide range of molecular targets in the body, including cannabinoid receptors and other pain and inflammation-related receptors [72,73]. Several studies conducted in the past ten years demonstrated PEA's ability to protect against neuroinflammation and neurodegeneration, demonstrating the compound's exceptional potential as a novel treatment for neurodegenerative disorders [74–78].

PEA's multifaceted effects are caused by its distinct mechanisms of action, which affect multiple pathways at various sites (**Figure 4**) [79]. PEA primarily targets the nuclear receptor peroxisome proliferator-activated alpha (PPAR- $\alpha$ ), but it also acts on novel cannabinoid receptors, G protein-coupled receptor 55 (GPR55) and G protein-coupled receptor 119

(GPR119) [80,81]. Furthermore, it indirectly activates CB1 and CB2 by inhibiting the degradation of AEA, a phenomenon known as the entourage effect [71,80].

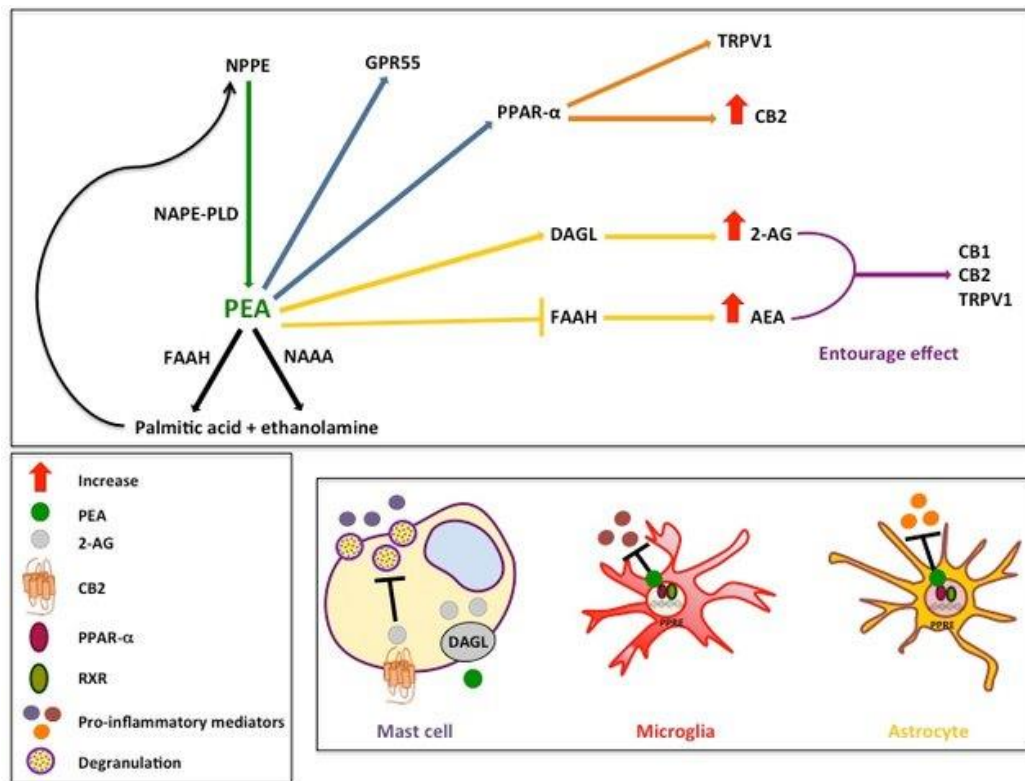


**Figure 4.** Metabolic pathways and mechanisms of action of PEA. PEA is synthesized by NAPE-PLD (green arrow) and hydrolyzed to palmitic acid and ethanolamine by FAAH and NAAA (black arrows). PEA directly activates GPR55 and PPAR- $\alpha$  receptors (blue arrows). PEA activates TRPV1 receptors and increases the expression of CB2 receptors (orange arrows) via direct activation of PPAR- $\alpha$  receptors (blue arrow). PEA, through the stimulation of the activity of DAGL or the inhibition of the expression of FAAH (yellow arrows), increases the endogenous levels of 2-AG and AEA, respectively, which directly activate CB1, CB2, and TRPV1 receptors ("entourage effect") (violet arrow). PEA, possibly through an allosteric modulation of TRPV1 receptors, potentiates the actions of AEA and 2-AG at TRPV1 receptors ("entourage effect. PEA inhibits the activation of mast cells through an indirect CB2-mediated mechanism (i.e., increased 2-AG synthesis). (used with permission from [82]).

PEA has previously been shown to protect dentate gyrus granule cells during secondary neuronal damage [83]. Another study found that repeated PEA treatment reduced the decrease in axon diameter and myelin thickness in a chronic constriction injury model of neuropathic pain [84]. Furthermore, PEA protects neurons from excitotoxicity and has a local anti-injury effect by inhibiting mast cell activation [85]. PEA enhances neurobehavioral functions, including memory and learning, in animal models of neurodegeneration by reducing oxidative stress, pro-inflammatory, and astrocyte marker expression, and rebalancing glutamatergic transmission [86]. Additionally, PEA showed neuroprotective effects in organotypic hippocampal slices and mixed neuroglial cultures through a peroxisome proliferator-activated

receptor-mediated mechanisms [87]. As a result, the potential protective effects of PEA against the side effects of chemotherapeutic agents that cause peripheral neuropathy, such as paclitaxel, are crucial.

## 1.5 Objectives

The aims of this thesis were the:

1. Isolation, purification, and culturing of DRG neuronal and non-neuronal cells.
2. Investigation of the toxicity of paclitaxel on cell viability, neurite length, and cell soma of rat DRG neurons as well as on cell viability, cell death, cell proliferation, and cell morphology of DRG non-neuronal cells at different time points.
3. Analysis the potential protective effects of PEA on DRG neuronal and non-neuronal cells.
4. Elucidation if paclitaxel effects or/and PEA on DRG neuronal and non-neuronal cells are concentration- or/and time-dependent or not.
5. Evaluation whether PEA influences the anti-tumoral effects of paclitaxel treatment on different human breast cancer cells or not.

## 2. Discussion

The protective effects of PEA against toxicity of paclitaxel were assessed in rat primary DRG neuronal and non-neuronal cells. The safety of PEA was tested on the efficacy of paclitaxel against different Human breast cancer cells (HBCCs). This dissertation is based on the publications that have addressed the research questions (**Introduction 1. 5**). In the first publication, we investigated the neuroprotective effects of PEA against the toxicity of paclitaxel on primary DRG neurons. In the second publication, the adverse effects of paclitaxel on primary DRG non-neuronal cells were investigated. Then, we evaluated the protective effects of PEA on DRG non-neuronal cells as well as the effects of PEA on anti-cancer efficacy of paclitaxel (data not published, briefly discussed).

### 2.1. Effects of paclitaxel on DRG neuronal and non-neuronal cells

In the first and second publications, primary DRG were isolated from 6-8 weeks aged Wistar rats, then DRG neuronal and non-neuronal cells were separated using density gradient centrifugation method using 15 % Bovine serum albumin (BSA). DRG neuronal and non-

neuronal cells were then exposed to paclitaxel at various concentrations (0.01  $\mu\text{M}$ , 0.1  $\mu\text{M}$ , 1  $\mu\text{M}$ , 10  $\mu\text{M}$ ) then the effects were analyzed at 24 h, 48 h, and 72 h post-treatment. Our findings revealed that paclitaxel showed toxic effects on neuronal cells including reduction in neuronal viability, a strong reduction in neurite length and enlargement of neuronal cell bodies at all investigated time windows (**publication 1**). These results are in line with previous findings reporting about a significant reduction in neurite length when DRG neurons were exposed to 10  $\mu\text{M}$  paclitaxel for 24 h [44]. Paclitaxel treatment caused a significant increase in DRG neuron soma size after 24 h of treatment [55,88] and induced a significant enlargement of DRG nucleolus size [89]. The data imply the fact that DRG neurons are highly susceptible to paclitaxel accumulation, possibly because of higher permeability of the blood-nerve barrier when compared to blood-brain barrier [90]. Therefore, paclitaxel seems to act directly on axons and causes axonal degeneration probably through local mechanisms [91]. Additionally, paclitaxel disrupted intracellular microtubules and bindings with beta-tubulin inside cell soma, resulting in accumulation of non-functional beta-tubulin units of microtubules, vacuolization of mitochondria and cytoplasm in neuronal cell bodies, and cell enlargement [92].

In the second publication, paclitaxel showed a set of toxicological effects on primary DRG non-neuronal cells that included a decline in cell viability, an increase in cell death, inhibition of cell proliferation, and morphological changes. These effects might have adverse effects on the function of neurons and the management of peripheral neuropathy. Our findings are in agreement with earlier studies representing an affected viability of SCs isolated from the sciatic nerve [56], and suppressed cell proliferation of SGCs after 24 h of paclitaxel treatment [57]. In addition, a loss or shortening of processes was induced in non-neuronal cells in primary DRG co-culture [56,88]. These effects were attributed to paclitaxel's fast and strong mechanism of action on primary DRG non-neuronal cells, as these cells are non-transformed and proliferating cells. Therefore, paclitaxel selectively causes the death of transformed cells, possibly by arresting the cell cycle at G1 as well as G2/M phases [1,93–96]. The adverse effects of paclitaxel on DRG neuronal and non-neuronal cells were concentration- and time-dependent (**Publications 1&2**).

## **2.2. Effects of PEA against paclitaxel toxicity on DRG neuronal and non-neuronal cells**

In the first publication, primary DRG neuronal cells were treated with different concentrations of PEA (0.1  $\mu\text{M}$ , 1  $\mu\text{M}$ , 10  $\mu\text{M}$ ) either alone or in combination with different concentrations of paclitaxel (0.01  $\mu\text{M}$ , 0.1  $\mu\text{M}$ , 1  $\mu\text{M}$ , 10  $\mu\text{M}$ ) at various investigated time points. PEA alone did not show any effects on DRG neurons compared to the control group; however, it showed

neuroprotective effects by partially reversing the toxic effects of paclitaxel including increasing cell viability, enhancing DRG neuron neurite outgrowth, and decreasing swelling of neuronal soma (**Publication 1**). These data were also consistent with previous research demonstrating that different PEA concentrations increased the cell viability in astrocytes [97]. Further, our data are in agreement to research reporting a reduction of positive propidium iodide (PI) neuronal nuclei after application of PEA to N-methyl D-aspartate-treated

organotypic hippocampal slice cultures [83]. In line with previous evidence PEA effects on preserving myelin sheet thickness and axonal diameter and preventing myelin degeneration [84]. Additionally, in a rat model of oxaliplatin-induced neurotoxicity, administration of PEA substantially relieved pain after 30 minutes [98].

Our findings also demonstrated that PEA could reverse the toxic effects of paclitaxel on DRG non-neuronal cells by increasing cell viability, improving cell survival as well as accelerating the rate of cell proliferation. It showed protective effects on cell viability particularly against higher concentrations of paclitaxel (1  $\mu$ M, and 10  $\mu$ M) (**Figure 5a**). This could be due to high concentrations of paclitaxel causing high toxicity and a significant reduction in the number of viable cells. As a result, any protective signaling amplified by PEA would be more visible and effective. These findings are in line with the data that found a significant increase in viability of DRG neurons when co-treated with PEA plus paclitaxel at different concentrations (**Publication 1**). Furthermore, our findings are consistent with previous research demonstrating the importance of PEA in improving astrocyte cell viability [97]. Interestingly, PEA maintained a nearly similar positive PI ratio (indicative of cell death) as well as positive bromodeoxyuridine (BrdU) ratio (indicative of cell proliferation) in cells treated with higher concentrations of paclitaxel compared to cells treated with the lowest concentration of paclitaxel (0.01  $\mu$ M) at different time points (**Figure 5 b, c**), even though there were concentration-dependent effects (more toxicity) at these endpoints when cells have been exposed to different paclitaxel concentrations (**Publication 2**). In line with the majority of experimental evidences, cannabinoids protect neurons and glial cells from apoptosis and oxidative damage. Therefore, cannabinoids are very likely to regulate cell survival and cell death pathways in non-transformed cells [99]. Daily PEA-OXA treatment for 14 days after sciatic nerve crush showed analgesic protective effect on hypersensitivity and improved functional recovery after nerve crush [100]. Our results shed more light on the PEA mode of action against paclitaxel toxic effects and how it might protect DRG non-neuronal cells, which is critical in the management of peripheral neuropathy and the protection of DRG neurons.



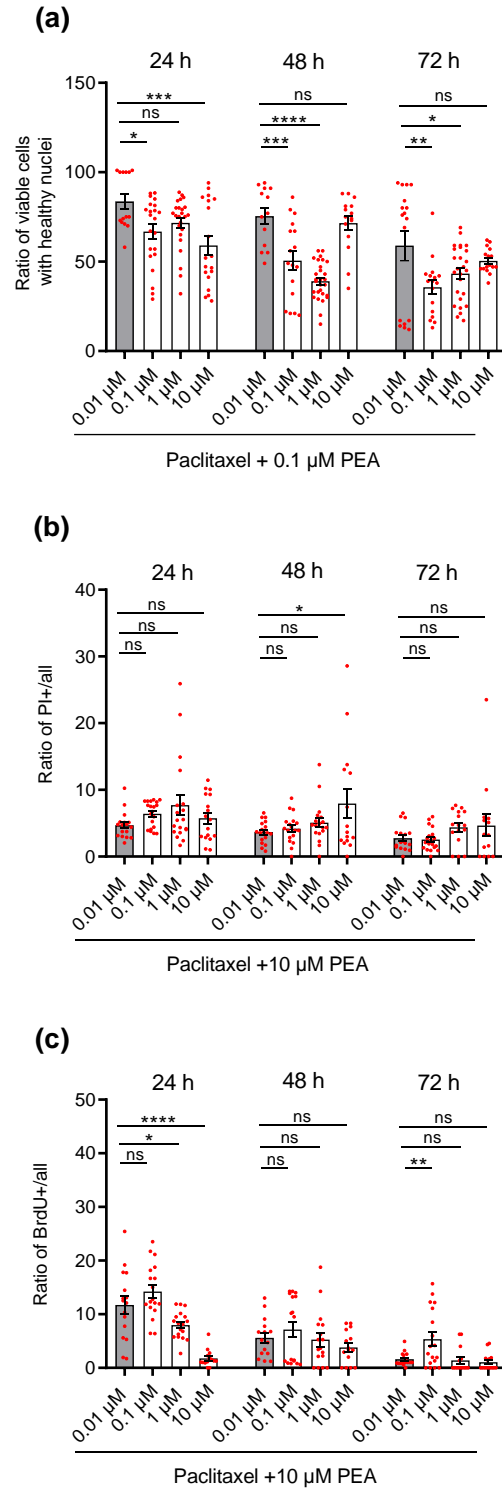


**Figure 5.** Effects of different paclitaxel concentrations (0.01 μM, 0.1 μM, 1 μM, and 10 μM) combined with either 0.1 μM PEA on (a) the ratio of viable DRG non-neuronal cells with healthy nuclei at 24 h, 48 h, and 72 h post-treatment using DAPI staining assay or 10 μM PEA to study effects on (b) cell death of DRG non-neuronal cells at various investigated time points using PI assay, and (c) cell proliferation of DRG non-neuronal cells using BrdU assay. The data represent only one example of the effects comparing the effect in combinations of PEA (0.1 μM) + gradual or/and higher concentrations (10x) of paclitaxel with the effect in the combination of the lowest paclitaxel concentration (0.01 μM) plus the same PEA concentration

used using One-way ANOVA followed by Bonferroni-post hook test,  $*P < 0.05$ ). Data represented as mean  $\pm$  SEM and the experiments were performed three independent times with  $n = 15$  replicas. The asterisk denotes significant results ( $**p < 0.01$ ,  $***p < 0.001$ ,  $****p < 0.0001$ ) regarding the respective measurement indicated with the bar graph. Only the non-significant differences are of biological importance which indicates the role of the PEA in maintaining a similar survival ratio of the cells, positive PI (cell death), and positive BrdU (cell proliferation) even at higher concentrations of paclitaxel.

Live cell imaging is less prone to experimental artifacts and usually gives more reliable and useful information on time dependent processes than microscopy of fixed cells [101]. In the current study, live imaging records of the cells treated with paclitaxel or/and PEA, either individually or in combination revealed a protective effect of PEA against the toxic action of paclitaxel (**Figure 6, supplementary videos**). PEA effects included changing in cell behavior and assisting cells to resist paclitaxel induced effects by recovering from mitotic arrest. The cells returned to their normal morphology indicating for contribution of PEA to slowing down the cell death. Paclitaxel is known to disrupt microtubule dynamics, causing the cell cycle to stop at G1 and G2/M phases [96]. Considerably, the here presented findings show that PEA effects to prevent cell death are not restricted to neurons [42] but can be extended to safeguarding non-neuronal cells within the DRG. The data is consistent and support earlier findings that cannabinoids, both *in vivo* and *in vitro*, prevent astrocyte apoptosis induced by ceramide [102]. In addition, cannabinoids protect oligodendrocytes from cell death caused by growth factor deficiency [103].

After the demonstrated protective effects of PEA against toxicity of paclitaxel on neuronal and non-neuronal cells as discussed above, it is very important to ensure that PEA will not affect the efficacy of paclitaxel against tumor cells. Therefore, the effects of different concentrations of PEA or/and paclitaxel either individually or in combination on three different breast cancer cell lines, namely MCF-7, MDA-MB-231, and SK-BR-3 representing early, invasive, and metastatic pathological stages of breast tumor, respectively were investigated (unpublished data, in preparation). We found that PEA treatment had no impact on the efficacy of paclitaxel in killing different stages of human breast cancer cells (HBCCs). The synergistic anti-cancer effects of PEA were visible when combined with paclitaxel at lower concentrations and were noticed only in early and invasive stages of HBCCs (**Figure 7**).

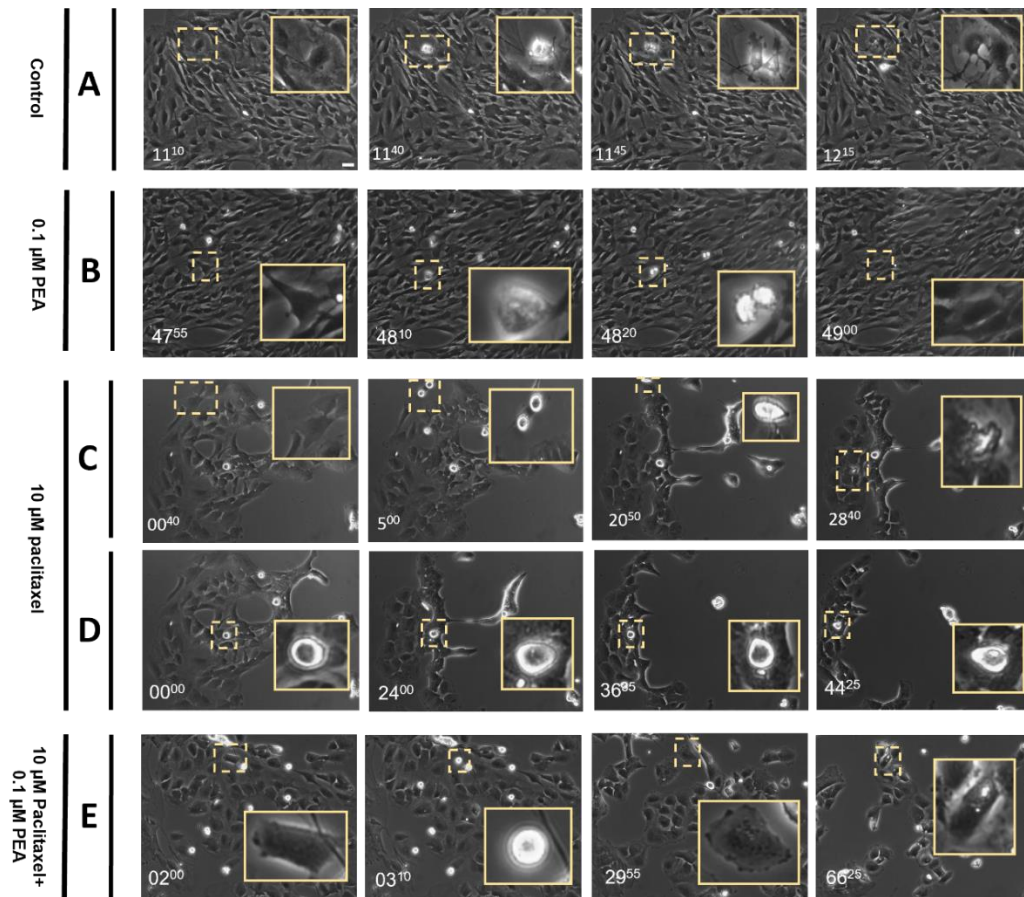


**Figure 6.** Representative images demonstrated the effects of 0.1  $\mu\text{M}$  PEA against 10  $\mu\text{M}$  paclitaxel on cell proliferation of DRG non-neuronal cells using a phase contrast live imaging setup for up to 72 h. Higher magnification of labeled areas showed different actions of cells related to effects on cell proliferation after treatment with 10  $\mu\text{M}$  paclitaxel and 0.1  $\mu\text{M}$  PEA either individually or in combination at different hours. Marked cells representing normal mitotic events resulting in two daughter cells as represented in the control (A) (Video S1), and 0.1  $\mu\text{M}$  PEA (B) (Video S2) groups. 10  $\mu\text{M}$  paclitaxel arrested cell proliferation through various mechanisms where some rounding cells closed together and became one live cell before being rounded again and then dead, as seen in the highlighted image in (C) (Video S3). Additionally, some cells changed their morphology to a rounding event then not divide, and finally died through apoptosis as indicated in (D) (Video S3). 0.1  $\mu\text{M}$  PEA partially reversed the effects of 10  $\mu\text{M}$  paclitaxel on cell division, in which some cells changed their morphology to a mitotic rounding event then back again to a single cell, but not two cells, then later, the cell started to be round and merged with the other surrounding cell as shown in (E) (Video S4). The experiments were conducted three times independently,  $n=15-20$  replicates. The white numbers in the left lower corner of each image indicate the time of detection of various events in hours and minutes. Scale bars = 100  $\mu\text{m}$ .

Anticancer effects of paclitaxel are mainly due to its ability to target microtubules. In addition to its effects on mitosis, paclitaxel plays as a microtubule target agent (MTA) important roles in cellular functions throughout the cell cycle, where p53, c-Myc, BRCA1, androgen receptor, APC, and Src, proteins involved in oncogenesis, are known to associate with and/or traffic along microtubules [104,105]. Paclitaxel's ability to disrupt interphase microtubule functions

was expected to reduce the activity of these and other proteins implicated in cancer maintenance and progression [106]. Our findings are in similarity with previous literatures elucidating paclitaxel-induced cell death by apoptosis in different HBCCs [27,107–110].

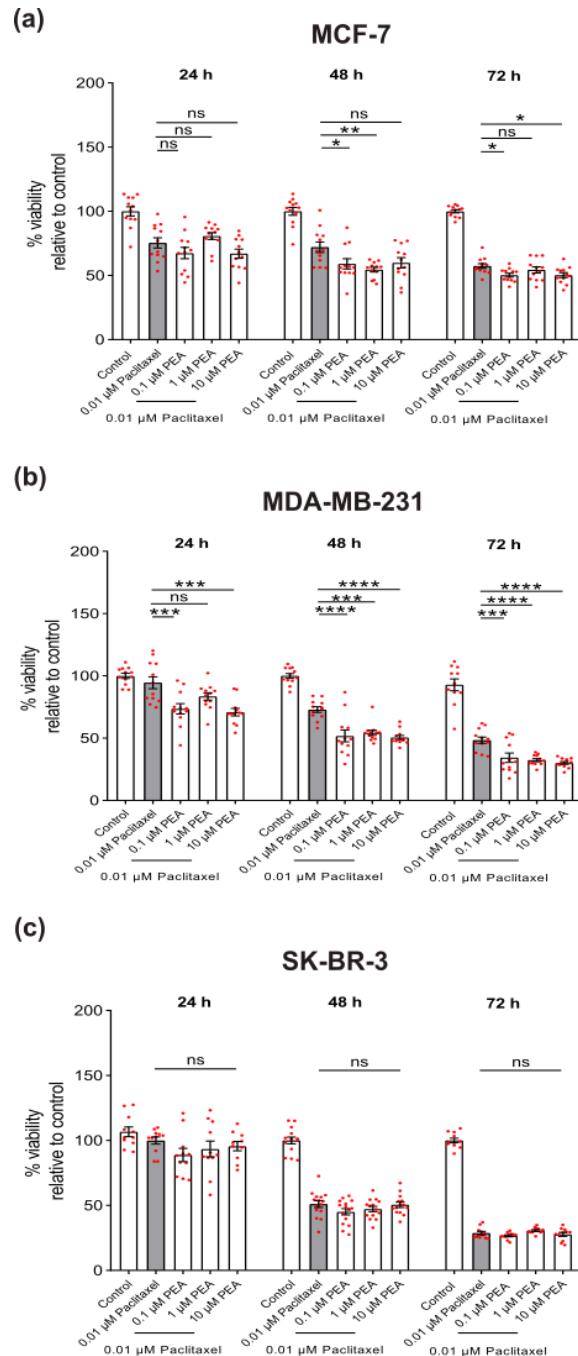


**Figure 7.** Effects of different concentrations of PEA (0.1 μM, 1 μM, and 10 μM) combined with 0.01 μM Paclitaxel on the viability of different breast tumor cells (MCF-7, MDA-MB-231, and SK-BR-3) at 24 h, 48 h, and 72 h post-treatment using MTT assay. PEA plus 0.01 μM paclitaxel showed a significant suppression in the viability of (a) MCF-7 cells at 48 h and 72 h after application compared to paclitaxel alone (\* $p < 0.05$ , \*\* $p < 0.01$ ). (b) Significant reduction in the viability of MDA-MB-231 cells compared to the paclitaxel group (\*\*\* $p < 0.001$ , \*\*\*\* $p < 0.0001$ ) at 24 h, 48 h, and 72 h post-treatment. (c) No significant effects against paclitaxel

were found at different PEA concentrations on the viability of SK-BR-3 compared to paclitaxel ( $p > 0.05$ ) at all investigated time windows. The asterisks denote significant results regarding the respective measurement indicated with the bar. Values are given as the mean  $\pm$  SEM of three independent experiments conducted in 12 replicates, ns: non-significant.

Our findings indicated that PEA plus paclitaxel exhibited synergistic anti-cancer effects in distinct cell lines like MCF-7 or MDA-MB-231 cells by significantly reducing the viability of cells, at various investigated time points. This combined effect might involve the entourage effect increasing AEA concentration as an endogenous enhancer of some biological actions, resulting in a positive interaction (additive-synergistic) [111]. Previous research also discovered that PEA inhibits colon carcinoma cell proliferation by inhibiting the Akt/mechanistic target of rapamycin (mTOR) pathway by involving PPAR alpha [112], enhancing inhibition of proliferation by AEA by virtue of its action as positive allosteric modulator of TRPV1 [113] and by permissively enhancing AEA effects by downregulation of FAAH expression and activity [114].

Notably, these additive-synergistic interaction effects were only visible at low paclitaxel concentrations. Low- dose combination treatments of paclitaxel and 5-Demethylnobiletin, exhibited synergistic effects in lung cancer cells [115]. Additionally, our results revealed that these synergistic interactive effects of PEA and paclitaxel depended on the stage of the breast cancer, as MCF-7 and MDA-MB-231 cells were more susceptible to paclitaxel and PEA, whereas no effect was apparent in late-stage breast tumor (SK-BR-3) cells. This may be because SK-BR-3 cells are more aggressive and demonstrated hypersensitivity to paclitaxel induced apoptotic cell death [116].

### **2.3. Conclusions**

Paclitaxel treatment exhibited a set of toxicological effects on primary DRG neuronal and non-neuronal cells. It led to a reduction in neuronal viability, a strong reduction in neurite length, and an increase in size of neuronal cell bodies at all investigated time windows. In addition, paclitaxel showed adverse effects on primary DRG non-neuronal cells including suppression in number of viable cells, an increase in cell death, decrease of cell proliferation rate, as well as morphological changes. The effects of paclitaxel on primary DRG neuronal and non-neuronal cells were concentration- and time- dependent. PEA, on the other hand, demonstrated neuroprotective effects by partially mitigating the toxic effects of paclitaxel by increasing cell viability, inducing DRG neuron neurite outgrowth, and decreasing swelling of neuronal soma. Furthermore, PEA at various concentrations protects DRG non-neuronal cells from the adverse

effects of paclitaxel, including increased cell viability, improved cell survival, and accelerated cell proliferation. These findings shed more light on the PEA mode of action against the toxic effects of paclitaxel and might be important for a better management of peripheral neuropathy and the protection of DRG neurons and non-neuronal cells. Further, our findings demonstrated the safety of PEA as an endocannabinoid-like substance in combination with paclitaxel against HBCCs, suggesting that it could be used to treat peripheral neuropathy caused by paclitaxel. PEA could be used in conjunction with paclitaxel to treat breast cancer patients with CIPN. Taken together, more research is required to identify the signaling pathways underlying the additive-synergistic interaction effect of PEA and paclitaxel on the viability of HBCCs.

### 3. References

1. Jemal, A.; Center, M. M.; DeSantis, C.; Ward, E. M. Global Patterns of Cancer Incidence and Mortality Rates and Trends. *Cancer Epidemiol. Biomarkers Prev.* **2010**, *19* (8), 1893–1907. <https://doi.org/10.1158/1055-9965.EPI-10-0437>.
2. Willson, M. L.; Burke, L.; Ferguson, T.; Ghersi, D.; Nowak, A. K.; Wilcken, N. Taxanes for Adjuvant Treatment of Early Breast Cancer. *Cochrane Database Syst. Rev.* **2019**. <https://doi.org/10.1002/14651858.CD004421.pub3>.
3. Argyriou, A. A.; Koltzenburg, M.; Polychronopoulos, P.; Papapetropoulos, S.; Kalofonos, H. P. Peripheral Nerve Damage Associated with Administration of Taxanes in Patients with Cancer. *Crit. Rev. Oncol. Hematol.* **2008**, *66* (3), 218–228. <https://doi.org/10.1016/j.critrevonc.2008.01.008>.
4. Carozzi, V. A.; Canta, A.; Chiorazzi, A. Chemotherapy-Induced Peripheral Neuropathy: What Do We Know about Mechanisms? *Neurosci. Lett.* **2015**, *596*, 90–107. <https://doi.org/10.1016/j.neulet.2014.10.014>.
5. Duregon, F.; Vendramin, B.; Bullo, V.; Gobbo, S.; Cugusi, L.; Di Blasio, A.; Neunhaeuserer, D.; Zaccaria, M.; Bergamin, M.; Ermolao, A. Effects of Exercise on Cancer Patients Suffering Chemotherapy-Induced Peripheral Neuropathy Undergoing Treatment: A Systematic Review. *Crit. Rev. Oncol. Hematol.* **2018**, *121*, 90–100. <https://doi.org/10.1016/j.critrevonc.2017.11.002>.
6. Ibrahim, E. Y.; Ehrlich, B. E. Prevention of Chemotherapy-Induced Peripheral Neuropathy: A Review of Recent Findings. *Crit. Rev. Oncol. Hematol.* **2020**, *145*, 102831. <https://doi.org/10.1016/j.critrevonc.2019.102831>.
7. Pachman, D. R.; Qin, R.; Seisler, D. K.; Smith, E. M. L.; Beutler, A. S.; Ta, L. E.; Lafky, J. M.; Wagner-Johnston, N. D.; Ruddy, K. J.; Dakhil, S.; Staff, N. P.; Grothey, A.; Loprinzi, C. L. Clinical Course of Oxaliplatin-Induced Neuropathy: Results From the Randomized Phase III Trial N08CB (Alliance). *J. Clin. Oncol.* **2015**, *33* (30), 3416–3422. <https://doi.org/10.1200/JCO.2014.58.8533>.
8. Kelley, M. R.; Fehrenbacher, J. C. Challenges and Opportunities Identifying Therapeutic Targets for Chemotherapy-Induced Peripheral Neuropathy Resulting from Oxidative DNA Damage. *Neural Regen. Res.* **2017**, *12* (1), 72–74. <https://doi.org/10.4103/1673-5374.198986>.
9. Song, S. J.; Min, J.; Suh, S. Y.; Jung, S. H.; Hahn, H. J.; Im, S.-A.; Lee, J.-Y. Incidence of Taxane-Induced Peripheral Neuropathy Receiving Treatment and Prescription Patterns in Patients with Breast Cancer. *Support. Care Cancer* **2017**, *25* (7), 2241–2248. <https://doi.org/10.1007/s00520-017-3631-x>.
10. Hershman, D. L.; Lacchetti, C.; Dworkin, R. H.; Lavoie Smith, E. M.; Bleeker, J.; Cavaletti, G.;

- Chauhan, C.; Gavin, P.; Lavino, A.; Lustberg, M. B.; Paice, J.; Schneider, B.; Smith, M. Lou; Smith, T.; Terstriep, S.; Wagner-Johnston, N.; Bak, K.; Loprinzi, C. L.; American Society of Clinical Oncology. Prevention and Management of Chemotherapy-Induced Peripheral Neuropathy in Survivors of Adult Cancers: American Society of Clinical Oncology Clinical Practice Guideline. *J. Clin. Oncol.* **2014**, *32* (18), 1941–1967. <https://doi.org/10.1200/JCO.2013.54.0914>.
11. Majithia, N.; Temkin, S. M.; Ruddy, K. J.; Beutler, A. S.; Hershman, D. L.; Loprinzi, C. L. National Cancer Institute-Supported Chemotherapy-Induced Peripheral Neuropathy Trials: Outcomes and Lessons. *Support. Care Cancer* **2016**, *24* (3), 1439–1447. <https://doi.org/10.1007/s00520-015-3063-4>.
  12. Pike, C. T.; Birnbaum, H. G.; Muehlenbein, C. E.; Pohl, G. M.; Natale, R. B. Healthcare Costs and Workloss Burden of Patients with Chemotherapy-Associated Peripheral Neuropathy in Breast, Ovarian, Head and Neck, and Non-small Cell Lung Cancer. *Chemother. Res. Pract.* **2012**, *2012*, 1–10. <https://doi.org/10.1155/2012/913848>.
  13. Dorsey, S. G.; Kleckner, I. R.; Barton, D.; Mustian, K.; O'Mara, A.; St. Germain, D.; Cavaletti, G.; Danhauer, S. C.; Hershman, D. L.; Hohmann, A. G.; Hoke, A.; Hopkins, J. O.; Kelly, K. P.; Loprinzi, C. L.; McLeod, H. L.; Mohile, S.; Paice, J.; Rowland, J. H.; Salvemini, D.; Segal, R. A.; Smith, E. L.; Stevens, W. M.; Janelins, M. C. The National Cancer Institute Clinical Trials Planning Meeting for Prevention and Treatment of Chemotherapy-Induced Peripheral Neuropathy. *JNCI J. Natl. Cancer Inst.* **2019**, *111* (6), 531–537. <https://doi.org/10.1093/jnci/djz011>.
  14. Yang, Y.; Zhao, B.; Gao, X.; Sun, J.; Ye, J.; Li, J.; Cao, P. Targeting Strategies for Oxaliplatin-Induced Peripheral Neuropathy: Clinical Syndrome, Molecular Basis, and Drug Development. *J. Exp. Clin. Cancer Res.* **2021**, *40* (1), 331. <https://doi.org/10.1186/s13046-021-02141-z>.
  15. Rowinsky, E. K.; Donehower, R. C. Paclitaxel (Taxol). *N. Engl. J. Med.* **1995**, *332* (15), 1004–1014. <https://doi.org/10.1056/NEJM199504133321507>.
  16. Škubník, J.; Pavlíčková, V.; Ruml, T.; Rimpelová, S. Current Perspectives on Taxanes: Focus on Their Bioactivity, Delivery and Combination Therapy. *Plants (Basel, Switzerland)* **2021**, *10* (3). <https://doi.org/10.3390/plants10030569>.
  17. Maloney, S. M.; Hoover, C. A.; Morejon-Lasso, L. V.; Prospero, J. R. Mechanisms of Taxane Resistance. *Cancers (Basel)*. **2020**, *12* (11), 3323. <https://doi.org/10.3390/cancers12113323>.
  18. Rowinsky, MD, E. K. The Development and Clinical Utility of the Taxane Class of Antimicrotubule Chemotherapy Agents. *Annu. Rev. Med.* **1997**, *48* (1), 353–374. <https://doi.org/10.1146/annurev.med.48.1.353>.
  19. Lee, J. J.; Swain, S. M. Peripheral Neuropathy Induced by Microtubule-Stabilizing Agents. *J. Clin. Oncol.* **2006**, *24* (10), 1633–1642. <https://doi.org/10.1200/JCO.2005.04.0543>.
  20. Schiff, P. B.; Horwitz, S. B. Taxol Stabilizes Microtubules in Mouse Fibroblast Cells. *Proc. Natl. Acad. Sci. U. S. A.* **1980**, *77* (3), 1561–1565. <https://doi.org/10.1073/pnas.77.3.1561>.
  21. Weaver, B. A. How Taxol/Paclitaxel Kills Cancer Cells. *Mol. Biol. Cell* **2014**, *25* (18), 2677–2681. <https://doi.org/10.1091/mbc.e14-04-0916>.
  22. Jordan, M. A.; Wilson, L. Microtubules as a Target for Anticancer Drugs. *Nat. Rev. Cancer* **2004**, *4* (4), 253–265. <https://doi.org/10.1038/nrc1317>.
  23. Ren, X.; Zhao, B.; Chang, H.; Xiao, M.; Wu, Y.; Liu, Y. Paclitaxel Suppresses Proliferation and Induces Apoptosis through Regulation of ROS and the AKT/MAPK Signaling Pathway in Canine Mammary Gland Tumor Cells. *Mol. Med. Rep.* **2018**. <https://doi.org/10.3892/mmr.2018.8868>.
  24. Strobel, T.; Swanson, L.; Korsmeyer, S.; Cannistra, S. A. BAX Enhances Paclitaxel-Induced

- Apoptosis through a P53-Independent Pathway. *Proc. Natl. Acad. Sci.* **1996**, *93* (24), 14094–14099. <https://doi.org/10.1073/pnas.93.24.14094>.
25. Yang, M.; Wang, B.; Gao, J.; Zhang, Y.; Xu, W.; Tao, L. Spinosad Induces Programmed Cell Death Involves Mitochondrial Dysfunction and Cytochrome C Release in *Spodoptera Frugiperda* Sf9 Cells. *Chemosphere* **2017**, *169*, 155–161. <https://doi.org/10.1016/j.chemosphere.2016.11.065>.
  26. Suh, D. H.; Kim, M.-K.; Kim, H. S.; Chung, H. H.; Song, Y. S. Mitochondrial Permeability Transition Pore as a Selective Target for Anti-Cancer Therapy. *Front. Oncol.* **2013**, *3*. <https://doi.org/10.3389/fonc.2013.00041>.
  27. Abu Samaan, T. M.; Samec, M.; Liskova, A.; Kubatka, P.; Büsselberg, D. Paclitaxel's Mechanistic and Clinical Effects on Breast Cancer. *Biomolecules* **2019**, *9* (12), 789. <https://doi.org/10.3390/biom9120789>.
  28. Gornstein, E.; Schwarz, T. L. The Paradox of Paclitaxel Neurotoxicity: Mechanisms and Unanswered Questions. *Neuropharmacology* **2014**, *76*, 175–183. <https://doi.org/10.1016/j.neuropharm.2013.08.016>.
  29. Cavaletti, G.; Tredici, G.; Braga, M.; Tazzari, S. Experimental Peripheral Neuropathy Induced in Adult Rats by Repeated Intraperitoneal Administration of Taxol. *Exp. Neurol.* **1995**, *133* (1), 64–72. <https://doi.org/10.1006/exnr.1995.1008>.
  30. Peters, C. M.; Jimenez-Andrade, J. M.; Kuskowski, M. A.; Ghilardi, J. R.; Mantyh, P. W. An Evolving Cellular Pathology Occurs in Dorsal Root Ganglia, Peripheral Nerve and Spinal Cord Following Intravenous Administration of Paclitaxel in the Rat. *Brain Res.* **2007**, *1168*, 46–59. <https://doi.org/10.1016/j.brainres.2007.06.066>.
  31. Shemesh, O. A.; Spira, M. E. Paclitaxel Induces Axonal Microtubules Polar Reconfiguration and Impaired Organelle Transport: Implications for the Pathogenesis of Paclitaxel-Induced Polyneuropathy. *Acta Neuropathol.* **2010**, *119* (2), 235–248. <https://doi.org/10.1007/s00401-009-0586-0>.
  32. Cavaletti, G.; Cavalletti, E.; Montaguti, P.; Oggioni, N.; De Negri, O.; Tredici, G. Effect on the Peripheral Nervous System of the Short-Term Intravenous Administration of Paclitaxel in the Rat. *Neurotoxicology* **1997**, *18* (1), 137–145.
  33. Scripture, C.; Figg, W.; Sparreboom, A. Peripheral Neuropathy Induced by Paclitaxel: Recent Insights and Future Perspectives. *Curr. Neuropharmacol.* **2006**, *4* (2), 165–172. <https://doi.org/10.2174/157015906776359568>.
  34. Gießen-Jung, C.; von Baumgarten, L. Chemotherapie-Induzierte Periphere Neuropathie. *DMW - Dtsch. Medizinische Wochenschrift* **2018**, *113* (13), 970–978. <https://doi.org/10.1055/s-0043-120839>.
  35. Zajączkowska, R.; Kocot-Kępska, M.; Leppert, W.; Wrzosek, A.; Mika, J.; Wordliczek, J. Mechanisms of Chemotherapy-Induced Peripheral Neuropathy. *Int. J. Mol. Sci.* **2019**, *20* (6), 1451. <https://doi.org/10.3390/ijms20061451>.
  36. Windebank, A. J.; Smith, A. G.; Russell, J. W. The Effect of Nerve Growth Factor, Ciliary Neurotrophic Factor, and ACTH Analogs on Cisplatin Neurotoxicity in Vitro. *Neurology* **1994**, *44* (3 Pt 1), 488–494. [https://doi.org/10.1212/wnl.44.3\\_part\\_1.488](https://doi.org/10.1212/wnl.44.3_part_1.488).
  37. Melli, G.; Höke, A. Dorsal Root Ganglia Sensory Neuronal Cultures: A Tool for Drug Discovery for Peripheral Neuropathies. *Expert Opin. Drug Discov.* **2009**, *4* (10), 1035–1045. <https://doi.org/10.1517/17460440903266829>.
  38. Li, Y.; Marri, T.; North, R. Y.; Rhodes, H. R.; Uhelski, M. L.; Tatsui, C. E.; Rhines, L. D.; Rao, G.; Corrales, G.; Abercrombie, T. J.; Johansson, C. A.; Dougherty, P. M. Chemotherapy-Induced Peripheral Neuropathy in a Dish: Dorsal Root Ganglion Cells Treated in Vitro with Paclitaxel



- Show Biochemical and Physiological Responses Parallel to That Seen in Vivo. *Pain* **2021**, *162* (1), 84–96. <https://doi.org/10.1097/j.pain.0000000000002005>.
39. Zhang, H.; Dougherty, P. M. Enhanced Excitability of Primary Sensory Neurons and Altered Gene Expression of Neuronal Ion Channels in Dorsal Root Ganglion in Paclitaxel-Induced Peripheral Neuropathy. *Anesthesiology* **2014**, *120* (6), 1463–1475. <https://doi.org/10.1097/ALN.000000000000176>.
  40. Gill, J. S.; Windebank, A. J. Cisplatin-Induced Apoptosis in Rat Dorsal Root Ganglion Neurons Is Associated with Attempted Entry into the Cell Cycle. *J. Clin. Invest.* **1998**, *101* (12), 2842–2850. <https://doi.org/10.1172/JCI1130>.
  41. Fischer, S. J.; McDonald, E. S.; Gross, L.; Windebank, A. J. Alterations in Cell Cycle Regulation Underlie Cisplatin Induced Apoptosis of Dorsal Root Ganglion Neurons in Vivo. *Neurobiol. Dis.* **2001**, *8* (6), 1027–1035. <https://doi.org/10.1006/nbdi.2001.0426>.
  42. Elfarnawany, A.; Dehghani, F. Palmitoylethanolamide Mitigates Paclitaxel Toxicity in Primary Dorsal Root Ganglion Neurons. *Biomolecules* **2022**, *12* (12), 1873. <https://doi.org/10.3390/biom12121873>.
  43. Martin, S.; Reid, A.; Verkhatsky, A.; Magnaghi, V.; Faroni, A. Gene Expression Changes in Dorsal Root Ganglia Following Peripheral Nerve Injury: Roles in Inflammation, Cell Death and Nociception. *Neural Regen. Res.* **2019**, *14* (6), 939. <https://doi.org/10.4103/1673-5374.250566>.
  44. Park, S. H.; Eber, M. R.; Fonseca, M. M.; Patel, C. M.; Cunnane, K. A.; Ding, H.; Hsu, F.-C.; Peters, C. M.; Ko, M.-C.; Strowd, R. E.; Wilson, J. A.; Hsu, W.; Romero-Sandoval, E. A.; Shiozawa, Y. Usefulness of the Measurement of Neurite Outgrowth of Primary Sensory Neurons to Study Cancer-Related Painful Complications. *Biochem. Pharmacol.* **2021**, *188*, 114520. <https://doi.org/10.1016/j.bcp.2021.114520>.
  45. Delree, P.; Leprince, P.; Schoenen, J.; Moonen, G. Purification and Culture of Adult Rat Dorsal Root Ganglia Neurons. *J. Neurosci. Res.* **1989**, *23* (2), 198–206. <https://doi.org/10.1002/jnr.490230210>.
  46. Grothe, C.; Unsicker, K. Neuron-Enriched Cultures of Adult Rat Dorsal Root Ganglia: Establishment, Characterization, Survival, and Neuropeptide Expression in Response to Trophic Factors. *J. Neurosci. Res.* **1987**, *18* (4), 539–550. <https://doi.org/10.1002/jnr.490180406>.
  47. Li, R.; Sliwkowski, M. X.; Lo, J.; Mather, J. P. Establishment of Schwann Cell Lines from Normal Adult and Embryonic Rat Dorsal Root Ganglia. *J. Neurosci. Methods* **1996**, *67* (1), 57–69. [https://doi.org/10.1016/0165-0270\(96\)00028-3](https://doi.org/10.1016/0165-0270(96)00028-3).
  48. Wrathall, J. R.; Rigamonti, D. D.; Braford, M. R.; Kao, C. C. Non-Neuronal Cell Cultures from Dorsal Root Ganglia of the Adult Cat: Production of Schwann-like Cell Lines. *Brain Res.* **1981**, *229* (1), 163–181. [https://doi.org/10.1016/0006-8993\(81\)90753-8](https://doi.org/10.1016/0006-8993(81)90753-8).
  49. Ji, R.-R.; Berta, T.; Nedergaard, M. Glia and Pain: Is Chronic Pain a Gliopathy? *Pain* **2013**, *154* (Supplement 1), S10–S28. <https://doi.org/10.1016/j.pain.2013.06.022>.
  50. Ji, R.-R.; Chamesian, A.; Zhang, Y.-Q. Pain Regulation by Non-Neuronal Cells and Inflammation. *Science* (80-. ). **2016**, *354* (6312), 572–577. <https://doi.org/10.1126/science.aaf8924>.
  51. Lipton, R. B.; Apfel, S. C.; Dutcher, J. P.; Rosenberg, R.; Kaplan, J.; Berger, A.; Einzig, A. I.; Wiernik, P.; Schaumburg, H. H. Taxol Produces a Predominantly Sensory Neuropathy. *Neurology* **1989**, *39* (3), 368–368. <https://doi.org/10.1212/WNL.39.3.368>.
  52. Apfel, S. C.; Lipton, R. B.; Arezzo, J. C.; Kessler, J. A. Nerve Growth Factor Prevents Toxic Neuropathy in Mice. *Ann. Neurol.* **1991**, *29* (1), 87–90. <https://doi.org/10.1002/ana.410290115>.
  53. Rowinsky, E. K.; Chaudhry, V.; Cornblath, D. R.; Donehower, R. C. Neurotoxicity of Taxol. *J.*

- Natl. Cancer Inst. Monogr.* **1993**, No. 15, 107–115. <https://doi.org/7912516>.
54. Vuorinen, V.; Rytte, M.; Raine, C. S. The Acute Response of Schwann Cells to Taxol after Nerve Crush. *Acta Neuropathol.* **1988**, *76* (1), 17–25. <https://doi.org/10.1007/BF00687676>.
  55. Scuteri, A.; Nicolini, G.; Miloso, M.; Bossi, M.; Cavaletti, G.; Windebank, A. J.; Tredici, G. Paclitaxel Toxicity in Post-Mitotic Dorsal Root Ganglion (DRG) Cells. *Anticancer Res.* **2006**, *26* (2A), 1065–1070. <https://doi.org/16619507>.
  56. Imai, S.; Koyanagi, M.; Azimi, Z.; Nakazato, Y.; Matsumoto, M.; Ogihara, T.; Yonezawa, A.; Omura, T.; Nakagawa, S.; Wakatsuki, S.; Araki, T.; Kaneko, S.; Nakagawa, T.; Matsubara, K. Taxanes and Platinum Derivatives Impair Schwann Cells via Distinct Mechanisms. *Sci. Rep.* **2017**, *7* (1), 5947. <https://doi.org/10.1038/s41598-017-05784-1>.
  57. Klein, I.; Boenert, J.; Lange, F.; Christensen, B.; Wassermann, M. K.; Wiesen, M. H. J.; Olschewski, D. N.; Rabenstein, M.; Müller, C.; Lehmann, H. C.; Fink, G. R.; Schroeter, M.; Rueger, M. A.; Vay, S. U. Glia from the Central and Peripheral Nervous System Are Differentially Affected by Paclitaxel Chemotherapy via Modulating Their Neuroinflammatory and Neuroregenerative Properties. *Front. Pharmacol.* **2022**, *13*. <https://doi.org/10.3389/fphar.2022.1038285>.
  58. Gadgil, S.; Ergün, M.; van den Heuvel, S. A.; van der Wal, S. E.; Scheffer, G. J.; Hooijmans, C. R. A Systematic Summary and Comparison of Animal Models for Chemotherapy Induced (Peripheral) Neuropathy (CIPN). *PLoS One* **2019**, *14* (8), e0221787. <https://doi.org/10.1371/journal.pone.0221787>.
  59. Seretny, M.; Currie, G. L.; Sena, E. S.; Ramnarine, S.; Grant, R.; MacLeod, M. R.; Colvin, L. A.; Fallon, M. Incidence, Prevalence, and Predictors of Chemotherapy-Induced Peripheral Neuropathy: A Systematic Review and Meta-Analysis. *Pain* **2014**, *155* (12), 2461–2470. <https://doi.org/10.1016/j.pain.2014.09.020>.
  60. Mielke, S.; Sparreboom, A.; Mross, K. Peripheral Neuropathy: A Persisting Challenge in Paclitaxel-Based Regimes. *Eur. J. Cancer* **2006**, *42* (1), 24–30. <https://doi.org/10.1016/j.ejca.2005.06.030>.
  61. Pachman, D. R.; Watson, J. C.; Lustberg, M. B.; Wagner-Johnston, N. D.; Chan, A.; Broadfield, L.; Cheung, Y. T.; Steer, C.; Storey, D. J.; Chandwani, K. D.; Paice, J.; Jean-Pierre, P.; Oh, J.; Kamath, J.; Fallon, M.; Strik, H.; Koeppen, S.; Loprinzi, C. L. Management Options for Established Chemotherapy-Induced Peripheral Neuropathy. *Support. Care Cancer* **2014**, *22* (8), 2281–2295. <https://doi.org/10.1007/s00520-014-2289-x>.
  62. Hershman, D. L.; Lacchetti, C.; Dworkin, R. H.; Lavoie Smith, E. M.; Bleeker, J.; Cavaletti, G.; Chauhan, C.; Gavin, P.; Lavino, A.; Lustberg, M. B.; Paice, J.; Schneider, B.; Smith, M. Lou; Smith, T.; Terstriep, S.; Wagner-Johnston, N.; Bak, K.; Loprinzi, C. L. Prevention and Management of Chemotherapy-Induced Peripheral Neuropathy in Survivors of Adult Cancers: American Society of Clinical Oncology Clinical Practice Guideline. *J. Clin. Oncol.* **2014**, *32* (18), 1941–1967. <https://doi.org/10.1200/JCO.2013.54.0914>.
  63. Kalant, H. Medicinal Use of Cannabis: History and Current Status. *Pain Res. Manag.* **2001**, *6* (2), 80–91. <https://doi.org/10.1155/2001/469629>.
  64. Pacher, P.; Kunos, G. Modulating the Endocannabinoid System in Human Health and Disease - Successes and Failures. *FEBS J.* **2013**, *280* (9), 1918–1943. <https://doi.org/10.1111/febs.12260>.
  65. Mendizábal, V. E.; Adler-Graschinsky, E. Cannabinoids as Therapeutic Agents in Cardiovascular Disease: A Tale of Passions and Illusions. *Br. J. Pharmacol.* **2007**, *151* (4), 427–440. <https://doi.org/10.1038/sj.bjp.0707261>.
  66. Eid, B. G. Cannabinoids for Treating Cardiovascular Disorders: Putting Together a Complex Puzzle. *J. Microsc. Ultrastruct.* **2018**, *6* (4), 171–176.

[https://doi.org/10.4103/JMAU.JMAU\\_42\\_18](https://doi.org/10.4103/JMAU.JMAU_42_18).

67. Di Marzo, V. The Endocannabinoid System: Its General Strategy of Action, Tools for Its Pharmacological Manipulation and Potential Therapeutic Exploitation. *Pharmacol. Res.* **2009**, *60* (2), 77–84. <https://doi.org/10.1016/j.phrs.2009.02.010>.
68. Munro, S.; Thomas, K. L.; Abu-Shaar, M. Molecular Characterization of a Peripheral Receptor for Cannabinoids. *Nature* **1993**, *365* (6441), 61–65. <https://doi.org/10.1038/365061a0>.
69. Yang, F.; Zheng, J. Understand Spiciness: Mechanism of TRPV1 Channel Activation by Capsaicin. *Protein Cell* **2017**, *8* (3), 169–177. <https://doi.org/10.1007/s13238-016-0353-7>.
70. Dariš, B.; Tancer Verboten, M.; Knez, Ž.; Ferik, P. Cannabinoids in Cancer Treatment: Therapeutic Potential and Legislation. *Bosn. J. Basic Med. Sci.* **2019**, *19* (1), 14–23. <https://doi.org/10.17305/bjbms.2018.3532>.
71. Beggiato, S.; Tomasini, M. C.; Ferraro, L. Palmitoylethanolamide (PEA) as a Potential Therapeutic Agent in Alzheimer's Disease. *Front. Pharmacol.* **2019**, *10*. <https://doi.org/10.3389/fphar.2019.00821>.
72. Tsuboi, K.; Uyama, T.; Okamoto, Y.; Ueda, N. Endocannabinoids and Related N-Acylethanolamines: Biological Activities and Metabolism. *Inflamm. Regen.* **2018**, *38* (1), 28. <https://doi.org/10.1186/s41232-018-0086-5>.
73. Petrosino, S.; Di Marzo, V. The Pharmacology of Palmitoylethanolamide and First Data on the Therapeutic Efficacy of Some of Its New Formulations. *Br. J. Pharmacol.* **2017**, *174* (11), 1349–1365. <https://doi.org/10.1111/bph.13580>.
74. Hansen, H. S. Palmitoylethanolamide and Other Anandamide Congeners. Proposed Role in the Diseased Brain. *Exp. Neurol.* **2010**, *224* (1), 48–55. <https://doi.org/10.1016/j.expneurol.2010.03.022>.
75. Skaper, S. D.; Facci, L.; Giusti, P. Mast Cells, Glia and Neuroinflammation: Partners in Crime? *Immunology* **2014**, *141* (3), 314–327. <https://doi.org/10.1111/imm.12170>.
76. Brotini, S.; Schievano, C.; Guidi, L. Ultra-Micronized Palmitoylethanolamide: An Efficacious Adjuvant Therapy for Parkinson's Disease. *CNS Neurol. Disord. - Drug Targets* **2017**, *16* (6). <https://doi.org/10.2174/1871527316666170321124949>.
77. D'Orio, B.; Fracassi, A.; Paola Cerù, M.; Moreno, S. Targeting PPARalpha in Alzheimer's Disease. *Curr. Alzheimer Res.* **2018**, *15* (4), 345–354. <https://doi.org/10.2174/1567205014666170505094549>.
78. Scuderi, C.; Bronzuoli, M. R.; Facchinetti, R.; Pace, L.; Ferraro, L.; Broad, K. D.; Serviddio, G.; Bellanti, F.; Palombelli, G.; Carpinelli, G.; Canese, R.; Gaetani, S.; Steardo, L.; Steardo, L.; Cassano, T. Ultramicronized Palmitoylethanolamide Rescues Learning and Memory Impairments in a Triple Transgenic Mouse Model of Alzheimer's Disease by Exerting Anti-Inflammatory and Neuroprotective Effects. *Transl. Psychiatry* **2018**, *8* (1), 32. <https://doi.org/10.1038/s41398-017-0076-4>.
79. Esposito, E.; Cuzzocrea, S. Palmitoylethanolamide in Homeostatic and Traumatic Central Nervous System Injuries. *CNS Neurol. Disord. Drug Targets* **2013**, *12* (1), 55–61. <https://doi.org/10.2174/1871527311312010010>.
80. Rankin, L.; Fowler, C. J. The Basal Pharmacology of Palmitoylethanolamide. *Int. J. Mol. Sci.* **2020**, *21* (21), 7942. <https://doi.org/10.3390/ijms21217942>.
81. Nau, R.; Ribes, S.; Djukic, M.; Eiffert, H. Strategies to Increase the Activity of Microglia as Efficient Protectors of the Brain against Infections. *Front. Cell. Neurosci.* **2014**, *8*. <https://doi.org/10.3389/fncel.2014.00138>.

82. Petrosino, S.; Schiano Moriello, A. Palmitoylethanolamide: A Nutritional Approach to Keep Neuroinflammation within Physiological Boundaries—A Systematic Review. *Int. J. Mol. Sci.* **2020**, *21* (24), 9526. <https://doi.org/10.3390/ijms21249526>.
83. Koch, M.; Kreutz, S.; Böttger, C.; Benz, A.; Maronde, E.; Ghadban, C.; Korf, H.-W.; Dehghani, F. Palmitoylethanolamide Protects Dentate Gyrus Granule Cells via Peroxisome Proliferator-Activated Receptor-Alpha. *Neurotox. Res.* **2011**, *19* (2), 330–340. <https://doi.org/10.1007/s12640-010-9166-2>.
84. Di Cesare Mannelli, L.; D’Agostino, G.; Pacini, A.; Russo, R.; Zanardelli, M.; Ghelardini, C.; Calignano, A. Palmitoylethanolamide Is a Disease-Modifying Agent in Peripheral Neuropathy: Pain Relief and Neuroprotection Share a PPAR-Alpha-Mediated Mechanism. *Mediators Inflamm.* **2013**, *2013*, 1–12. <https://doi.org/10.1155/2013/328797>.
85. Landolfo, E.; Cutuli, D.; Petrosini, L.; Caltagirone, C. Effects of Palmitoylethanolamide on Neurodegenerative Diseases: A Review from Rodents to Humans. *Biomolecules* **2022**, *12* (5), 667. <https://doi.org/10.3390/biom12050667>.
86. Colizzi, M.; Bortoletto, R.; Colli, C.; Bonomo, E.; Pagliaro, D.; Maso, E.; Di Gennaro, G.; Balestrieri, M. Therapeutic Effect of Palmitoylethanolamide in Cognitive Decline: A Systematic Review and Preliminary Meta-Analysis of Preclinical and Clinical Evidence. *Front. Psychiatry* **2022**, *13*. <https://doi.org/10.3389/fpsy.2022.1038122>.
87. Scuderi, C.; Valenza, M.; Stecca, C.; Esposito, G.; Carratù, M. R.; Steardo, L. Palmitoylethanolamide Exerts Neuroprotective Effects in Mixed Neuroglial Cultures and Organotypic Hippocampal Slices via Peroxisome Proliferator-Activated Receptor- $\alpha$ . *J. Neuroinflammation* **2012**, *9* (1), 49. <https://doi.org/10.1186/1742-2094-9-49>.
88. Guo, L.; Hamre, J.; Eldridge, S.; Behrsing, H. P.; Cutuli, F. M.; Mussio, J.; Davis, M. Multiparametric Image Analysis of Rat Dorsal Root Ganglion Cultures to Evaluate Peripheral Neuropathy-Inducing Chemotherapeutics. *Toxicol. Sci.* **2017**, kfw254. <https://doi.org/10.1093/toxsci/kfw254>.
89. Jamieson, S. M. F.; Liu, J.; Hsu, T.; Baguley, B. C.; McKeage, M. J. Paclitaxel Induces Nucleolar Enlargement in Dorsal Root Ganglion Neurons in Vivo Reducing Oxaliplatin Toxicity. *Br. J. Cancer* **2003**, *88* (12), 1942–1947. <https://doi.org/10.1038/sj.bjc.6601012>.
90. Cavaletti, G.; Cavalletti, E.; Oggioni, N.; Sottani, C.; Minoia, C.; D’Incalci, M.; Zucchetti, M.; Marmiroli, P.; Tredici, G. Distribution of Paclitaxel within the Nervous System of the Rat after Repeated Intravenous Administration. *Neurotoxicology* **2000**, *21* (3), 389–393.
91. Yang, I. H.; Siddique, R.; Hosmane, S.; Thakor, N.; Höke, A. Compartmentalized Microfluidic Culture Platform to Study Mechanism of Paclitaxel-Induced Axonal Degeneration. *Exp. Neurol.* **2009**, *218* (1), 124–128. <https://doi.org/10.1016/j.expneurol.2009.04.017>.
92. Barbuti, A. M.; Chen, Z.-S. Paclitaxel Through the Ages of Anticancer Therapy: Exploring Its Role in Chemoresistance and Radiation Therapy. *Cancers (Basel)*. **2015**, *7* (4), 2360–2371. <https://doi.org/10.3390/cancers7040897>.
93. Trielli, M. O.; Andreassen, P. R.; Lacroix, F. B.; Margolis, R. L. Differential Taxol-Dependent Arrest of Transformed and Nontransformed Cells in the G1 Phase of the Cell Cycle, and Specific-Related Mortality of Transformed Cells. *J. Cell Biol.* **1996**, *135* (3), 689–700. <https://doi.org/10.1083/jcb.135.3.689>.
94. Wang, T.-H.; Wang, H.-S.; Soong, Y.-K. Paclitaxel-Induced Cell Death. *Cancer* **2000**, *88* (11), 2619–2628. [https://doi.org/10.1002/1097-0142\(20000601\)88:11<2619::AID-CNCR26>3.0.CO;2-J](https://doi.org/10.1002/1097-0142(20000601)88:11<2619::AID-CNCR26>3.0.CO;2-J).
95. Hammad, A.; Mohamed M, S. A.; Khalifa, M.; El-Daly, M. Mechanisms of Paclitaxel-Induced Peripheral Neuropathy. *J. Adv. Biomed. Pharm. Sci.* **2023**, *6* (1), 25–35.

<https://doi.org/10.21608/jabps.2022.170238.1172>.

96. Klein, I.; Lehmann, H. Pathomechanisms of Paclitaxel-Induced Peripheral Neuropathy. *Toxics* **2021**, *9* (10), 229. <https://doi.org/10.3390/toxics9100229>.
97. Morsanuto, V.; Galla, R.; Molinari, C.; Uberti, F. A New Palmitoylethanolamide Form Combined with Antioxidant Molecules to Improve Its Effectiveness on Neuronal Aging. *Brain Sci.* **2020**, *10* (7), 457. <https://doi.org/10.3390/brainsci10070457>.
98. Di Cesare Mannelli, L.; Pacini, A.; Corti, F.; Boccella, S.; Luongo, L.; Esposito, E.; Cuzzocrea, S.; Maione, S.; Calignano, A.; Ghelardini, C. Antineuropathic Profile of N-Palmitoylethanolamine in a Rat Model of Oxaliplatin-Induced Neurotoxicity. *PLoS One* **2015**, *10* (6), e0128080. <https://doi.org/10.1371/journal.pone.0128080>.
99. Guzmán, M. Effects on Cell Viability. In *Cannabinoids*; Springer-Verlag: Berlin/Heidelberg, 2005; pp 627–642. [https://doi.org/10.1007/3-540-26573-2\\_21](https://doi.org/10.1007/3-540-26573-2_21).
100. Gugliandolo, E.; D'amico, R.; Cordaro, M.; Fusco, R.; Siracusa, R.; Crupi, R.; Impellizzeri, D.; Cuzzocrea, S.; Di Paola, R. Effect of PEA-OXA on Neuropathic Pain and Functional Recovery after Sciatic Nerve Crush. *J. Neuroinflammation* **2018**, *15* (1), 264. <https://doi.org/10.1186/s12974-018-1303-5>.
101. Cole, R. Live-Cell Imaging. *Cell Adh. Migr.* **2014**, *8* (5), 452–459. <https://doi.org/10.4161/cam.28348>.
102. Gómez del pulgar, T.; Velasco, G.; Sánchez, C.; Haro, A.; Guzmán, M. De Novo-Synthesized Ceramide Is Involved in Cannabinoid-Induced Apoptosis. *Biochem. J.* **2002**, *363* (1), 183. <https://doi.org/10.1042/0264-6021:3630183>.
103. Molina-Holgado, E.; Vela, J. M.; Arévalo-Martín, A.; Almazán, G.; Molina-Holgado, F.; Borrell, J.; Guaza, C. Cannabinoids Promote Oligodendrocyte Progenitor Survival: Involvement of Cannabinoid Receptors and Phosphatidylinositol-3 Kinase/Akt Signaling. *J. Neurosci.* **2002**, *22* (22), 9742–9753. <https://doi.org/10.1523/JNEUROSCI.22-22-09742.2002>.
104. Komlodi-Pasztor, E.; Sackett, D.; Wilkerson, J.; Fojo, T. Mitosis Is Not a Key Target of Microtubule Agents in Patient Tumors. *Nat. Rev. Clin. Oncol.* **2011**, *8* (4), 244–250. <https://doi.org/10.1038/nrclinonc.2010.228>.
105. Parker, A. L.; Kavallaris, M.; McCarroll, J. A. Microtubules and Their Role in Cellular Stress in Cancer. *Front. Oncol.* **2014**, *4*. <https://doi.org/10.3389/fonc.2014.00153>.
106. Risinger, A. L.; Dybdal-Hargreaves, N. F.; Mooberry, S. L. Breast Cancer Cell Lines Exhibit Differential Sensitivities to Microtubule-Targeting Drugs Independent of Doubling Time. *Anticancer Res.* **2015**, *35* (11), 5845–5850.
107. Zasadil, L. M.; Andersen, K. A.; Yeum, D.; Rocque, G. B.; Wilke, L. G.; Tevaarwerk, A. J.; Raines, R. T.; Burkard, M. E.; Weaver, B. A. Cytotoxicity of Paclitaxel in Breast Cancer Is Due to Chromosome Missegregation on Multipolar Spindles. *Sci. Transl. Med.* **2014**, *6* (229). <https://doi.org/10.1126/scitranslmed.3007965>.
108. Motiwala, M. N.; Rangari, V. D. Combined Effect of Paclitaxel and Piperine on a MCF-7 Breast Cancer Cell Line in Vitro: Evidence of a Synergistic Interaction. *Synergy* **2015**, *2* (1), 1–6. <https://doi.org/10.1016/j.synres.2015.04.001>.
109. Němcová-Fürstová, V.; Kopperová, D.; Balušíková, K.; Ehrlichová, M.; Brynychová, V.; Václavíková, R.; Daniel, P.; Souček, P.; Kovář, J. Characterization of Acquired Paclitaxel Resistance of Breast Cancer Cells and Involvement of ABC Transporters. *Toxicol. Appl. Pharmacol.* **2016**, *310*, 215–228. <https://doi.org/10.1016/j.taap.2016.09.020>.
110. Aborehab, N. M.; Elnagar, M. R.; Waly, N. E. Gallic Acid Potentiates the Apoptotic Effect of Paclitaxel and Carboplatin via Overexpression of Bax and P53 on the MCF-7 Human Breast

- Cancer Cell Line. *J. Biochem. Mol. Toxicol.* **2021**, *35* (2). <https://doi.org/10.1002/jbt.22638>.
111. De Petrocellis, L.; Bisogno, T.; Ligresti, A.; Bifulco, M.; Melck, D.; Di Marzo, V. Effect on Cancer Cell Proliferation of Palmitoylethanolamide, a Fatty Acid Amide Interacting with Both the Cannabinoid and Vanilloid Signalling Systems. *Fundam. Clin. Pharmacol.* **2002**, *16* (4), 297–302. <https://doi.org/10.1046/j.1472-8206.2002.00094.x>.
  112. Sarnelli, G.; D'Alessandro, A.; Iuvone, T.; Capoccia, E.; Gigli, S.; Pesce, M.; Seguella, L.; Nobile, N.; Aprea, G.; Maione, F.; de Palma, G. D.; Cuomo, R.; Steardo, L.; Esposito, G. Palmitoylethanolamide Modulates Inflammation-Associated Vascular Endothelial Growth Factor (VEGF) Signaling via the Akt/MTOR Pathway in a Selective Peroxisome Proliferator-Activated Receptor Alpha (PPAR- $\alpha$ )-Dependent Manner. *PLoS One* **2016**, *11* (5), e0156198. <https://doi.org/10.1371/journal.pone.0156198>.
  113. Huang, S. M.; Bisogno, T.; Trevisani, M.; Al-Hayani, A.; De Petrocellis, L.; Fezza, F.; Tognetto, M.; Petros, T. J.; Krey, J. F.; Chu, C. J.; Miller, J. D.; Davies, S. N.; Geppetti, P.; Walker, J. M.; Di Marzo, V. An Endogenous Capsaicin-like Substance with High Potency at Recombinant and Native Vanilloid VR1 Receptors. *Proc. Natl. Acad. Sci.* **2002**, *99* (12), 8400–8405. <https://doi.org/10.1073/pnas.122196999>.
  114. Bisogno, T.; Hanuš, L.; De Petrocellis, L.; Tchilibon, S.; Ponde, D. E.; Brandi, I.; Moriello, A. S.; Davis, J. B.; Mechoulam, R.; Di Marzo, V. Molecular Targets for Cannabidiol and Its Synthetic Analogues: Effect on Vanilloid VR1 Receptors and on the Cellular Uptake and Enzymatic Hydrolysis of Anandamide. *Br. J. Pharmacol.* **2001**, *134* (4), 845–852. <https://doi.org/10.1038/sj.bjp.0704327>.
  115. Tan, K.-T.; Li, S.; Li, Y. R.; Cheng, S.-L.; Lin, S.-H.; Tung, Y.-T. Synergistic Anticancer Effect of a Combination of Paclitaxel and 5-Demethylnobiletin Against Lung Cancer Cell Line In Vitro and In Vivo. *Appl. Biochem. Biotechnol.* **2019**, *187* (4), 1328–1343. <https://doi.org/10.1007/s12010-018-2869-1>.
  116. Miyato, H.; Kitayama, J.; Yamashita, H.; Souma, D.; Asakage, M.; Yamada, J.; Nagawa, H. Pharmacological Synergism Between Cannabinoids and Paclitaxel in Gastric Cancer Cell Lines. *J. Surg. Res.* **2009**, *155* (1), 40–47. <https://doi.org/10.1016/j.jss.2008.06.045>.

## 4. Theses

- 1) Chemotherapy-induced peripheral neuropathy (CIPN) is a type of nerve damage caused by anticancer agents such as paclitaxel, and this side effect disrupts and decreases the quality of patients' life.
- 2) The endocannabinoid-like substance, palmitoylethanolamide (PEA) or /and paclitaxel at various concentrations affect primary dorsal root ganglion (DRG) neuronal and non-neuronal cells in a time-dependent manner.
- 3) Paclitaxel showed toxic effects on neuronal cells including a reduction in neuronal viability, suppression in neurite length, and an enlargement in neuronal cell bodies at all investigated time windows. In addition, primary DRG non-neuronal cells responded with a decrease in number of viable cells, an increase in cell death, a decrease of cell proliferation rate, as well as morphological changes.
- 4) PEA showed neuroprotective effects by partially mitigating the toxic effects of paclitaxel by increasing cell viability, inducing DRG neuron neurite outgrowth, and decreasing swelling of neuronal soma.
- 5) PEA exerted protective effects against paclitaxel adverse effects on DRG non-neuronal cells including increasing cell viability, improving cell survival as well as accelerating the rate of cell proliferation.
- 6) PEA did not have effects on the efficacy of paclitaxel on human breast cancer cells MCF-7, MDA-MB-231, and SK-BR-3, but it showed synergistic anti-cancer effects with paclitaxel by increasing the drop in viability.
- 7) PEA might be a promising therapeutic substance for cancer patients suffering from CIPN.

# Publications

## List of publications

1. Elfarnawany, A., & Dehghani, F. (2022). Palmitoylethanolamide Mitigates Paclitaxel Toxicity in Primary Dorsal Root Ganglion Neurons. *Biomolecules*, *12*(12), 1873.
2. Elfarnawany, A., & Dehghani, F. (2023). Time-and Concentration-Dependent Adverse Effects of Paclitaxel on Non-Neuronal Cells in Rat Primary Dorsal Root Ganglia. *Toxics*, *11*(7), 581.



# Publication 1

---


The following article [Elfarnawany, A.; Dehghani, F, *Biomolecules*, **2022**] has been published under the terms and conditions of the Creative Commons Attribution (CC BY) license (<https://creativecommons.org/licenses/by/4.0/>) that permits unrestricted use, distribution, and reproduction in any medium under specification of the authors (see the article) and the source (*Biomolecules* **2022**, 12, 1873. <https://doi.org/10.3390/biom12121873>). The link back to the article on the publisher's website is (<https://www.mdpi.com/journal/biomolecules>).

## **Contribution as an author:**

I have contributed to the conception and design of the work, formal data analysis, the results interpretation, investigation, data curation, writing original draft preparation, data visualization, data review, and editing.

## Article

# Palmitoylethanolamide Mitigates Paclitaxel Toxicity in Primary Dorsal Root Ganglion Neurons

Amira Elfarnawany<sup>1,2</sup> and Faramarz Dehghani<sup>1,\*</sup> 

<sup>1</sup> Department of Anatomy and Cell Biology, Medical Faculty, Martin Luther University Halle-Wittenberg, Grosse Steinstrasse 52, 06108 Halle (Saale), Germany

<sup>2</sup> Zoology Department, Faculty of Science, Tanta University, Tanta 31527, Egypt

\* Correspondence: faramarz.dehghani@medizin.uni-halle.de

**Abstract:** Chemotherapy-induced peripheral neuropathy (CIPN) is a common side effect of several chemotherapeutic agents, such as Paclitaxel. The main symptoms of CIPN are pain and numbness in the hands and feet. Paclitaxel is believed to accumulate in the dorsal root ganglia and free nerve endings. Novel therapeutic agents might help to mitigate or prevent Paclitaxel toxicity on dorsal root ganglion (DRG) neurons. Thus, we used primary DRG neurons as a model to investigate the potential neuroprotective effects of the endocannabinoid-like substance, palmitoylethanolamide (PEA). DRG neurons were isolated from cervical to sacral segments of spinal nerves of Wistar rats (6–8 weeks old). After isolation and purification of neuronal cell populations, different concentrations of Paclitaxel (0.01–10  $\mu$ M) or PEA (0.1–10  $\mu$ M) or their combination were tested on cell viability by MTT assay at 24 h, 48, and 72 h post-treatment. Furthermore, morphometric analyses of neurite length and soma size for DRG neurons were performed. Adverse Paclitaxel effects on cell viability were apparent at 72 h post-treatment whereas Paclitaxel significantly reduced the neurite length in a concentration-dependent manner nearly at all investigated time points. However, Paclitaxel significantly increased the size of neuronal cell bodies at all time windows. These phenotypic effects were significantly reduced in neurons additionally treated with PEA, indicating the neuroprotective effect of PEA. PEA alone led to a significant increase in neuron viability regardless of PEA concentrations, apparent improvements in neurite outgrowth as well as a significant decrease in soma size of neurons at different investigated time points. Taken together, PEA showed promising protective effects against Paclitaxel-related toxicity on DRG neurons.

**Keywords:** peripheral neuropathic pain; neurotoxicity; dorsal root ganglion neurons; palmitoylethanolamide; paclitaxel; neurite length; soma size; MTT assay



**Citation:** Elfarnawany, A.; Dehghani, F. Palmitoylethanolamide Mitigates Paclitaxel Toxicity in Primary Dorsal Root Ganglion Neurons. *Biomolecules* **2022**, *12*, 1873. <https://doi.org/10.3390/biom12121873>

Academic Editors: Rosalia Crupi and Salvatore Cuzzocrea

Received: 22 November 2022

Accepted: 10 December 2022

Published: 14 December 2022

**Publisher's Note:** MDPI stays neutral with regard to jurisdictional claims in published maps and institutional affiliations.



**Copyright:** © 2022 by the authors. Licensee MDPI, Basel, Switzerland. This article is an open access article distributed under the terms and conditions of the Creative Commons Attribution (CC BY) license (<https://creativecommons.org/licenses/by/4.0/>).

## 1. Introduction

Chemotherapy-induced neuropathic pain (CINP) is a dose-limiting side effect of some anticancer drugs, such as bortezomib, cisplatin, oxaliplatin, paclitaxel, thalidomide, and vincristine [1]. The incidence of CINP in patients ranges from 12.1% to 96.2%, depending on the chemotherapeutic agent used and the type of cancer treated [2]. Taxanes are a class of chemotherapy drugs that promote tubulin polymerization into highly stable intracellular microtubules and cause cell death by intermixing with microtubules via normal cell division [3,4]. Paclitaxel is a Taxane derivative that has been used successfully as a first-line treatment for a variety of solid tumors, including ovarian cancer, breast cancer, cervical cancer, lung carcinomas, and other solid tumors [5–7].

Unfortunately, peripheral neuropathic pain (PNP) is a common side effect of Paclitaxel treatment affecting around 70.8% (95% CI 43.5–98.1) of patients [8]. The incidence ranges from 30 to 50% after a single dose and rises to more than 50% after a second dose [9]. Hyperalgesia, allodynia, and sporadic burning, shooting, numbness, spasm, and prickling sensations are some of CINP signs, and these can drastically lower the patient's quality

of life [10,11]. Chemotherapy-induced peripheral neuropathy (CIPN) is predominately a sensory axonopathy and neuronopathy, and the sensory neurons residing in dorsal root ganglions (DRGs) are the primary targets. Therefore, DRG explants have been shown to represent a good, simple, and well-accepted model for studying peripheral neuropathy induced by antineoplastic agents [12]. The ability of DRG explants to outgrow neurites in vitro when exposed to nerve growth factor (NGF), as well as the interference with neurite elongation by toxic substances, is the basis for their use in drug neurotoxicity assessment [12–14].

The neurotoxic effect of Paclitaxel on neurite length of DRG was shown to be dose- and time-dependent [15,16], and DRG dissociated post-mitotic neurons were observed to die by necrosis [15]. Paclitaxel also caused the enlargement of neuronal cell bodies, and suppression of DRGs neuritis [17]. Paclitaxel has shown to demonstrate concentration- and time-dependent effects on vesicular trafficking and membrane localization of Nav1.7 in sensory axons of DRGs, providing a possible mechanistic explanation for increased excitability of primary afferents and pain [18]. Paclitaxel was reported to alter intracellular trafficking in both *Drosophila* and mouse models of CIPN by inducing recycling defects in mouse DRG neurons in vitro [19]. Currently, tricyclic antidepressants and analgesic drugs such as amitriptyline, morphine, gabapentin, and duloxetine display limited efficacy for preventing and alleviating paclitaxel-induced peripheral neuropathic pain and/or suffering of patients from serious side effects [20–23]. As a result, finding novel therapeutic agents that can mitigate or prevent Paclitaxel neurotoxicity on DRG neurons is very crucial.

The endocannabinoid system (ECS) is an important biological system that regulates and balances a wide range of physiological functions in the body, making it a target for many drugs and therapies [24]. Modulating the ECS activity showed promising therapeutic effects in a wide range of diseases and pathological conditions, including neurodegenerative, cardiovascular, and inflammatory disorders, obesity/metabolic syndrome, cachexia, chemotherapy-induced nausea and vomiting, tissue injury, and pain [25]. Palmitoylethanolamide (PEA), an endogenous fatty acid amide analogue of the endocannabinoid anandamide, has an important role in tissue protective mechanisms [26,27]. PEA was discovered nearly 5 decades ago in lipid extracts of various natural products, and its anti-inflammatory and antinociceptive properties were later described [28].

There is evidence for PEA synthesis during inflammation and tissue damage. PEA has a variety of beneficial effects, including the relief of inflammation and pruritus, and is effective in the control of neurogenic and neuropathic pain [29]. The hypothesized theories for PEA's mode of action include modulating endocannabinoid signaling and indirectly activating cannabinoid receptors via “entourage” effects [30–33].

PEA acts primarily through the direct activation of the nuclear receptor PPAR- $\alpha$  [34]. After the activation of PPAR- $\alpha$  receptor, a chain of events leads to suppression of pain and inflammatory signals, including the inhibition of the release of pro-inflammatory cytokines such as IL-1 $\beta$  and IL-6 [35]. Previous studies showed a PEA-mediated protection of dentate gyrus granule cells during secondary neuronal damage, which was mediated by PPAR- $\alpha$  activation and influenced by reduction in inflammatory processes [36]. In a chronic constriction injury model of neuropathic pain, repeated PEA treatment (30 mg/kg) not only decreased edema and macrophage infiltrates, but also declined the decrease in axon diameter and myelin thickness [37]. However, research on studying the protective role of PEA against the toxicity of Paclitaxel on DRG neurons is still lacking.

In the present study, the effects of different Paclitaxel and PEA concentrations were investigated, either individually or in combination, on the viability, morphology, and neurite length of primary DRG neurons at various time points. We hypothesized that PEA might reduce the neurotoxicity induced by Paclitaxel on DRG neurons in a concentration- or/and time-dependent manner.

## 2. Materials and Methods

### 2.1. Ethics Statement

All animal experiments were carried out in accordance with the policy on ethics and the policy on the use of animals in neuroscience research, as specified in directive 2010/63/EU of the European Parliament and of the Council of the European Union on the protection of animals used for scientific purposes and were approved by local authorities for laboratory animal care and use (State of Saxony-Anhalt, Germany, permission number: I11M27).

### 2.2. Materials

Experiments were conducted with Palmitoylethanolamide (PEA, Tocris Bioscience, cat No. 0879-10 mg, Bristol, UK), Paclitaxel (Taxol equivalent, Invitrogen, cat No. P3456-5 mg, Schwerte, Germany), Nerve Growth Factor-2.5S from the murine submaxillary gland (NGF, Sigma Aldrich, Merck, cat No. N6009-4X 25 µg, St. Louis, MO, USA) and glial cell-derived neurotrophic factor (GDNF, Sigma-Aldrich, cat No. SRP3309-10 µg, St. Louis, MO, USA), Uridine (Uridin, Sigma-Aldrich, U3003-5 g, Darmstadt, Germany), and 5-Fluoro-2-deoxyuridine (FudR, Sigma-Aldrich, cat No. F0503-100 mg, Darmstadt, Germany). PEA and Paclitaxel were dissolved in DMSO to obtain stock solutions of 10 mM PEA and 1 mM Paclitaxel and stored at  $-20\text{ }^{\circ}\text{C}$ , while NGF and GDNF dissolved in 0.1 % Bovine Serum Albumin (BSA, Sigma-Aldrich, cat No. A7906-10 g, St. Louis, MO, USA). A total of 20 mM uridine/5-fluorodeoxyuridine (UFdU) stock solution was prepared by mixing 48.8 mg uridine and 49.2 mg 5-fluorodeoxyuridine in 10 mL distilled water, and 100 µL aliquots were prepared and frozen at  $-20\text{ }^{\circ}\text{C}$ . Notably, controls contained the similar highest concentration of DMSO (0.1%) to exclude any effects on investigated parameters.

### 2.3. Isolation and Preparation of DRG Neurons

DRG tissues isolated from 6–8 weeks of age Wister rats. In brief, rats were deeply anesthetized with isoflurane (Florene, 100% (V/V), 250 mL, Abcam, cat No. B506, Carros, France) by inhalation and sacrificed by decapitation with a commercial guillotine. Under aseptic conditions, the vertebral column was isolated and carefully cleared from all surrounding muscle, fat, and other soft tissue. The spinal cord was then exposed and scooped out. Following the dorsal roots. DRGs were localized, removed, collected from intervertebral foramina at both sides, and placed in a 3 mL sterile dish containing Hanks balanced salt solutions without  $\text{Mg}^{2+}/\text{Ca}^{2+}$  (HBSS, Invitrogen, REF. 24020-091, Schwerte, Germany). Dorsal root neuronal culture was prepared according to a previously published protocol [38] with some modifications. Briefly, isolated DRGs were enzymatically digested in the first enzymatic solution, which contained 60 U/mL papain solution (Sigma-Aldrich, cat No. P4762-100 mg, St. Louis, MO, USA), 3 µL of 80 mg/mL saturated sodium hydrogen carbonate solution ( $\text{NaHCO}_3$ , Merck, cat No. k22399729, Darmstadt, Germany), and 0.6 mg/mL L-Cysteine (L-Cys, Sigma-Aldrich, Cat No. C7352-25 g, St. Louis, MO, USA) dissolved in 1.5 mL of HBSS without  $\text{Mg}^{2+}/\text{Ca}^{2+}$ . Afterwards, DRGs were incubated in a papain solution for 15 min in a  $37\text{ }^{\circ}\text{C}$  water bath, then incubated in a second solution which consisted of 4 mg/mL collagenase type II solution (CLS2, Sigma-Aldrich, Cat No. C6885-1 gm, St. Louis, MO, USA) and 4.6 mg/mL dispase type II (Dispase II, Sigma-Aldrich, Cat No. D4693-1 gm, St. Louis, MO, USA) solution in 3 mL HBSS without  $\text{Mg}^{2+}/\text{Ca}^{2+}$ . The DRGs were mixed gently in collagenase solution and incubated again for 15 min in a water bath at  $37\text{ }^{\circ}\text{C}$ .

The resulting cell suspension was centrifuged at  $200\times g$  for 1 min. The collagenase solution was carefully aspirated, and the DRGs were washed with 2ml of titration media consisting of high glucose Dulbecco's Modified Eagle Medium (DMEM, Invitrogen, Ref. 41965-039, Schwerte, Germany) containing 10% heat-inactivated Fetal Bovine Serum (FBS, Invitrogen, REF. 10270-106, Schwerte, Germany). The DRGs were triturated 10–15 times by using p1000 pipette tips until the cell suspension became cloudy. Bovine serum albumin (BSA) was used for purification (15% (W/V) BSA solution) to obtain nearly pure neurons without myelin debris. After trituration, single-cell suspensions from DRGs were

centrifuged through 15% (W/V) BSA solution in DMEM, 3 mL of 15% BSA solution: 1 mL of cell suspension in a 15 mL conical tube at 300 g for 8 min at room temperature (RT) to separate sensory neurons in the pellet from non-neuronal cells and debris [39]. The BSA solution was removed and the pellet containing neurons was re-suspended in 1 mL of culture medium consisting of 445 mL of F12 medium (1X, Invitrogen, REF.11765-054, Schwerte, Germany), 50 mL of FBS and 5 mL of 0.1 mg/mL streptomycin/penicillin (Sigma Aldrich, cat No. P4333/100 mL, Darmstadt, Germany). The cell suspension was filtered by a 40  $\mu$ m cell strainer (SARSTEDT, cat No. D-51588, Schwerte, Germany) to obtain single-cell suspensions and remove undigested tissue debris.

#### 2.4. Seeding and Growth of DRG Neurons

Coverslips 12 mm round were pre-coated with 2 mg/mL Poly-D-lysine (PDL, Sigma Aldrich, cat No. P6407, St. Louis, MO, USA) and 0.2 mg/mL laminin (Sigma Aldrich, cat No. L2020-1 mg, St. Louis, MO, USA) for at least 1 h or overnight in 4 °C, then washed one time with distilled H<sub>2</sub>O directly before seeding the cells in culture medium. DRG neuronal cells (5000 cells in 50  $\mu$ L culture medium) were then pre-seeded onto the center of the coated coverslips for 2 h in an incubator with 37 °C and 5% CO<sub>2</sub>. Then, 1 mL of warm culture medium adjusted at pH 7.4 containing 50 ng/mL NGF and 20 ng/mL GDNF (which is essential for growing neuritis of neurons) and 20  $\mu$ M UFDU (for inhibiting the growth of any remains of supporting cells in culture) was gently added to the wells, and the cells were maintained again at 37 °C with 5% CO<sub>2</sub>. The growth and morphology of neurons were monitored after 2, 24, 48, and 72 h to detect the suitable time of treatment (Figure 1a).

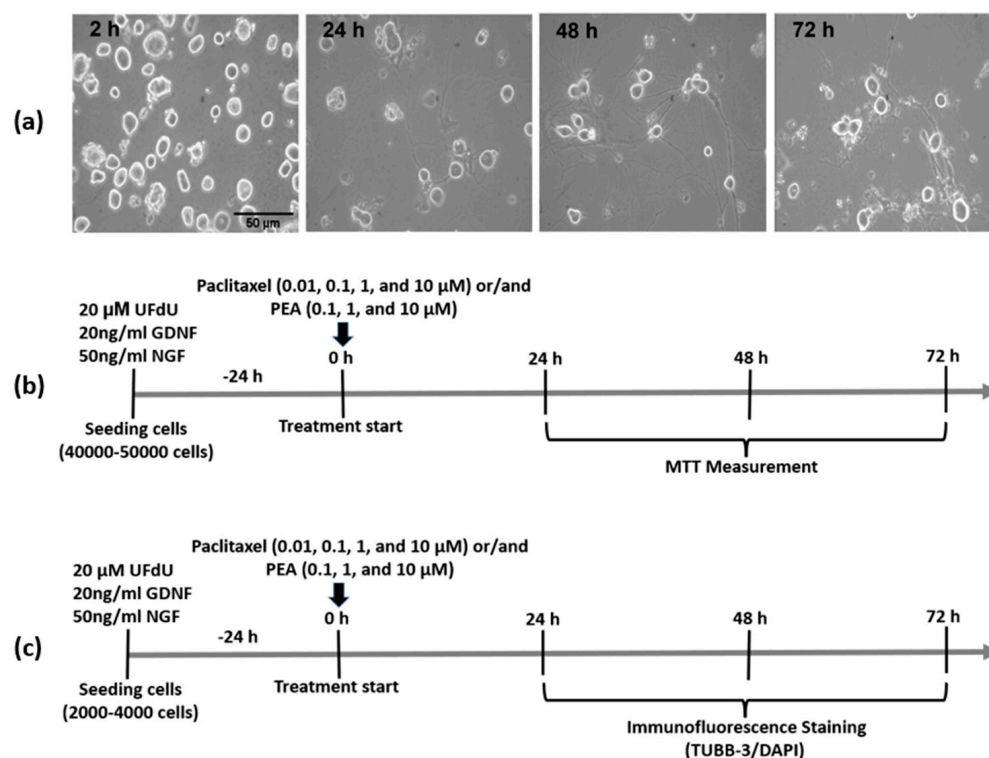


**Figure 1.** Morphological features and treatment protocols of DRG neurons. (a) Representative images show the morphology and growth of DRG neurons at different time points after BSA purification. Scale bars = 50  $\mu$ m. (b,c) treatment protocols for studying the effects of Paclitaxel or /and palmitoylethanolamide (PEA) on DRG neurons viability and morphology (Neurite length measurement) respectively, at 24, 48, and 72-h post-treatment.

#### 2.5. Cell Viability (MTT Assay)

DRG neurons were treated 24 h after seeding. Cells were treated with different concentrations of Paclitaxel (0.01, 0.1, 1, 10  $\mu$ M) and PEA (0.1, 1, 10  $\mu$ M), either individually

or simultaneously combined to study the effects on cell viability. Paclitaxel concentrations were selected based on the literature [15–19,40,41] as well as PEA [42–44]. DRG neurons ( $4\text{--}5 \times 10^4$  cells/well) in 96 well plates were treated with different concentrations of Paclitaxel and PEA alone or in combination for 24, 48, and 72 h. (Figure 1b). Then, cell viability (%) was measured at the different time points using MTT assay. Four hours before termination of experiments at different time points, 3-(4,5-dimethylthiazol-2-yl)-2,5-diphenyltetrazolium bromide solution (MTT, Invitrogen, cat. No M6494, 5 mg/mL, Eugene, OR, USA) was added. Cells were further incubated for 4 h at 37 °C and 5% CO<sub>2</sub>. After removing MTT solution, formazan crystals dissolved in 100 µL of dimethyl sulfoxide (DMSO, Sigma-Aldrich, cat No. D4540-500 mL, Lyon, France) were added and, after another 20 min absorbance values, were measured at wavelengths (540 nm and 720 nm) by a microplate reader (SynergyTMMx, BioTek Instruments, Winooski, VT, USA). DRG neurons cultured in normal media free of Paclitaxel or/and PEA were used as control groups. Controls contained the similar highest concentration of DMSO (0.1%) to exclude any solvent effects on cell viability. All experiments were performed three times independently with 2–3 technical replica for each treatment.

### 2.6. Immunofluorescence Staining and Microscopy

To investigate the effects of various treatments on the morphology of DRG neurons, cells ( $2\text{--}4 \times 10^3$  cells/well) were seeded on 12 mm sterile coverslips in a 24-well plate (Greiner Bio-One, Cat No. 662160, Frickenhausen, Germany), cultured for 24 h until most neurites outgrew, and then treated with different concentrations of Paclitaxel or PEA, either alone or in combination (Figure 1c). At the end of each time point, the cells were fixed with 4% paraformaldehyde (PFA, AppliChem, cat No.141451.1211, Darmstadt, Germany) for 15 min at RT and immediately subjected to immunofluorescence or stored in  $1 \times$  PBS at 4 °C until further use. For immunofluorescence staining, fixed cells were washed 3 times with 0.02 M PBS for 10 min before unspecific bindings were blocked by incubating cells in normal goat serum (NGS, Sigma Aldrich, cat No. G9023-10 mL, Taufkirchen, Germany, 1:20) in 0.02 M PBS/0.3% (*v/v*) Triton) for 30 min. Afterward, cells were incubated with neuronal marker mouse anti-β-III tubulin antibody (TUBB3, Biolegend, San Diego, cat No: 801201, CA, USA, 1:1000) overnight for labelling the cytoskeleton of neurons. Coverslips were thereafter washed thrice for 10 min in PBS, incubated with the secondary antibody goat anti-mouse Alexa Fluor® 488 conjugated (Life Technologies, cat No. 2066710, Darmstadt, Germany, 1:200) for 1 h, washed again 3 times with PBS, and stained with DAPI (4',6-Diamin-2-phenylindol, Sigma-Aldrich, Munich, Germany, cat No. D9542) for visualization of nuclei. The stained cells were washed in distilled water and covered with DAKO fluorescence mounting medium (DAKO, Agilent Technologies, Inc., Santa Clara, CA 95051, USA). The DRG neurons photomicrographs were captured by using a Leica DMi8 (Wetzlar, Germany) microscope, and five images were randomly taken from each coverslip. The experiment was performed 3 times independently.

### 2.7. Image Analysis and Determination of Neurite Lengths and Soma Sizes

Measurement of neurite length as a marker for investigating the neurotoxicity of DRG neurons was assessed by using Neurite Tracer, a plugin for ImageJ software version v1.52 used for automated neurite tracing as previously described [45] with some adjustments (Figure S1). Briefly, a sample image pair from cultures of DRG neurons fluorescently labelled with TUBB3 as neuronal marker and DAPI as nuclear marker were opened in Image J (v1.46r (National Institutes of Health, Laboratory for Optical and Computational Instrumentation, University of Wisconsin, Madison, WI, USA) and converted to 8-bit grayscale, and then individually opened in neurite tracer plugin. Large bright objects (somata of neurons) were removed from all images by application of Fiji software version 2.9.0 (accessed 15 January 2022) (<https://imagej.net/Fiji/Downloads>). Thereafter, the resulting images were inserted to neurite tracer. Afterwards, the threshold was adjusted manually before starting the automated tracing of neuritis. Images with the traced neuritis

were merged with RGB original images to ensure the reliability and accuracy of the tracing process. Afterwards, the number of neurons was determined by using a multi-point tool of ImageJ. Finally, traced neuritis lengths were normalized with the numbers of neurons to calculate the neurite length/cell. To determine the size of neuronal somata, soma areas of neurons were selected, and soma areas were measured. The results were normalized with those from the control group.

### 2.8. Statistical Analysis

Data analysis and visualization were carried out by using GraphPad Prism (GraphPad Software version 8.0.1 for Windows, La Jolla, CA, USA). The normal distribution of data was assessed by use of the Kolmogorov–Smirnov test. The effect of treatments on viability and neurite length of DRG neurons was assessed using one-way ANOVA (analysis of variance) followed by the Bonferroni multiple comparisons test ( $p < 0.05$ ). An alpha level of 0.05 was used for all tests.

## 3. Results

### 3.1. Characterization of DRG Neuronal Cells

DRG neurons cultures were examined under a light microscope at various time points (2, 24, 48, and 72 h) to track their growth and morphology. After 2 hours, neuron somas appeared round, bright, and refractile, with a large nucleus (Figure 1a). Three distinct subpopulations (small, medium, and large neurons) based on soma diameter were observed, (Figure 1a). Most of the DRG neurons extended long thin neuritis after 24 h of cells seeding, while, after 48 and 72 h of culturing, all sensory neurons had long neuritis which connected and formed networks together (Figure 1a).

### 3.2. Effects of Paclitaxel or/and PEA on Cell Viability of DRG Neurons

DRG neurons were treated with different concentrations of Paclitaxel for 24, 48, and 72 h, and we found a significant reduction in the viability of cells at only 72 h post-treatment, regardless of Paclitaxel concentrations, compared to the untreated control group ( $p < 0.001$ ) (Figure 2). Paclitaxel's effects on neuron viability were obviously time-dependent but not concentration-dependent. PEA, as expected, showed no statistically significant effect on the viability of cells in comparison to the untreated control group ( $p > 0.05$ ) at 72 h post-treatment (Figure S2).

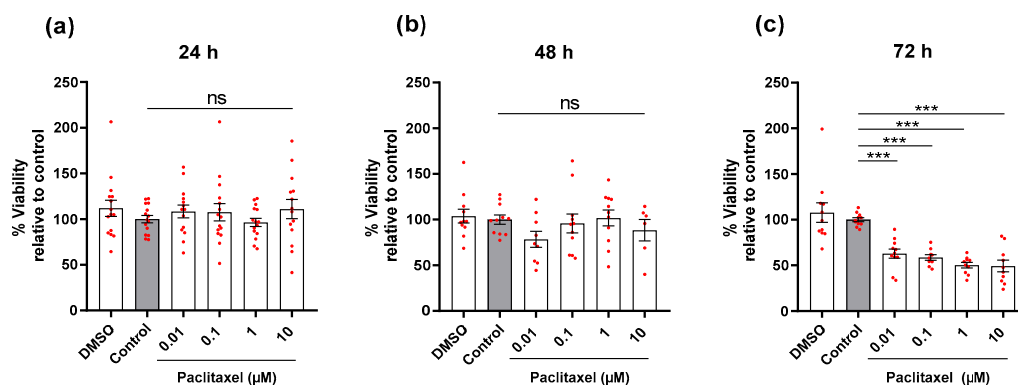


**Figure 2.** Effects of different concentrations of Paclitaxel on viability (%) of DRG neurons at different time points. Application of different concentrations of Paclitaxel showed no influence on the viability of neurons at (a) 24 h and (b) 48 h, whereas, at (c) 72 h post-treatment, Paclitaxel significantly reduced the viability of cells compared to control (\*\* $p < 0.001$ ). The asterisk denotes significant results regarding the respective measurement indicated with the bar. Values are served as mean  $\pm$  SEM of three independent experiments performed in triplicate. SEM: Standard error mean.

The effects of combined treatments (Paclitaxel plus PEA) were compared to the effect of Paclitaxel alone on viability (%) at 72 h post-treatment. A significant increase was observed

for almost all combinations of Paclitaxel (0.01–10  $\mu\text{M}$ ) plus PEA (0.1–10  $\mu\text{M}$ ) compared to cells treated with Paclitaxel alone. A significant effect was missed only for the combination (10  $\mu\text{M}$  Paclitaxel + 1  $\mu\text{M}$  PEA vs. 10  $\mu\text{M}$  Paclitaxel) ( $p < 0.05$ ) (Figure 3). Notably, the effect of PEA against Paclitaxel was clearly concentration independent.

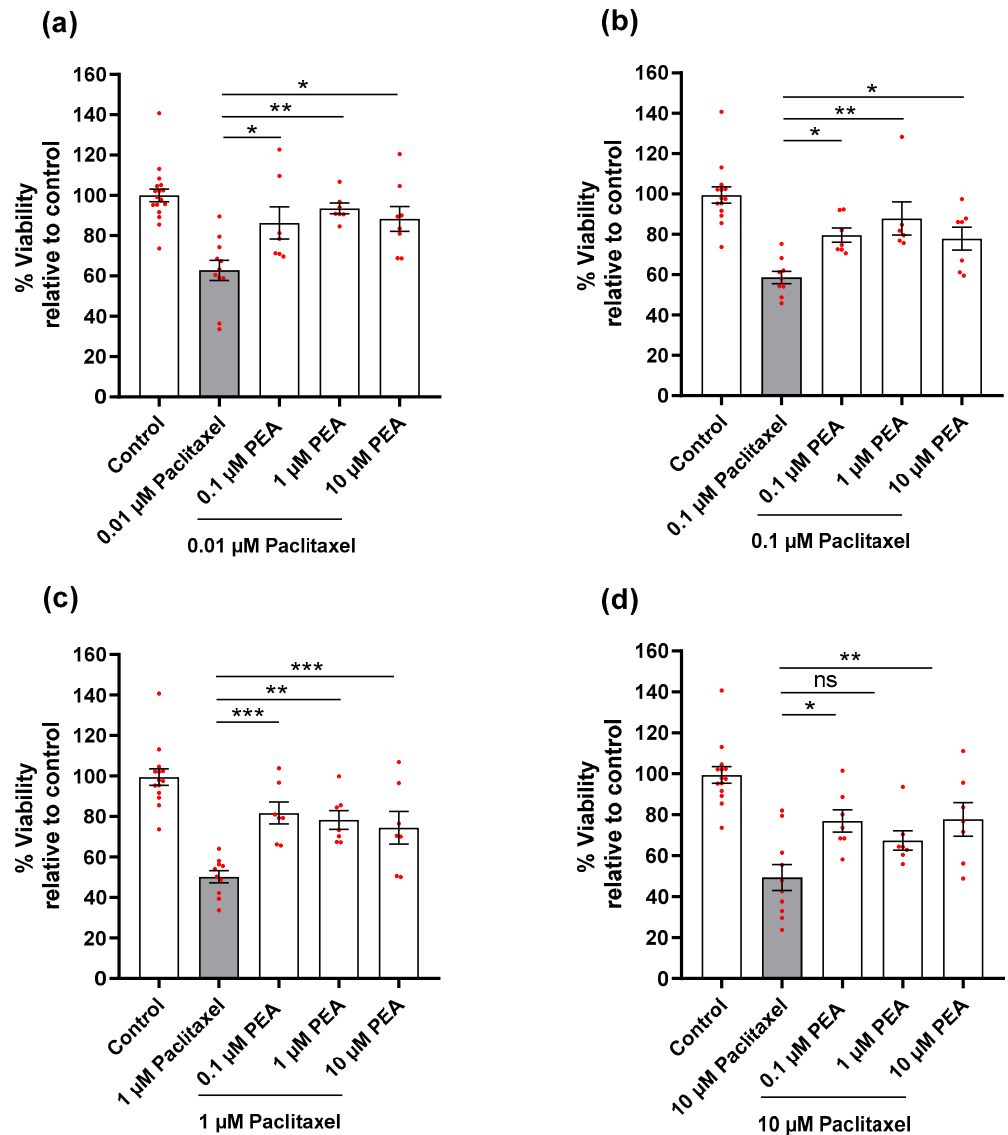


**Figure 3.** Effects of different concentrations of Paclitaxel (a) 0.01  $\mu\text{M}$ , (b) 0.1  $\mu\text{M}$ , (c) 1  $\mu\text{M}$ , and (d) 10  $\mu\text{M}$  either alone or in combination with different concentrations of PEA on viability (%) (mean  $\pm$  SEM) of DRG neurons at 72 h post-treatment by using MTT assay. The asterisk indicates a significant increase in viability of DRG neurons treated with different Paclitaxel concentrations in combination with different concentrations of PEA at 72 h post-treatment compared to cells treated with Paclitaxel only (\*  $p < 0.05$ , \*\*  $p < 0.01$ , and \*\*\*  $p < 0.001$ ). Data are (mean  $\pm$  SEM) of three independent experiments performed in duplicate.

### 3.3. Effects of Paclitaxel or/and PEA on Morphology of DRG Neurons

Toxic hallmarks of Paclitaxel were observed on the morphology of neurons such as suppression in neurite lengths of neurons, swelling of neuronal cell bodies, as well as retraction and blebbing formation at the distal endings of neurites (Figure 4a). To verify and quantify the Paclitaxel and PEA effects, two different endpoints were assessed, namely neurite length and soma size.



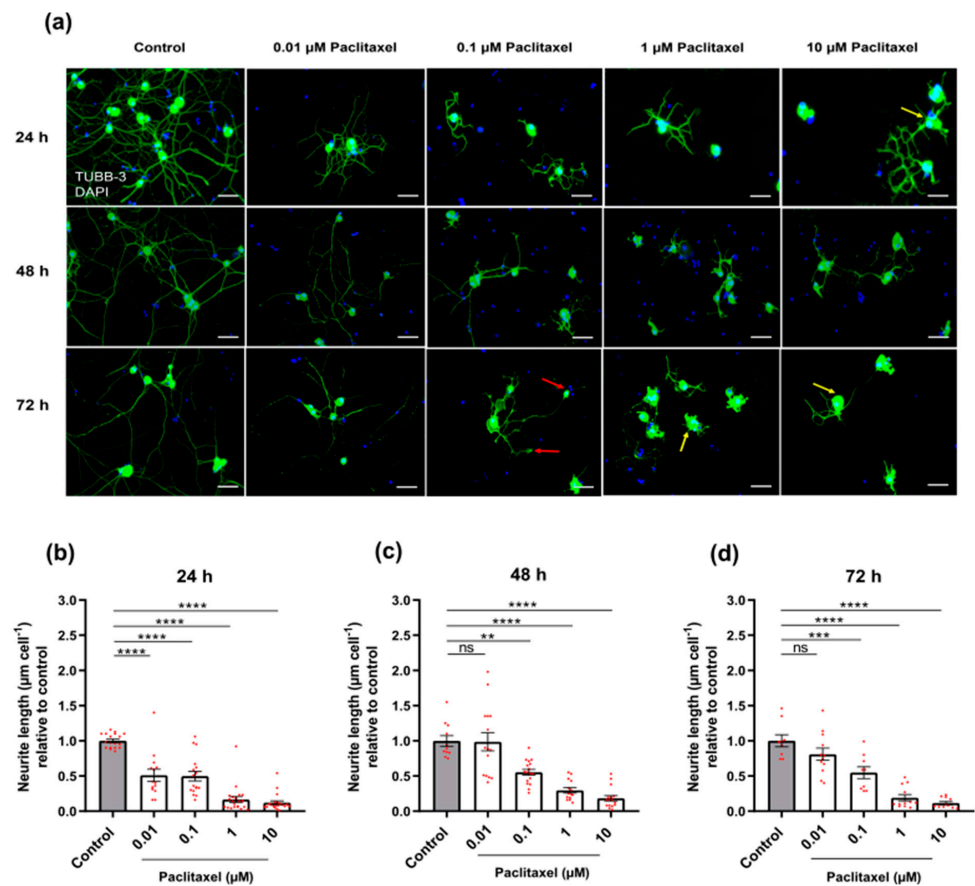


**Figure 4.** Effects of different Paclitaxel concentrations on morphology, neurite length, and soma size of DRG neurons. (a) Immunofluorescence staining of DRG neurons treated with different Paclitaxel concentrations (0.01, 0.1, 1, and 10 μM) labeled with anti-mouse beta III Tubulin antibody after 24, 48, and 72 h. Different concentrations of Paclitaxel had toxic effects leading to a reduction in neurite length and an increase in soma area (yellow arrows) at all time points. Additionally, other characteristics of Paclitaxel toxicity on neuronal morphology are visible, including swellings and blebbing at distal ends of neurites (red arrows). Nuclei were counterstained with DAPI. Five to eight regions were recorded randomly per each coverslip. Scale bars = 75 μm. (b–d) significant suppression in neurite lengths of DRG neurons treated with different Paclitaxel concentrations in comparison with the control group (\*\*  $p < 0.01$ , \*\*\*  $p < 0.001$ , \*\*\*\*  $p < 0.0001$ ) at 24, 48, and 72-h post-treatment, respectively. Data are (mean  $\pm$  SEM) of three independent experiments performed with (10–15) replicates.

### 3.3.1. Neurite Length

The treatment with the four different concentrations of Paclitaxel resulted in a significant reduction in neurite length 24 h after treatment when compared to the non-treated control group ( $p < 0.05$ ) (Figure 4b). At 48 and 72 h post-treatment, all studied Paclitaxel groups had an apparent reduction in neurite length except for 0.01 μM Paclitaxel relative to control group (Figure 4c,d). Interestingly, Paclitaxel effects on neurite length were clearly time- and concentration-dependent. No alterations in morphology and neurite length were found in DRG neurons treated with PEA in comparison to the vehicle control group ( $p > 0.05$ ) (Figure S3a–c).

The three different concentrations of PEA co-applied with 0.01 μM Paclitaxel had no significant protective effects on the neurite lengths of neurons at all investigated timelines compared to the 0.01 μM Paclitaxel group ( $p > 0.05$ ; Figure S4). All combined groups of PEA with 0.1 μM Paclitaxel did not cause any significant increase in neurite length at any time point when compared to the 0.1 μM Paclitaxel group alone ( $p > 0.05$ ); however, at 72 h

after application, 1  $\mu\text{M}$  PEA only plus 0.1  $\mu\text{M}$  Paclitaxel resulted in an apparent increase in neurite length of DRG neurons compared to 0.1  $\mu\text{M}$  Paclitaxel group ( $p < 0.05$ ; Figure S5).

However, PEA concentrations (0.1, 1, and 10  $\mu\text{M}$ ) showed a significant protective effect on neurite outgrowth of DRG neurons when combined with 1  $\mu\text{M}$  Paclitaxel and compared with 1  $\mu\text{M}$  Paclitaxel alone at 24 and 72-h post-treatment. A total of 0.1  $\mu\text{M}$  PEA combined with 1  $\mu\text{M}$  Paclitaxel had a significant protective effect on neurite lengths of DRG neurons 48 h after treatment when compared to Paclitaxel alone ( $p < 0.05$ ) (Figure 5).

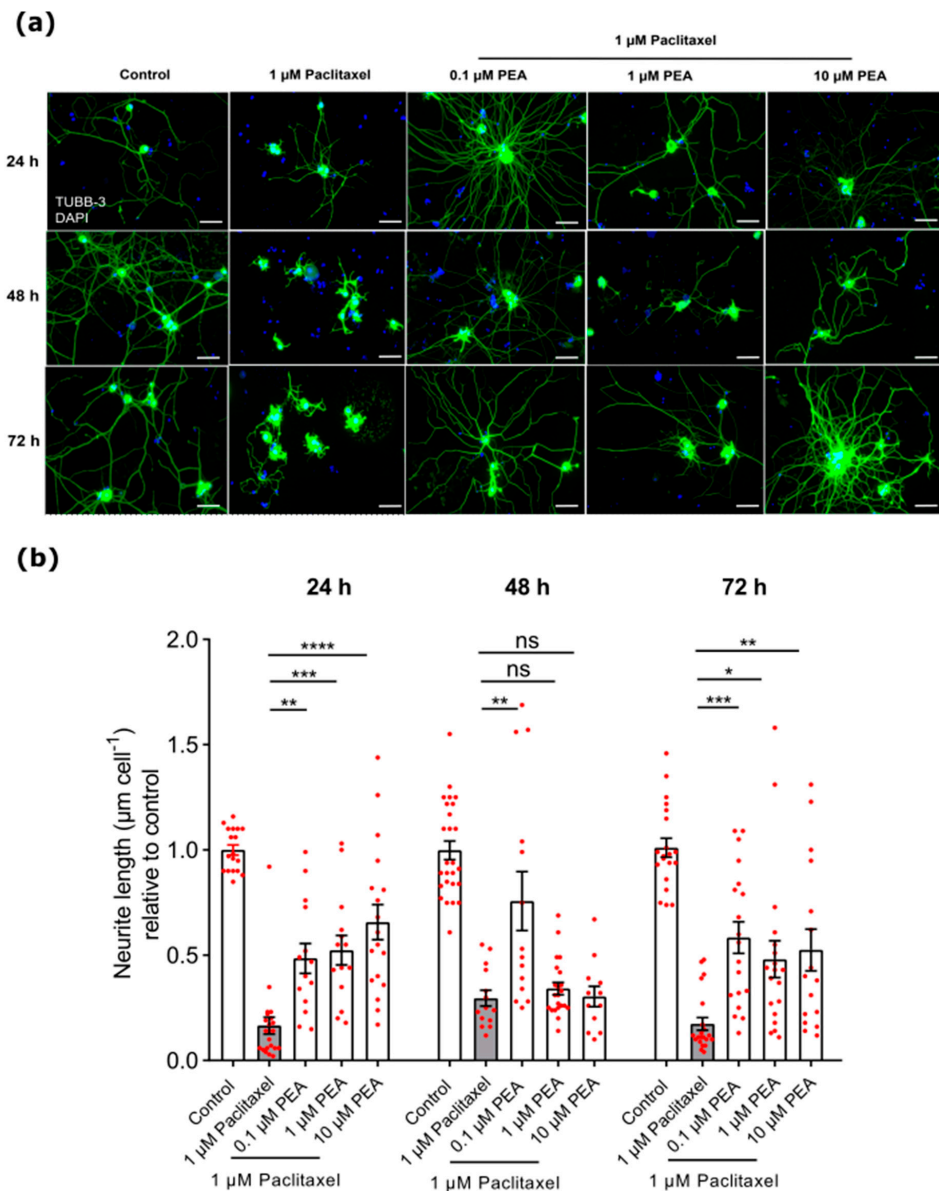


**Figure 5.** Showing protective effects of different PEA concentrations (0.1, 1, and 10  $\mu\text{M}$ ) co-applied with 1  $\mu\text{M}$  Paclitaxel on neurite lengths of DRG neurons compared to 1  $\mu\text{M}$  Paclitaxel alone at 24, 48, and 72 h post-treatment. (a) Representative microphotographs of DRG neurons stained with beta III Tubulin antibody for soma and neuritis (green) and DAPI for nuclei (blue). Scale bars = 75  $\mu\text{m}$ . (b) Bar graphs indicated a significant increase in neurite lengths of neurons treated with different concentrations of PEA at 24 h and 72 h post-treatment compared to cells treated with Paclitaxel only, while at 48 h post-treatment only 0.1  $\mu\text{M}$  PEA demonstrated a significant increase in neurite length against 1  $\mu\text{M}$  Paclitaxel (\*  $p < 0.05$ , \*\*  $p < 0.01$ , \*\*\*  $p < 0.001$ , \*\*\*\*  $p < 0.0001$ ). Data are (mean  $\pm$  SEM) of three independent experiments performed in 10–15 replicates. The asterisk denotes significant results regarding the respective measurement indicated with bar charts.

Regarding the protective effects of different PEA concentrations against 10  $\mu\text{M}$  Paclitaxel, we found 0.1 or 1  $\mu\text{M}$  PEA combined with 10  $\mu\text{M}$  Paclitaxel showed a significant increase in neurite lengths of DRG neurons at 24, 48, and 72-h post-treatment compared to cells treated with 10  $\mu\text{M}$  Paclitaxel only ( $p < 0.05$ ) (Figure 6). Meanwhile, the 10  $\mu\text{M}$  PEA plus 10  $\mu\text{M}$  Paclitaxel group revealed a significant increase in neurite lengths only at 24 h post-treatment in comparison to the 10  $\mu\text{M}$  Paclitaxel group ( $p < 0.05$ ) (Figure 6).

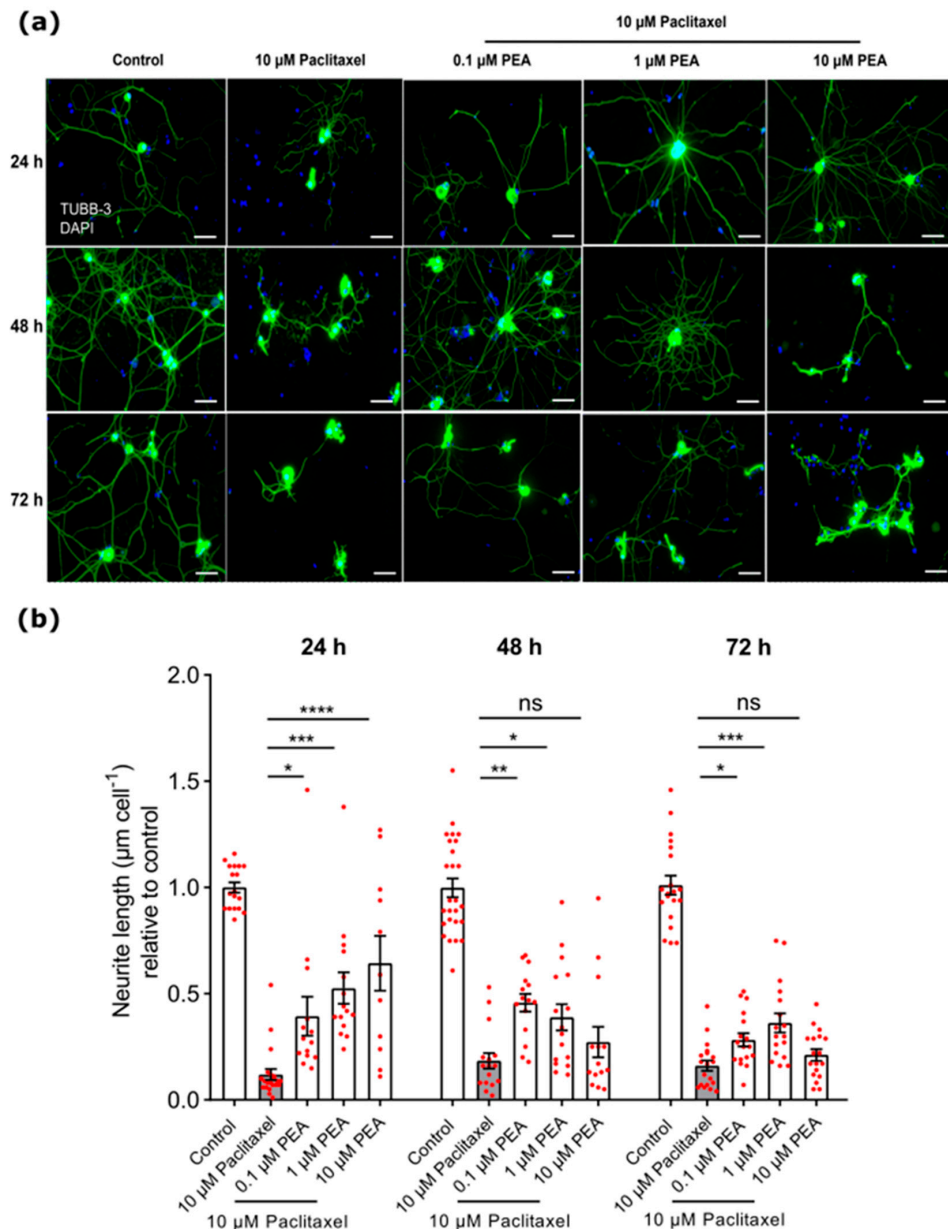


**Figure 6.** Effects of different PEA concentrations (0.1, 1, and 10  $\mu\text{M}$ ) combined with 10  $\mu\text{M}$  Paclitaxel at 24, 48, and 72 h post-treatment. (a) Representative immunofluorescence images show DRG neurons labeled with beta III Tubulin antibody (green) and DAPI for nuclei (blue). Scale bars = 75  $\mu\text{m}$ . (b) A significant increase in neurite length of neurons was found in groups treated with different concentrations of PEA at 24 h only compared to cells treated with Paclitaxel only. At 48 and 72-h post-treatment, 0.1  $\mu\text{M}$  PEA or 1  $\mu\text{M}$  PEA combined with 10  $\mu\text{M}$  Paclitaxel demonstrated a significant increasing effect on the neurite lengths in comparison with 10  $\mu\text{M}$  Paclitaxel alone (\*  $p < 0.05$ , \*\*  $p < 0.01$ , \*\*\*  $p < 0.001$ , \*\*\*\*  $p < 0.0001$ ). Data represented as (mean  $\pm$  SEM), and the experiments were performed at least 3 independent times and 10–15 replicas. The asterisk denotes significant results regarding the respective measurement indicated with the bar graphs.

### 3.3.2. Soma Size

The four different concentrations of Paclitaxel led to an increase in the soma size of neurons 24 h post-treatment when compared to the control group ( $p < 0.05$ ) (Figure 7a). At 48 and 72-h, all investigated groups treated with Paclitaxel showed apparent enlargements in areas of neuronal somata except for 0.01  $\mu\text{M}$  of Paclitaxel when compared to the control group ( $p < 0.05$ ) (Figure 7b,c). Effects of Paclitaxel on soma size of neuronal cell bodies were obviously time- and concentration-dependent. Treatment with PEA alone demonstrated no significant effects on the size of neuronal bodies at any time point when compared to control group ( $p > 0.05$ ) (Figure S3d–f).

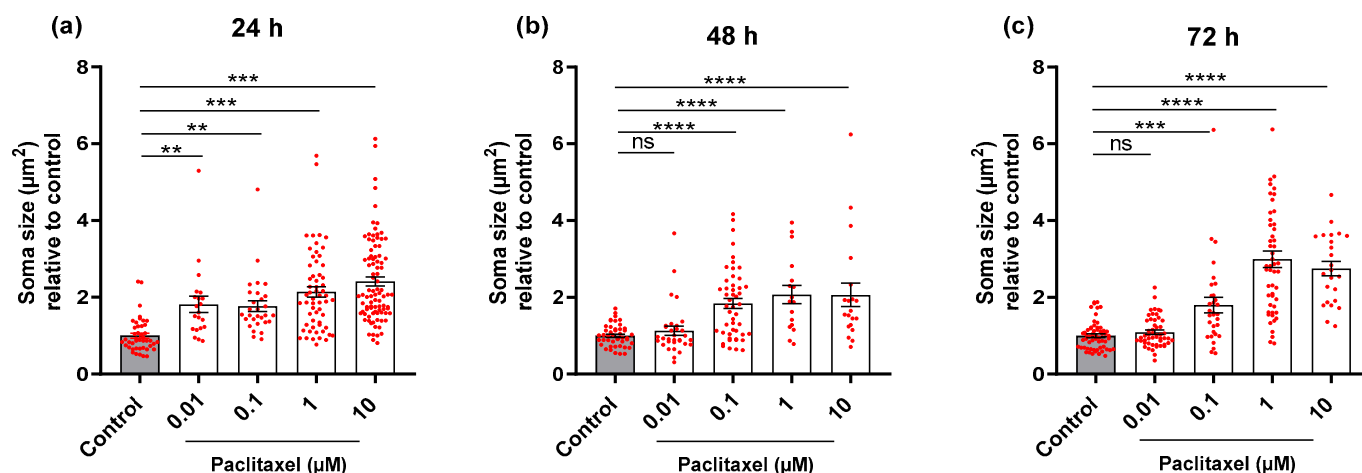


**Figure 7.** Effects of different Paclitaxel concentrations on soma size of DRG neurons at different time points. Bar charts show a significant increase in the soma size of DRG neurons after the application of different Paclitaxel concentrations at (a) 24 h, (b) 48 h, and (c) 72 h post-treatment compared to the control (\*\*  $p < 0.01$ , \*\*\*  $p < 0.001$ , \*\*\*\*  $p < 0.0001$ ). Asterisks denote significant results regarding the respective measurement indicated with the bar. Values are served as mean  $\pm$  SEM of three independent experiments,  $n = 30$ – $45$  replicates. SEM: Standard error mean.

The effects of different combined groups of Paclitaxel plus PEA on soma size of DRG neurons were investigated in comparison to the cells treated with Paclitaxel alone. An increase in soma size was found for 0.01  $\mu\text{M}$  Paclitaxel only at 24 h after treatment compared to control group. A total of 10  $\mu\text{M}$  PEA combined with 0.01  $\mu\text{M}$  Paclitaxel was the only group that demonstrated a significant decrease in neurons soma size in comparison to Paclitaxel group ( $p < 0.05$ ) at 24 h after application, while 0.1 and 1  $\mu\text{M}$  PEA did not show any protective effects against 0.01  $\mu\text{M}$  Paclitaxel group ( $p > 0.05$ ) at the same time point (Figure S6).

The 0.1 and 10  $\mu\text{M}$  PEA co-applied with 0.1  $\mu\text{M}$  Paclitaxel revealed an apparent decrease in neuronal somata sizes, whereas 1  $\mu\text{M}$  PEA had no effect compared to neurons treated with Paclitaxel only at 24 h after treatment ( $p < 0.05$ ) (Figure 8a). At 48 h post-treatment, 1 and 10  $\mu\text{M}$  of PEA combined with 0.1  $\mu\text{M}$  Paclitaxel were the only groups with a significant neuroprotective effect on somata sizes when compared to 0.1  $\mu\text{M}$  Paclitaxel ( $p < 0.05$ ) (Figure 8a). At 72 h after application, all PEA concentrations combined with 0.1  $\mu\text{M}$  Paclitaxel showed considerable protectant action except for the 10  $\mu\text{M}$  PEA + 0.1  $\mu\text{M}$  Paclitaxel group when compared to Paclitaxel only (Figure 8a).

Treatment of neurons with the three different concentrations of PEA co-applied with 1  $\mu\text{M}$  Paclitaxel demonstrated a significant protective effect on somata sizes when compared to cells exposed to 1  $\mu\text{M}$  Paclitaxel alone at 24- and 72-h time points ( $p < 0.05$ ) (Figure 8b). At 48 h post-treatment, 1  $\mu\text{M}$  of Paclitaxel in combination with 10  $\mu\text{M}$  of PEA was the only group without any protective effects, whereas the other two combined groups led to a strong decrease when compared to individual Paclitaxel treated cells ( $p < 0.05$ ) (Figure 8b).

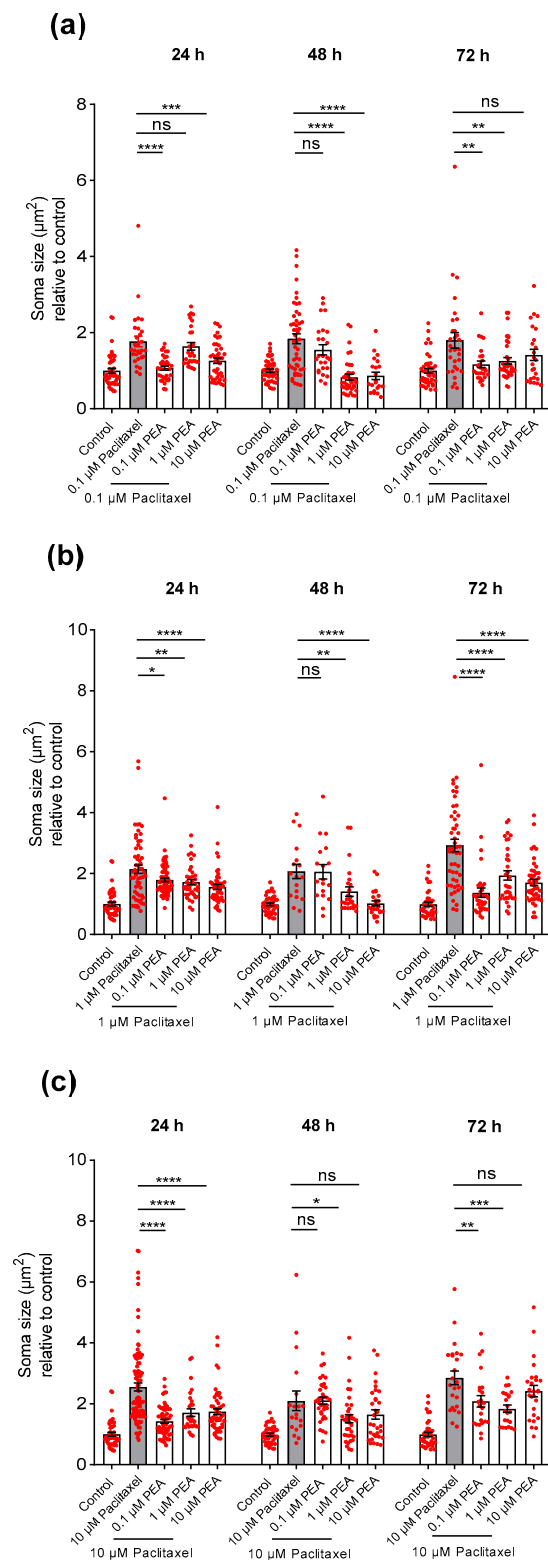


**Figure 8.** Effects of different PEA concentrations (0.1, 1, and 10  $\mu\text{M}$ ) in combination with different concentrations of Paclitaxel (a) 0.1  $\mu\text{M}$ , (b) 1  $\mu\text{M}$ , and (c) 10  $\mu\text{M}$  on soma sizes of DRG neurons at 24, 48, and 72-h post-treatment. The combined groups of Paclitaxel plus PEA demonstrated a varied significant decrease in DRG neuronal cell bodies in comparison with neurons treated with Paclitaxel only (\*  $p < 0.05$ , \*\*  $p < 0.01$ , \*\*\*  $p < 0.001$ , \*\*\*\*  $p < 0.0001$ ). Data represented as (mean  $\pm$  SEM), and the experiments were performed at least 3 independent times with  $n = 30\text{--}45$  replicas. The asterisk denotes significant results regarding the respective measurement indicated with the bar graphs.

The three concentrations of PEA co-applied with 10  $\mu$ M Paclitaxel showed statistically significant protective effects on DRG neurons' cell bodies against the 10  $\mu$ M Paclitaxel group at 24 h after treatment ( $p < 0.05$ ) (Figure 8c). Similarly, both concentrations, 0.1 and 1  $\mu$ M of PEA, combined with 10  $\mu$ M of Paclitaxel showed a significant neuroprotective effect on soma sizes, while the combination of 10  $\mu$ M Paclitaxel and 10  $\mu$ M PEA did not have any protective effect at 72 h post-treatment compared to Paclitaxel alone ( $p < 0.05$ ) (Figure 8c). The 10  $\mu$ M Paclitaxel plus 1  $\mu$ M PEA group demonstrated a significant protective effect; however, 0.1 and 10  $\mu$ M of PEA combined with 10  $\mu$ M Paclitaxel groups did not reveal any protective effect on the size of cell bodies of neurons when compared to neurons treated only with 10  $\mu$ M Paclitaxel at 48 h after treatment ( $p < 0.05$ ) (Figure 8c).

Overall, the neuroprotective actions of PEA against the induced toxicity of Paclitaxel on soma size of DRG neurons were time and concentration independent ( $p < 0.05$ ).

#### 4. Discussion

Peripheral neuropathy (PN) is one of the most common side effects of Paclitaxel, affecting up to 97% of all gynecological and urological cancer patients [46,47]. Paclitaxel causes cell death in cancer cells by interfering with mitosis via microtubule stabilization; however, Paclitaxel also affects the peripheral nervous system, causing PN [48]. The primary symptoms are hand and foot numbness besides pain caused by Paclitaxel accumulation in the DRG. DRG neurons are highly susceptible to Paclitaxel accumulation presumably due to a more permeable blood nerve barrier [49]. In the current study, the toxicity of Paclitaxel on viability of neurons was apparent at only 72 h post-treatment in comparison to the control group, while, at all-time windows studied, different Paclitaxel concentrations resulted in a significant reduction in neurite length of DRG neurons. These findings were in line with previous research on Paclitaxel-induced peripheral neuropathy with axonal sensory neuropathy that was length-dependent [50]. A significant reduction in neurite length was reported when DRG neurons were exposed to 10  $\mu$ M Paclitaxel for 24 h [17]. In addition, Paclitaxel's toxic effects on neurons resulted in the enlargement of neuronal cell bodies obviously at 24, 48, and 72 h post-treatment. These findings are in agreement with previous findings, in which Paclitaxel treatment caused a significant increase in DRG neuron soma size after 24 h of treatment [15,16] and induced a significant enlargement of DRG nucleolus size [51].

Our data obviously demonstrated that Paclitaxel neurotoxicity on neurite outgrowth and soma size is time- and dose-dependent. Similar earlier studies reported on a dose- and infusion time-dependent-induced neurotoxicity that could be exacerbated by underlying conditions or co-application with other drugs [52,53]. The differences in toxic effects of Paclitaxel on the viability and morphology of neurons might possibly be due to higher susceptibility or vulnerability of neurites to toxins than neuronal somata [15,16]. As a result, the toxic effects of Paclitaxel were more rapid, with a significant reduction in neurite length of neurons after 24 h post-treatment. The data are in agreement with a previous work reporting on reduction of axon length after Paclitaxel treatment. Therefore, Paclitaxel seems to act directly on axons and causes axonal degeneration probably through local mechanisms [54]. Additionally, Paclitaxel disrupted intracellular microtubules and bindings with beta-tubulin inside cell soma, resulting in accumulation of non-functional beta-tubulin units of microtubules, vacuolization of mitochondria and cytoplasm in neuronal cell bodies, and cell enlargement [55]. Paclitaxel increased cell size, and, after 72 h of treatment, neurons may explode and die due to a non-apoptotic effect. Taken together, Paclitaxel targets the nerve fibers and causes local axonopathy in still viable neurons with increased soma sizes.

PEA is a bioactive lipid that is used as an anti-nociceptive agent in different animal models of neuropathic pain, including spinal cord injury [56] and diabetes-induced peripheral neuropathy [57]. In humans, PEA accumulates in painful tissues, as observed in the trapezius muscle of women suffering from chronic neck pain [58]. Moreover, PEA protected nerve tissue in neuropathic conditions [37] and prevented neurotoxicity and neurodegeneration [59,60]. Furthermore, PEA also alleviated painful diabetic neuropathy,

chemotherapy neuropathy, idiopathic axonal neuropathy, nonspecific neuropathy, and sciatic and lumbosacral spine disease pain [61]. Here, we demonstrated that PEA partially counteracted the toxicity of Paclitaxel on DRG neurons. Regardless of PEA concentration, combining PEA with Paclitaxel significantly increased neuron cell viability compared to treatment with Paclitaxel at 72 h after treatment. These results were consistent with a previous study that showed a reduction of positive propidium iodide (PI) neuronal nuclei after the application of PEA to N-methyl D-aspartate (NMDA)-treated organotypic hippocampal slice cultures [36]. The positive effects on cell viability seem not to be confined to neurons. In astrocytes, different PEA concentrations increased the cell viability from 30 min to 18 h [62]. The data imply for Paclitaxel the need for a longer interaction with damaged cells. Paclitaxel's slow action might provide a good opportunity for PEA to exert protective effects and reverse the toxic effects of Paclitaxel, resulting in increasing the viability of DRG neurons.

In the present study, PEA plus Paclitaxel groups showed a significant increase in neurite length and a strongly decreased soma size of DRG neurons at all studied time points when compared to individual Paclitaxel treatment groups. Interestingly, at 24 h after treatment, PEA produced a protective effect on neurite length and size of cell bodies of neurons against toxicity of Paclitaxel, independent of PEA concentration. This phenomenon might be attributed to the short period of exposure of DRG neurons to Paclitaxel and PEA treatment, allowing PEA to mask and alleviate the toxicity of Paclitaxel. In line with previous evidence in a rat model of Oxaliplatin-induced neurotoxicity, acute intraperitoneal administration of PEA (30 mg kg<sup>-1</sup>) substantially relieved pain 30 min after administration [63].

Notably, 10  $\mu$ M PEA did not show any significant protective effect on neurite outgrowth at 48 h post-treatment, although it enhanced neurite extension at 72 h after treatment. The results might be interpreted as an attempt of damaged neurons to develop a survival pressure to resist death caused by Paclitaxel toxicity. They retract and aggregate short neurites. Therefore, neurite extension might become a secondary process at 48 h post-treatment and, as a result, PEA remains unable to express any protective effects. These data are agreed with previous studies on PEA effects on preserving myelin sheet thickness and axonal diameter and preventing myelin degeneration [37]. PEA reduced myelin loss caused by sciatic nerve injury, maintained neuron cell diameters, reduced nerve edema, and restored nerve function, all of which were associated with decreased hypersensitivity [64].

In summary, PEA induced strong neuroprotective actions against Paclitaxel toxicity in DRG neurons and improved their viability and morphology.

## 5. Conclusions

Our findings showed the ability of PEA to attenuate the toxicity of Paclitaxel on DRG neurons. The effects of Paclitaxel on neuronal viability alone were apparent at 72 h post-treatment only. Furthermore, treatment with Paclitaxel led to a strong reduction in neurite length and enlargement of neuronal cell bodies at all investigated time windows. PEA showed neuroprotective effects by partially reversing the toxic effects of Paclitaxel, including increasing cell viability, enhancing DRG neuron neurite outgrowth, and decreasing swelling of neuronal soma. These findings contribute to our understanding of Paclitaxel's site and mode of action on the peripheral nervous system and highlight the critical need for novel peripheral neuropathy protective strategies. More research will be needed to elucidate the signaling pathways underlying PEA's neuroprotective effects against Paclitaxel neurotoxicity. With these results, PEA might be a promising therapeutic option for cancer patients suffering from CIPN.

**Supplementary Materials:** The following supporting information can be downloaded at: <https://www.mdpi.com/article/10.3390/biom12121873/s1>. Figure S1: Representative example for tracing neurites by ImageJ program; Figure S2: Effects of different PEA concentrations on neuronal cell viability (%) (mean  $\pm$  SEM) at 72 h post-treatment; Figure S3: Effects of different concentrations of PEA on neurite lengths and soma sizes (mean  $\pm$  SEM) of DRG neurons at 24, 48, and 72-h post-treatment; Figure S4: Effects of different PEA concentrations (0.1, 1, and 10  $\mu$ M) combined with 0.01  $\mu$ M Paclitaxel on neurite length of DRG neurons at 24, 48, and 72-h post-treatment; Figure S5: Effects of different PEA concentrations (0.1, 1, and 10  $\mu$ M) combined with 0.1  $\mu$ M Paclitaxel at 24, 48, and 72-h post-treatment; Figure S6: The effects of different PEA concentrations (0.1, 1, and 10  $\mu$ M) co-applied with 0.01  $\mu$ M Paclitaxel on soma sizes of DRG neurons at 24, 48, and 72-h post-treatment.

**Author Contributions:** Conceptualization, F.D. and A.E.; methodology, A.E.; formal analysis, A.E.; investigation, A.E.; resources, F.D.; data curation, A.E.; writing—original draft preparation, A.E. and F.D.; writing—review and editing, F.D. and A.E.; visualization, A.E.; supervision, F.D.; project administration, F.D. All authors have read and agreed to the published version of the manuscript.

**Funding:** This research received no external funding.

**Institutional Review Board Statement:** All animal experiments were carried out in accordance with the policy on ethics and the policy on the use of animals in neuroscience research, as specified in directive 2010/63/EU of the European Parliament and of the Council of the European union on the protection of animals used for scientific purposes and were approved by local authorities for laboratory animal care and use (State of Saxony-Anhalt, Germany, permission number: I11M27).

**Informed Consent Statement:** Not applicable.

**Data Availability Statement:** The data presented in this study are available on request from the authors.

**Acknowledgments:** We acknowledge Katholischer akademischer Ausländer-Dienst (KAAD) for the Ph.D. scholarship to A.E. Authors would like to thank Chalid Ghadban and Candy Rothgänger-Strube for excellent technical assistance and Tim Hohmann, Marc Richard Kolbe, Urszula Hohmann, Johanna Marie Dela Cruz, Derek C Molliver, and Steven Fagan for helpful discussions. We acknowledge the financial support of the Open Access Publication Fund of the Martin Luther University Halle-Wittenberg.

**Conflicts of Interest:** The authors declare no conflict of interest.

## References

1. Grisold, W.; Cavaletti, G.; Windebank, A.J. Peripheral Neuropathies from Chemotherapeutics and Targeted Agents: Diagnosis, Treatment, and Prevention. *Neuro. Oncol.* **2012**, *14* (Suppl. 4), iv45–iv54. [[CrossRef](#)]
2. Masocha, W. Targeting the Endocannabinoid System for Prevention or Treatment of Chemotherapy-Induced Neuropathic Pain: Studies in Animal Models. *Pain Res. Manag.* **2018**, *2018*, 5234943. [[CrossRef](#)]
3. Rowinsky, E.K.; Donehower, R.C. Paclitaxel (Taxol). *N. Engl. J. Med.* **1995**, *332*, 1004–1014. [[CrossRef](#)]
4. Tankanow, R.M. Docetaxel: A Taxoid for the Treatment of Metastatic Breast Cancer. *Am. J. Health Pharm.* **1998**, *55*, 1777–1791. [[CrossRef](#)]
5. Vyas, D.M.; Kadow, J.F. 6 Paclitaxel: A Unique Tubulin Interacting Anticancer Agent. *Prog. Med. Chem.* **1995**, *32*, 289–337. [[CrossRef](#)]
6. Schiff, P.B.; Fant, J.; Horwitz, S.B. Promotion of Microtubule Assembly in Vitro by Taxol. *Nature* **1979**, *277*, 665–667. [[CrossRef](#)]
7. Rowinsky, E.K.; Cazenave, L.A.; Donehower, R.C. Taxol: A Novel Investigational Antimicrotubule Agent. *JNCI J. Natl. Cancer Inst.* **1990**, *82*, 1247–1259. [[CrossRef](#)]
8. Seretny, M.; Currie, G.L.; Sena, E.S.; Ramnarine, S.; Grant, R.; MacLeod, M.R.; Colvin, L.A.; Fallon, M. Incidence, Prevalence, and Predictors of Chemotherapy-Induced Peripheral Neuropathy: A Systematic Review and Meta-Analysis. *Pain* **2014**, *155*, 2461–2470. [[CrossRef](#)]
9. Farquhar-Smith, P. Chemotherapy-Induced Neuropathic Pain. *Curr. Opin. Support. Palliat. Care* **2011**, *5*, 1–7. [[CrossRef](#)]
10. Dougherty, P.M.; Cata, J.P.; Cordella, J.V.; Burton, A.; Weng, H.-R. Taxol-Induced Sensory Disturbance Is Characterized by Preferential Impairment of Myelinated Fiber Function in Cancer Patients. *Pain* **2004**, *109*, 132–142. [[CrossRef](#)]
11. Sharma, S.; Venkitaraman, R.; Vas, P.R.J.; Rayman, G. Assessment of Chemotherapy-Induced Peripheral Neuropathy Using the LDI FLARE Technique: A Novel Technique to Detect Neural Small Fiber Dysfunction. *Brain Behav.* **2015**, *5*, e00354. [[CrossRef](#)]
12. Windebank, A.J.; Smith, A.G.; Russell, J.W. The Effect of Nerve Growth Factor, Ciliary Neurotrophic Factor, and ACTH Analogs on Cisplatin Neurotoxicity in Vitro. *Neurology* **1994**, *44 Pt 1*, 488–494. [[CrossRef](#)]
13. Gill, J.S.; Windebank, A.J. Cisplatin-Induced Apoptosis in Rat Dorsal Root Ganglion Neurons Is Associated with Attempted Entry into the Cell Cycle. *J. Clin. Investig.* **1998**, *101*, 2842–2850. [[CrossRef](#)]



14. Fischer, S.J.; McDonald, E.S.; Gross, L.; Windebank, A.J. Alterations in Cell Cycle Regulation Underlie Cisplatin Induced Apoptosis of Dorsal Root Ganglion Neurons in Vivo. *Neurobiol. Dis.* **2001**, *8*, 1027–1035. [[CrossRef](#)]
15. Scuteri, A.; Nicolini, G.; Miloso, M.; Bossi, M.; Cavaletti, G.; Windebank, A.J.; Tredici, G. Paclitaxel Toxicity in Post-Mitotic Dorsal Root Ganglion (DRG) Cells. *Anticancer Res.* **2006**, *26*, 1065–1070.
16. Guo, L.; Hamre, J.; Eldridge, S.; Behrsing, H.P.; Cutuli, F.M.; Mussio, J.; Davis, M. Multiparametric Image Analysis of Rat Dorsal Root Ganglion Cultures to Evaluate Peripheral Neuropathy-Inducing Chemotherapeutics. *Toxicol. Sci.* **2017**, *156*, kfw254. [[CrossRef](#)]
17. Park, S.H.; Eber, M.R.; Fonseca, M.M.; Patel, C.M.; Cunnane, K.A.; Ding, H.; Hsu, F.-C.; Peters, C.M.; Ko, M.-C.; Strowd, R.E.; et al. Usefulness of the Measurement of Neurite Outgrowth of Primary Sensory Neurons to Study Cancer-Related Painful Complications. *Biochem. Pharmacol.* **2021**, *188*, 114520. [[CrossRef](#)]
18. Akin, E.J.; Alsaloum, M.; Higerd, G.P.; Liu, S.; Zhao, P.; Dib-Hajj, F.B.; Waxman, S.G.; Dib-Hajj, S.D. Paclitaxel Increases Axonal Localization and Vesicular Trafficking of Nav1.7. *Brain* **2021**, *144*, 1727–1737. [[CrossRef](#)]
19. Shin, G.J.; Pero, M.E.; Hammond, L.A.; Burgos, A.; Kumar, A.; Galindo, S.E.; Lucas, T.; Bartolini, F.; Grueber, W.B. Integrins Protect Sensory Neurons in Models of Paclitaxel-Induced Peripheral Sensory Neuropathy. *Proc. Natl. Acad. Sci. USA* **2021**, *118*, e2006050118. [[CrossRef](#)]
20. Rao, S.S.C.; Seaton, K.; Miller, M.; Brown, K.; Nygaard, I.; Stumbo, P.; Zimmerman, B.; Schulze, K. Randomized Controlled Trial of Biofeedback, Sham Feedback, and Standard Therapy for Dyssynergic Defecation. *Clin. Gastroenterol. Hepatol.* **2007**, *5*, 331–338. [[CrossRef](#)]
21. Kautio, A.-L.; Haanpää, M.; Leminen, A.; Kalso, E.; Kautiainen, H.; Saarto, T. Amitriptyline in the Prevention of Chemotherapy-Induced Neuropathic Symptoms. *Anticancer Res.* **2009**, *29*, 2601–2606.
22. Hershman, D.L.; Lacchetti, C.; Loprinzi, C.L. Prevention and Management of Chemotherapy-Induced Peripheral Neuropathy in Survivors of Adult Cancers: American Society of Clinical Oncology Clinical Practice Guideline Summary. *J. Oncol. Pract.* **2014**, *10*, e421–e424. [[CrossRef](#)]
23. Kim, J.H.; Dougherty, P.M.; Abdi, S. Basic Science and Clinical Management of Painful and Non-Painful Chemotherapy-Related Neuropathy. *Gynecol. Oncol.* **2015**, *136*, 453–459. [[CrossRef](#)]
24. Aizpurua-Olaizola, O.; Elezgarai, I.; Rico-Barrio, I.; Zarandona, I.; Etxebarria, N.; Usobiaga, A. Targeting the Endocannabinoid System: Future Therapeutic Strategies. *Drug Discov. Today* **2017**, *22*, 105–110. [[CrossRef](#)]
25. Pacher, P.; Kunos, G. Modulating the Endocannabinoid System in Human Health and Disease—Successes and Failures. *FEBS J.* **2013**, *280*, 1918–1943. [[CrossRef](#)]
26. Skaper, S.D.; Facci, L.; Barbierato, M.; Zusso, M.; Bruschetta, G.; Impellizzeri, D.; Cuzzocrea, S.; Giusti, P. N-Palmitoylethanolamine and Neuroinflammation: A Novel Therapeutic Strategy of Resolution. *Mol. Neurobiol.* **2015**, *52*, 1034–1042. [[CrossRef](#)]
27. di Marzo, V.D.; Skaper, S. Editorial (Hot Topic: Palmitoylethanolamide: Biochemistry, Pharmacology and Therapeutic Use of a Pleiotropic Anti-Inflammatory Lipid Mediator). *CNS Neurol. Disord. Drug Targets* **2013**, *12*, 4–6. [[CrossRef](#)]
28. Re, G.; Barbero, R.; Miolo, A.; Di Marzo, V. Palmitoylethanolamide, Endocannabinoids and Related Cannabimimetic Compounds in Protection against Tissue Inflammation and Pain: Potential Use in Companion Animals. *Vet. J.* **2007**, *173*, 21–30. [[CrossRef](#)]
29. Esposito, E.; Cuzzocrea, S. Palmitoylethanolamide in Homeostatic and Traumatic Central Nervous System Injuries. *CNS Neurol. Disord. Drug Targets* **2013**, *12*, 55–61. [[CrossRef](#)]
30. Petrosino, S.; Schiano Moriello, A.; Cerrato, S.; Fusco, M.; Puigdemont, A.; De Petrocellis, L.; Di Marzo, V. The Anti-Inflammatory Mediator Palmitoylethanolamide Enhances the Levels of 2-Arachidonoyl-Glycerol and Potentiates Its Actions at TRPV1 Cation Channels. *Br. J. Pharmacol.* **2016**, *173*, 1154–1162. [[CrossRef](#)]
31. Iannotti, F.A.; Vitale, R.M. The Endocannabinoid System and PPARs: Focus on Their Signalling Crosstalk, Action and Transcriptional Regulation. *Cells* **2021**, *10*, 586. [[CrossRef](#)]
32. Ho, W.-S.V.; Barrett, D.A.; Randall, M.D. “Entourage” Effects of N-Palmitoylethanolamide and N-Oleoylethanolamide on Vasorelaxation to Anandamide Occur through TRPV1 Receptors. *Br. J. Pharmacol.* **2008**, *155*, 837–846. [[CrossRef](#)]
33. Hohmann, U.; Pelzer, M.; Kleine, J.; Hohmann, T.; Ghadban, C.; Dehghani, F. Opposite Effects of Neuroprotective Cannabinoids, Palmitoylethanolamide, and 2-Arachidonoylglycerol on Function and Morphology of Microglia. *Front. Neurosci.* **2019**, *13*, 1180. [[CrossRef](#)]
34. Lo Verme, J.; Fu, J.; Astarita, G.; La Rana, G.; Russo, R.; Calignano, A.; Piomelli, D. The Nuclear Receptor Peroxisome Proliferator-Activated Receptor-Alpha Mediates the Anti-Inflammatory Actions of Palmitoylethanolamide. *Mol. Pharmacol.* **2005**, *67*, 15–19. [[CrossRef](#)]
35. Bougarne, N.; Weyers, B.; Desmet, S.J.; Deckers, J.; Ray, D.W.; Staels, B.; De Bosscher, K. Molecular Actions of PPAR $\alpha$  in Lipid Metabolism and Inflammation. *Endocr. Rev.* **2018**, *39*, 760–802. [[CrossRef](#)]
36. Koch, M.; Kretz, S.; Böttger, C.; Benz, A.; Maronde, E.; Ghadban, C.; Korf, H.-W.; Dehghani, F. Palmitoylethanolamide Protects Dentate Gyrus Granule Cells via Peroxisome Proliferator-Activated Receptor-Alpha. *Neurotox. Res.* **2011**, *19*, 330–340. [[CrossRef](#)]
37. Di Cesare Mannelli, L.; D’Agostino, G.; Pacini, A.; Russo, R.; Zanardelli, M.; Ghelardini, C.; Calignano, A. Palmitoylethanolamide Is a Disease-Modifying Agent in Peripheral Neuropathy: Pain Relief and Neuroprotection Share a PPAR-Alpha-Mediated Mechanism. *Mediat. Inflamm.* **2013**, *2013*, 328797. [[CrossRef](#)]
38. Malin, S.A.; Davis, B.M.; Molliver, D.C. Production of Dissociated Sensory Neuron Cultures and Considerations for Their Use in Studying Neuronal Function and Plasticity. *Nat. Protoc.* **2007**, *2*, 152–160. [[CrossRef](#)]

39. Tolkovsky, A.M.; Brelstaff, J. Sensory Neurons from Tau Transgenic Mice and Their Utility in Drug Screening. *Methods Mol. Biol.* **2018**, *1727*, 93–105. [[CrossRef](#)]
40. Liebmann, J.; Cook, J.; Lipschultz, C.; Teague, D.; Fisher, J.; Mitchell, J. Cytotoxic Studies of Paclitaxel (Taxol®) in Human Tumour Cell Lines. *Br. J. Cancer* **1993**, *68*, 1104–1109. [[CrossRef](#)]
41. Zasadil, L.M.; Andersen, K.A.; Yeum, D.; Rocque, G.B.; Wilke, L.G.; Tevaarwerk, A.J.; Raines, R.T.; Burkard, M.E.; Weaver, B.A. Cytotoxicity of Paclitaxel in Breast Cancer Is Due to Chromosome Missegregation on Multipolar Spindles. *Sci. Transl. Med.* **2014**, *6*, 229ra43. [[CrossRef](#)] [[PubMed](#)]
42. Musella, A.; Fresegna, D.; Rizzo, F.R.; Gentile, A.; Bullitta, S.; De Vito, F.; Guadalupi, L.; Centonze, D.; Mandolesi, G. A Novel Crosstalk within the Endocannabinoid System Controls GABA Transmission in the Striatum. *Sci. Rep.* **2017**, *7*, 7363. [[CrossRef](#)] [[PubMed](#)]
43. Scuderi, C.; Valenza, M.; Stecca, C.; Esposito, G.; Carratù, M.R.; Steardo, L. Palmitoylethanolamide Exerts Neuroprotective Effects in Mixed Neuroglial Cultures and Organotypic Hippocampal Slices via Peroxisome Proliferator-Activated Receptor- $\alpha$ . *J. Neuroinflammation* **2012**, *9*, 49. [[CrossRef](#)] [[PubMed](#)]
44. Beggiato, S.; Tomasini, M.C.; Cassano, T.; Ferraro, L. Chronic Oral Palmitoylethanolamide Administration Rescues Cognitive Deficit and Reduces Neuroinflammation, Oxidative Stress, and Glutamate Levels in A Transgenic Murine Model of Alzheimer's Disease. *J. Clin. Med.* **2020**, *9*, 428. [[CrossRef](#)] [[PubMed](#)]
45. Pool, M.; Thiemann, J.; Bar-Or, A.; Fournier, A.E. NeuriteTracer: A Novel ImageJ Plugin for Automated Quantification of Neurite Outgrowth. *J. Neurosci. Methods* **2008**, *168*, 134–139. [[CrossRef](#)] [[PubMed](#)]
46. Klein, I.; Lehmann, H. Pathomechanisms of Paclitaxel-Induced Peripheral Neuropathy. *Toxics* **2021**, *9*, 229. [[CrossRef](#)]
47. Mielke, S.; Sparreboom, A.; Mross, K. Peripheral Neuropathy: A Persisting Challenge in Paclitaxel-Based Regimes. *Eur. J. Cancer* **2006**, *42*, 24–30. [[CrossRef](#)]
48. Fukuda, Y.; Li, Y.; Segal, R.A. A Mechanistic Understanding of Axon Degeneration in Chemotherapy-Induced Peripheral Neuropathy. *Front. Neurosci.* **2017**, *11*, 481. [[CrossRef](#)]
49. Cavaletti, G.; Cavalletti, E.; Oggioni, N.; Sottani, C.; Minoia, C.; D'Incalci, M.; Zucchetti, M.; Marmiroli, P.; Tredici, G. Distribution of Paclitaxel within the Nervous System of the Rat after Repeated Intravenous Administration. *Neurotoxicology* **2000**, *21*, 389–393. [[CrossRef](#)]
50. Staff, N.P.; Grisold, A.; Grisold, W.; Windebank, A.J. Chemotherapy-Induced Peripheral Neuropathy: A Current Review. *Ann. Neurol.* **2017**, *81*, 772–781. [[CrossRef](#)]
51. Jamieson, S.M.F.; Liu, J.; Hsu, T.; Baguley, B.C.; McKeage, M.J. Paclitaxel Induces Nucleolar Enlargement in Dorsal Root Ganglion Neurons in vivo Reducing Oxaliplatin Toxicity. *Br. J. Cancer* **2003**, *88*, 1942–1947. [[CrossRef](#)] [[PubMed](#)]
52. Jaggi, A.S.; Singh, N. Mechanisms in Cancer-Chemotherapeutic Drugs-Induced Peripheral Neuropathy. *Toxicology* **2012**, *291*, 1–9. [[CrossRef](#)] [[PubMed](#)]
53. Carlson, K.; Ocean, A.J. Peripheral Neuropathy with Microtubule-Targeting Agents: Occurrence and Management Approach. *Clin. Breast Cancer* **2011**, *11*, 73–81. [[CrossRef](#)] [[PubMed](#)]
54. Yang, I.H.; Siddique, R.; Hosmane, S.; Thakor, N.; Höke, A. Compartmentalized Microfluidic Culture Platform to Study Mechanism of Paclitaxel-Induced Axonal Degeneration. *Exp. Neurol.* **2009**, *218*, 124–128. [[CrossRef](#)] [[PubMed](#)]
55. Barbuti, A.M.; Chen, Z.-S. Paclitaxel Through the Ages of Anticancer Therapy: Exploring Its Role in Chemoresistance and Radiation Therapy. *Cancers* **2015**, *7*, 2360–2371. [[CrossRef](#)]
56. Genovese, T.; Esposito, E.; Mazzon, E.; Paola, R.D.; Meli, R.; Bramanti, P.; Piomelli, D.; Calignano, A.; Cuzzocrea, S. Effects of Palmitoylethanolamide on Signaling Pathways Implicated in the Development of Spinal Cord Injury. *J. Pharmacol. Exp. Ther.* **2008**, *326*, 12–23. [[CrossRef](#)]
57. Donvito, G.; Bettoni, I.; Comelli, F.; Colombo, A.; Costa, B. Palmitoylethanolamide Relieves Pain and Preserves Pancreatic Islet Cells in a Murine Model of Diabetes. *CNS Neurol. Disord. Drug Targets* **2015**, *14*, 452–462. [[CrossRef](#)]
58. Ghafouri, N.; Ghafouri, B.; Larsson, B.; Stensson, N.; Fowler, C.J.; Gerdle, B. Palmitoylethanolamide and Stearoyl ethanolamide Levels in the Interstitium of the Trapezius Muscle of Women with Chronic Widespread Pain and Chronic Neck-Shoulder Pain Correlate with Pain Intensity and Sensitivity. *Pain* **2013**, *154*, 1649–1658. [[CrossRef](#)]
59. D'Agostino, G.; Russo, R.; Avagliano, C.; Cristiano, C.; Meli, R.; Calignano, A. Palmitoylethanolamide Protects Against the Amyloid-B25-35-Induced Learning and Memory Impairment in Mice, an Experimental Model of Alzheimer Disease. *Neuropsychopharmacology* **2012**, *37*, 1784–1792. [[CrossRef](#)]
60. Lambert, D.M.; Vandevoorde, S.; Diependaele, G.; Govaerts, S.J.; Robert, A.R. Anticonvulsant Activity of N-Palmitoylethanolamide, a Putative Endocannabinoid, in Mice. *Epilepsia* **2002**, *42*, 321–327. [[CrossRef](#)]
61. Andresen, S.R.; Bing, J.; Hansen, R.M.; Biering-Sørensen, F.; Johannesen, I.L.; Hagen, E.M.; Rice, A.S.C.; Nielsen, J.F.; Bach, F.W.; Finnerup, N.B. Ultramicrosized Palmitoylethanolamide in Spinal Cord Injury Neuropathic Pain: A Randomized, Double-Blind, Placebo-Controlled Trial. *Pain* **2016**, *157*, 2097–2103. [[CrossRef](#)] [[PubMed](#)]
62. Morsanuto, V.; Galla, R.; Molinari, C.; Uberti, F. A New Palmitoylethanolamide Form Combined with Antioxidant Molecules to Improve Its Effectiveness on Neuronal Aging. *Brain Sci.* **2020**, *10*, 457. [[CrossRef](#)] [[PubMed](#)]

63. Di Cesare Mannelli, L.; Pacini, A.; Corti, F.; Boccella, S.; Luongo, L.; Esposito, E.; Cuzzocrea, S.; Maione, S.; Calignano, A.; Ghelardini, C. Antineuropathic Profile of N-Palmitoylethanolamine in a Rat Model of Oxaliplatin-Induced Neurotoxicity. *PLoS ONE* **2015**, *10*, e0128080. [[CrossRef](#)] [[PubMed](#)]
64. Truini, A.; Biasiotta, A.; Di Stefano, G.; La Cesa, S.; Leone, C.; Cartoni, C.; Federico, V.T.; Petrucci, M.; Cruccu, G. Palmitoylethanolamide Restores Myelinated-Fibre Function in Patients with Chemotherapy-Induced Painful Neuropathy. *CNS Neurol. Disord. Drug Targets* **2011**, *10*, 916–920. [[CrossRef](#)]

## Publication 2

---


The following article [Elfarnawany, A.; Dehghani, F. *Toxics* **2023**] has been published under the terms and conditions of the Creative Commons Attribution (CC BY) license (<https://creativecommons.org/licenses/by/4.0/>) that permits unrestricted use, distribution, and reproduction in any medium under specification of the authors (see the article) and the source (*Toxics* **2023**, 11, 581. <https://doi.org/10.3390/toxics11070581>). The link back to the article on the publisher's website is (<https://www.mdpi.com/journal/toxics>).

### **Contribution as an author:**

I have contributed to the conception and design of the work, formal data analysis, the results interpretation, investigation, data curation, writing original draft preparation, data visualization, data review, and editing.

## Article

# Time- and Concentration-Dependent Adverse Effects of Paclitaxel on Non-Neuronal Cells in Rat Primary Dorsal Root Ganglia

Amira Elfarnawany<sup>1,2</sup> and Faramarz Dehghani<sup>1,\*</sup> 

<sup>1</sup> Department of Anatomy and Cell Biology, Medical Faculty, Martin Luther University Halle-Wittenberg, Grosse Steinstrasse 52, 06108 Halle (Saale), Germany; amira.elfarnawany@science.tanta.edu.eg

<sup>2</sup> Zoology Department, Faculty of Science, Tanta University, Tanta 31527, Egypt

\* Correspondence: faramarz.dehghani@medizin.uni-halle.de

**Abstract:** Paclitaxel is a chemotherapeutic agent used to treat a wide range of malignant tumors. Although it has anti-tumoral properties, paclitaxel also shows significant adverse effects on the peripheral nervous system, causing peripheral neuropathy. Paclitaxel has previously been shown to exert direct neurotoxic effects on primary DRG neurons. However, little is known about paclitaxel's effects on non-neuronal DRG cells. They provide mechanical and metabolic support and influence neuronal signaling. In the present study, paclitaxel effects on primary DRG non-neuronal cells were analyzed and their concentration or/and time dependence investigated. DRGs of Wistar rats (6–8 weeks old) were isolated, and non-neuronal cell populations were separated by the density gradient centrifugation method. Different concentrations of Paclitaxel (0.01  $\mu$ M–10  $\mu$ M) were tested on cell viability by MTT assay, cell death by lactate dehydrogenase (LDH) assay, and propidium iodide (PI) assay, as well as cell proliferation by Bromodeoxyuridine (BrdU) assay at 24 h, 48 h, and 72 h post-treatment. Furthermore, phenotypic effects have been investigated by using immunofluorescence techniques. Paclitaxel exhibited several toxicological effects on non-neuronal cells, including a reduction in cell viability, an increase in cell death, and an inhibition of cell proliferation. These effects were concentration- and time-dependent. Cellular and nuclear changes such as shrinkage, swelling of cell bodies, nuclear condensation, chromatin fragmentation, retraction, and a loss in processes were observed. Paclitaxel showed adverse effects on primary DRG non-neuronal cells, which might have adverse functional consequences on sensory neurons of the DRG, asking for consideration in the management of peripheral neuropathy.

**Keywords:** peripheral neuropathy; DRG non-neuronal cells; paclitaxel; MTT assay; LDH assay; BrdU assay



**Citation:** Elfarnawany, A.; Dehghani, F. Time- and Concentration-Dependent Adverse Effects of Paclitaxel on Non-Neuronal Cells in Rat Primary Dorsal Root Ganglia. *Toxics* **2023**, *11*, 581. <https://doi.org/10.3390/toxics11070581>

Academic Editor: Youssef Sari

Received: 23 May 2023

Revised: 27 June 2023

Accepted: 1 July 2023

Published: 4 July 2023



**Copyright:** © 2023 by the authors. Licensee MDPI, Basel, Switzerland. This article is an open access article distributed under the terms and conditions of the Creative Commons Attribution (CC BY) license (<https://creativecommons.org/licenses/by/4.0/>).

## 1. Introduction

Many chemotherapeutic agents may trigger chemotherapy-induced peripheral neuropathy (CIPN), which manifests as tingling, numbness, and burning pain in both hands and feet [1]. The high incidence of CIPN [2] frequently results in dose reduction or the discontinuation of chemotherapy regimens [2–4]. Additionally, CIPN symptoms can continue for a very long time after chemotherapy, significantly lowering patients' quality of life [5].

Sensory neurons are more vulnerable to the toxic effects of anticancer drugs, and patients with CIPN typically experience more sensory symptoms than those in the motor or autonomic systems [6,7]. Chemotherapeutic drugs cause toxicity in myelin sheaths (myelopathy), sensory cell bodies (neuronopathy), and axonal compartments (axonopathy) in the DRG by affecting ion channels, microtubules, mitochondria, and associated capillaries [7,8]. DRG explants have thus been demonstrated to be a good, simple, and well-accepted model for studying peripheral neuropathy caused by antineoplastic agents [9–11]. Peripheral sensory (somatic) neurons can easily be reached by chemotherapy drugs as they

are located outside the central nervous system without a brain–blood barrier and show strong vascularization due to fenestrated capillaries [12]. Additionally, chemotherapeutic drugs accumulate more in the sensory ganglia than in the peripheral nerves [13,14]. DRG explants' ability to outgrow neurites *in vitro*, as well as their response to toxic substances with neurite shortening, make them a reliable model in drug neurotoxicity assessment [9,15–17].

Primary DRG cultures consist of a diverse population of cells, including differentiated sensory post-mitotic neuronal cells (neurons) and proliferative non-neuronal cells (Satellite glial cells (SGCs), Schwann cells (SCs), and other glial cells) [18–21]. In parallel to the valuable impact of neurons, DRG non-neuronal cells are increasingly recognized as important in the development and maintenance of neuropathic pain [22,23]. SGCs, for instance, provide mechanical and metabolic support for neurons by forming an envelope surrounding their cell bodies [14,24]. Therefore, they closely monitor neuronal functions and interact with neurons using both diffusible (e.g., the paracrine release of glial modulators) and non-diffusive mechanisms (e.g., gap junctions) [25–28]. After nerve injury, SGCs become activated and contribute to the development of neuropathic pain [22,29]. SCs aid in myelinating axons, eliminate cellular debris [30], and play an important role in the outgrowth and guidance of re-growing peripheral axons [31]. SCs not only physically support the long axons, but they also have several growth factors that nourish and myelinate the large associated axons [32–34].

Paclitaxel is one of a wide range of commonly used chemotherapeutic agents. Although it has anti-tumoral properties, it also has significant adverse effects on the peripheral nervous system, causing peripheral neuropathy [2,17,35,36]. Paclitaxel shows neurotoxic effects on DRG neurons, including a significant reduction in neurite length and an increase in neuronal cell bodies at different investigated time points, as reported earlier [17,37]. The effects of paclitaxel on neuronal survival and neurite length in the DRG are shown to be dose- and time-dependent [17,37,38]. However, little is known about the effects of paclitaxel on primary DRG non-neuronal cells. The question is still open as to whether similar paclitaxel toxicity in primary DRG non-neuronal cells exists.

Previous research measured the process areas of non-neuronal cells of the DRG inside the mixed culture of neuronal and non-neuronal cells after 24 h of exposure to paclitaxel and found a decrease in the process areas of the non-neuronal cells [39]. In addition, paclitaxel has been shown to reduce cell viability and change the phenotype of SCs isolated from the sciatic nerve at 24 h and 48 h [31]. A recent study also investigated the impact of paclitaxel on the viability and proliferation of SGCs and found no effect on viability but a decrease in cell proliferation [14]. However, more research is needed to fully understand paclitaxel toxicity in the entire culture of non-neuronal cells (SCs, SGCs, and other glial cells). These outcomes may shed more light on the potential functional consequences of paclitaxel on primary DRG sensory neurons and the therapeutic interventions for peripheral neuropathy.

Therefore, the aim of this study was to investigate the effects of paclitaxel on primary DRG non-neuronal cells and determine the time course of those changes. DRG non-neuronal cells were isolated and treated with different concentrations of paclitaxel at different time points. Effects on viability, morphology, and proliferation were analyzed. We applied approaches such as the MTT assay to study cell viability [40], the lactate dehydrogenase (LDH) assay [41], and the propidium iodide (PI) assay to study cell death [42], as well as Bromodeoxyuridine (BrdU), to study cell proliferation [43]. These approaches are frequently employed in related studies [14,44–46]. We hypothesized that paclitaxel exposure would have severe toxic effects on DRG non-neuronal cells, which might be dose- or/and time-dependent.

## 2. Materials and Methods

### 2.1. Ethics Statement

All research involving animal material was carried out in accordance with the ethics policy and the policy on animal use in neuroscience research as outlined in Directive 2010/63/EU of the European Parliament and of the Council of the European Union on the protection of animals used for scientific purposes and was approved by local authorities for laboratory animal care and use (State of Saxony-Anhalt, Germany, permission number: I11M27).

### 2.2. Materials

Paclitaxel was used and administered into culture media in accordance with the treatment protocol (Taxol equivalent, Invitrogen, cat No. P3456-5 mg, Schwerte, Germany). Dimethyl sulfoxide (DMSO, Sigma–Aldrich, cat. No. D4540-500 mL, Lyon, France) was used to dissolve paclitaxel to obtain stock solutions of 1 mM and stored at  $-20\text{ }^{\circ}\text{C}$ .

### 2.3. Isolation and Preparation of Primary DRG Co-Culture

DRG tissues were isolated from Wister rats aged 6–8 weeks. Rats were deeply anesthetized before scarification by isoflurane (Florene, 100% (v/v), 250 mL, Abcam, cat No. B506, France). Under aseptic conditions, the vertebral column was isolated, and all surrounding muscle, fat, and soft tissue were carefully removed. The spinal cord was exposed, and after that, DRGs were located, removed, and collected from intervertebral foramina on both sides in a sterile dish containing 3 mL of Hanks balanced salt solutions without  $\text{Mg}^{2+}/\text{Ca}^{2+}$  (HBSS, Invitrogen, REF. 24020-091, Schwerte, Germany) (Figure S1). The culture of non-neuronal cells was conducted in accordance with a previously published protocol [47], with some modifications. In brief, isolated DRGs were enzymatically digested in the first enzymatic solution containing 60 U/mL papain (Sigma–Aldrich, cat No. P4762-100 mg, St. Louis, MO, USA), 3  $\mu\text{L}$  of 80 mg/mL saturated sodium hydrogen carbonate ( $\text{NaHCO}_3$ , Merck, cat No. k22399729, Darmstadt, Germany), and 0.6 mg/mL L-Cysteine (L-Cys, Sigma–Aldrich, Cat No. C7352-25 g, St. Louis, MO, USA) dissolved in 1.5 mL of HBSS without  $\text{Mg}^{2+}/\text{Ca}^{2+}$ . DRGs were then incubated for 15 min in a  $37\text{ }^{\circ}\text{C}$  water bath before being incubated in the second solution containing 4 mg/mL collagenase type II solution (CLS2, Sigma–Aldrich, Cat No. C6885-1 gm, St. Louis, MO, USA) and 4.6 mg/mL dispase type II (Dispase II, Sigma–Aldrich, Cat No. D4693-1 gm, St. Louis, MO, USA) solution in 3 mL HBSS without  $\text{Mg}^{2+}/\text{Ca}^{2+}$ . The DRGs were gently mixed with collagenase solution and incubated for an additional 15 min at  $37\text{ }^{\circ}\text{C}$ .

The resulting cell suspension underwent a one-minute centrifugation at 200 g. After carefully aspirating the collagenase solution, the DRGs were triturated 10–15 times with 1 mL of F12 medium (1X, Invitrogen, REF.11765-054, Schwerte, Germany) supplemented with 10 % of heat-inactivated Fetal Bovine Serum (FBS, Invitrogen, REF. 10270-106, Schwerte, Germany) and 1 % of 0.1 mg/mL streptomycin/penicillin (Sigma–Aldrich, cat No. P4333/100 mL, Darmstadt, Germany) by using 1000  $\mu\text{L}$  pipette tips till the cell suspension became cloudy.

### 2.4. Seeding and Growth of Primary DRG Co-Culture

Circular coverslips were pre-coated for at least 1 h or overnight at  $4\text{ }^{\circ}\text{C}$  with 2 mg/mL Poly-D-lysine (PDL, Sigma–Aldrich, cat No. P6407, St. Louis, MO, USA) and 0.2 mg/mL laminin (Sigma–Aldrich, cat No. L2020-1 mg, St. Louis, MO, USA), then washed once with dist.  $\text{H}_2\text{O}$  and added directly before seeding cells in the culture medium. DRGs (50,000 cells) co-cultured in 50  $\mu\text{L}$  culture medium were then pre-seeded on the coated coverslips for 2 h in an incubator at  $37\text{ }^{\circ}\text{C}$  and with 5%  $\text{CO}_2$ . One mL of warm culture medium adjusted to pH 7.4 was gently added to cells per well and maintained at  $37\text{ }^{\circ}\text{C}$  with 5%  $\text{CO}_2$ . Growth and morphology of co-cultivation of neurons and non-neurons were observed after 24 h, 72 h, 7 days, and 10 days (Figure 1a).

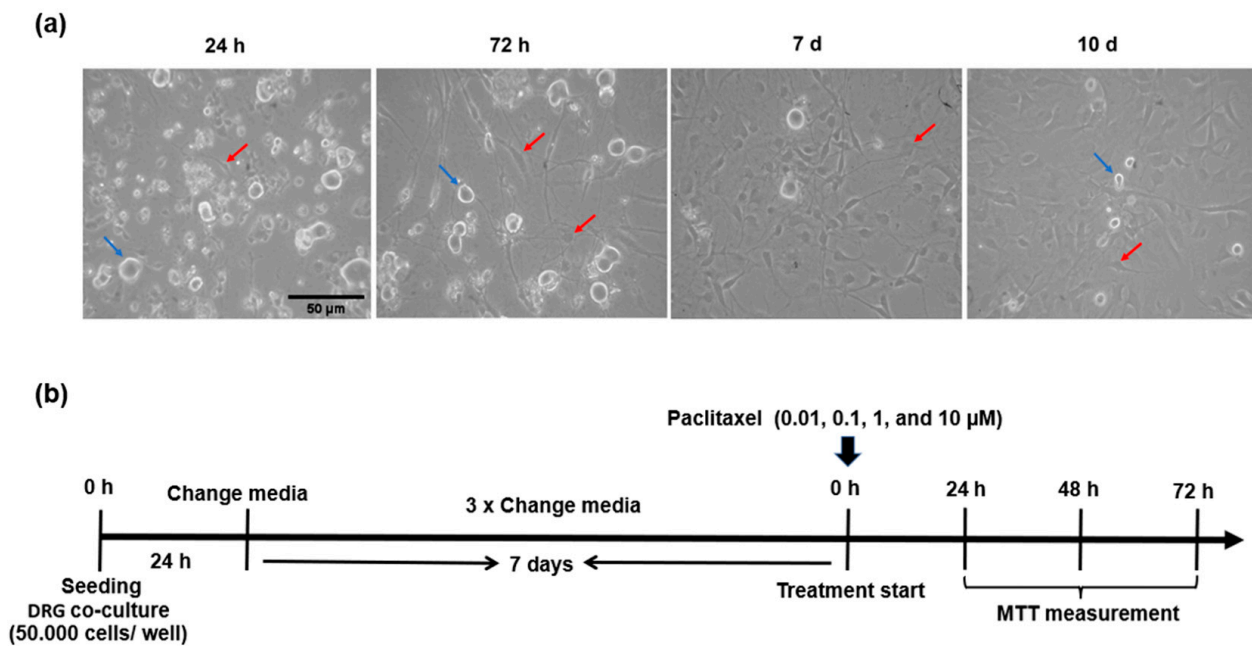


**Figure 1.** Morphological features and treatment protocol of primary DRG co-culture. (a) Representative images show the morphology and growth of DRG co-culture at different time points, blue arrows indicate neuronal populations, while red arrows indicate different subpopulations of DRG non-neuronal cells, Scale bar = 50  $\mu\text{m}$ . (b) Treatment protocol for studying the effects of paclitaxel on DRG co-culture viability by using MTT assays at 24 h, 48 h, and 72 h post-treatment.

### 2.5. Effects on Cell Viability of Primary DRG Co-Culture (MTT Assay)

DRG co-cultured cells ( $5 \times 10^4$  cells/well) were treated 8 days after seeding with different concentrations of paclitaxel (0.01–10  $\mu\text{M}$ ) at 24 h, 48 h, and 72 h post-treatment in 96 well plates to study the effects on cell viability (Figure 1b). Four concentrations were then chosen that were as close to clinically applied doses as possible. Furthermore, the selected paclitaxel concentrations are in line with earlier reports from the literature [37–39,48–51]. Cell viability (%) was measured at 24 h, 48 h, and 72 h post-treatment using MTT assay. Four hours prior to the end of the experiments at various time points, 3-(4,5-dimethylthiazol-2-yl)-2,5-diphenyltetrazolium bromide solution (MTT, Invitrogen, cat. No M6494, 5 mg/mL, Eugene, OR, USA) was added. After an additional 4 h of incubation, the MTT solution was removed from the cells, and formazan crystals were dissolved in 100  $\mu\text{L}$  of DMSO. Absorbance values were determined at two wavelengths (540 nm and 720 nm) by a microplate reader (SynergyTMMx, BioTek Instruments, Winooski, VT, USA) after another 20 min. Co-cultures maintained in standard media without paclitaxel were used as the control group. To rule out any effects of the solvent on cell viability, controls had DMSO at the same highest concentration (0.1%) as those used in other groups. For each treatment, three technical replicas were used in three biologically independent experiments.

### 2.6. Separation of Primary DRG Non-Neuronal Cells

To separate non-neuronal cells, density gradient centrifugation was applied by using bovine serum albumin (BSA, Sigma Aldrich, cat No.A7906-10 G, St. Louis, MO, USA) (15% (*w/v*) BSA solution) for purification [52]. The DRGs were triturated 10–15 times in 1 mL of high-glucose Dulbecco's Modified Eagle Medium (DMEM; Invitrogen; Ref. 41965-039; Schwerte, Germany) supplemented with 10 % FBS. Non-neuronal cells were separated from the DRG mixed culture by centrifuging single-cell suspensions through a 15% (*w/v*) BSA solution in DMEM. One milliliter of cell suspension was added to three milliliters of 15% BSA solution in a 15 mL conical tube and centrifuged at 300 g for 8 min at room temperature (RT) (Figure S1b). Thereafter, the layer of non-neuronal cells was carefully transferred to



a 15 mL conical tube by using 1000  $\mu$ L pipette tips. Then, 1 mL of warmed F12 medium supplemented with 10% FBS and 1% of 0.1 mg/mL streptomycin/penicillin was added, and the DRG non-neurons were suspended. A 40  $\mu$ m cell strainer (SARSTEDT, cat. no. D-51588, Schwerte, Germany) was then used to filter the cell suspension to remove cell debris and undigested tissue fragments.

### 2.7. Seeding and Growth of Primary DRG Non-Neuronal Cells

Sterilized 12 mm circular coverslips were used, and they were washed and dried once with dist. H<sub>2</sub>O. 50,000 cells resuspended in 50  $\mu$ L culture medium were then pre-seeded on the sterilized coverslips for 2 h in an incubator at 37 °C and with 5% CO<sub>2</sub>. One mL of warm culture medium adjusted to pH 7.4 was gently added to the cells, which were then preserved at 37 °C with 5% CO<sub>2</sub>. Growth and morphology of DRG non-neuronal cells were observed after 24 h, 48 h, 72 h, 96 h, and 7, 10 days.

### 2.8. Effects of Paclitaxel on DRG Non-Neuronal Cells

#### 2.8.1. Cell Viability (MTT Assay)

In 96 well plates, non-neuronal cells ( $15 \times 10^3$  cells/well) were seeded for 7 days, followed by treatment with four different concentrations of paclitaxel (0.01  $\mu$ M, 0.1  $\mu$ M, 1  $\mu$ M, and 10  $\mu$ M) at three different time points: 24 h, 48 h, and 72 h post treatment (Figure 2a). The effects of paclitaxel on the cell viability of non-neuronal cells were measured by MTT assay, as described above in Section 2.5.

#### 2.8.2. Determination of Cytotoxicity (LDH Assay)

In 24 well plates, DRG non-neuronal cells ( $7 \times 10^3$  cells/well) were seeded in DMEM/F12 free phenol red medium (1X, Gibco, REF.21041-025, Schwerte, Germany) supplemented with 10 % inactivated FBS and 1% of 0.1 mg/mL streptomycin/penicillin for 7 days, followed by treatment with four different concentrations of paclitaxel (0.01  $\mu$ M, 0.1  $\mu$ M, 1  $\mu$ M, and 10  $\mu$ M) prepared in culture media supplemented with 1% FBS at different time points: 24 h, 48 h, and 72 h post treatment (Figure 2b). Additional wells were filled without cells for culture media control (blank). For determination of maximum LDH release (positive LDH control, 100 % cell death), 1:10 of the LDH lysis kit (LDH, Sigma Aldrich, cat. No. TOX7, St. Louis, MO, USA) was added to some wells and incubated for 45 min. According to the manufacturer's instructions, culture media samples from cells or controls at certain time points were transferred to 1.5 mL tubes and then centrifuged at  $250 \times g$  for 4 min to pellet cells. Afterward, 40  $\mu$ L of the supernatant of different samples was added in 5 replicates to a clean flat-bottom 96-well plate and proceeded with enzymatic analysis. The LDH assay mixture was prepared at the time of use by adding 20  $\mu$ L per well. The plates were covered with aluminum foil for light protection and incubated at room temperature for 30 min. The reaction was then stopped by adding 6  $\mu$ L of 1 N Hydrochloric acid (HCl, Sigma Aldrich, cat. No. H9892, St. Louis, MO, USA) to each well. Absorbance values of samples were measured at a wavelength of 490 nm and the background absorbance of multi-well plates at 690 nm. Background absorbance values were subtracted from the primary wavelength measurements (490 nm). Finally, all controls, samples, and maximal measurements were normalized with blank measurements. Then the percent of cytotoxicity was calculated according to the below equation [53].

$$\% \text{ Cell death} = \frac{(\text{sample absorbance value} - \text{mean control value})}{(\text{mean complete kill result} - \text{mean control value})} \times 100$$

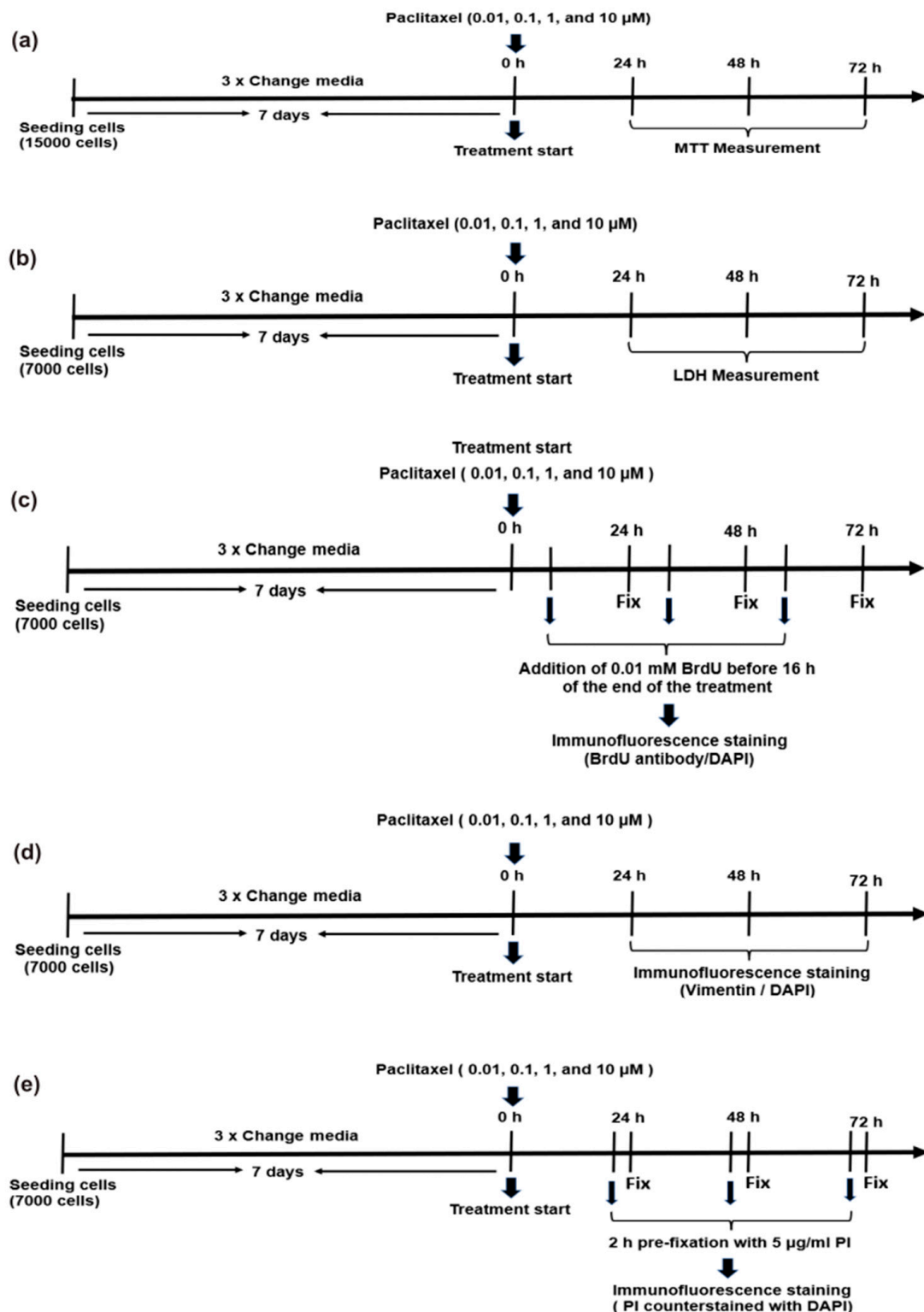


**Figure 2.** Various treatment protocols investigate the effects of different paclitaxel concentrations on primary DRG non-neuronal cells after 24 h, 48 h, and 72 h of the application. (a) The MTT assay was used for cell viability determination; (b) the LDH assay for cytotoxicity measurements; (c) the BrdU assay was used to detect cell proliferation; (d) treatment protocol for studying the effects of paclitaxel on cellular morphology through immunofluorescence staining; (e) detection of cell death by using the PI assay.

### 2.8.3. Detection of Cell Proliferation by BrdU Assay

To investigate the effects of paclitaxel on cell proliferation, DRG non-neuronal cells ( $7 \times 10^3$  cells/well) were seeded on 12 mm sterile coverslips in a 24 well plate, cultured for 7 days, and treated with various concentrations of paclitaxel at different time windows. Four  $\mu\text{L}$  of 0.01 mM 5-bromo-2'-deoxyuridine (BrdU, Sigma Aldrich, cat No. B5002-1G, St. Louis, MO, USA) was added to each well 16 h before fixation (Figure 2c). Cells were either immediately subjected to immunofluorescence or stored in 0.02 M PBS at 4 °C pending further use after fixation with 4% paraformaldehyde (PFA, AppliChem, cat No. 141451.1211, Darmstadt, Germany) for 15 min at room temperature. For labeling, non-specific bindings were blocked with normal goat serum (NGS, Sigma–Aldrich, cat. No. G9023-10 mL, Taufkirchen, Germany, 1:20) in 0.02 M PBS/0.3% (*v/v*) plus triton X-100 for 30 min. Thereafter, cells were washed three times with 0.02 M PBS for ten minutes each and incubated with a monoclonal mouse anti-BrdU antibody (Dako, cat. No. M0744-1 mL, Glostrup, Denmark, 1:200) overnight. Coverslips were then incubated with the goat anti-mouse Alexa Fluor® 488 conjugated secondary antibody (Life Technologies, cat. no. 2066710, Darmstadt, Germany, 1:200) for 1 h washed three times with PBS/triton for ten minutes. By using DAPI (4',6-Diamin-2-phenylindol, Sigma–Aldrich, Munich, Germany, cat No. D9542), nuclei were visualized, and coverslips were mounted with DAKO fluorescence mounting medium (DAKO, Agilent Technologies, Inc., Santa Clara, CA 95051, USA). A confocal laser scanning microscope (Leica DMI8, Wetzlar, Germany) was used to take photomicrographs from five to eight randomly chosen areas. BrdU-positive cells were manually counted with Image J's multipoint tool (version 1.46r, National Institutes of Health, Laboratory for Optical and Computational Instrumentation, University of Wisconsin, Madison, WI, USA), and the percentage of proliferating cells was determined by dividing the number of BrdU<sup>+</sup> cells by the total number of DAPI-stained nuclei. To obtain the data, three independent experiments were conducted.

### 2.8.4. Determination of Paclitaxel Effects on Cellular Morphology

To study the effects of paclitaxel on the morphology of DRG non-neuronal cells, cells ( $7 \times 10^3$  cells/well) were seeded on 12 mm sterile coverslips in a 24 well plate, cultured for 7 days to allow nearly all cells to proliferate, and then treated with various concentrations of paclitaxel at different time windows (Figure 2d). After fixation, the immunofluorescence staining procedure was followed as described in Section 2.8.3. Chicken anti-vimentin polyclonal primary antibody (Abcam, cat No. ab24525, Cambridge, UK, 1:1000) combined with goat anti-chicken IgY Alexa Fluor® 488 conjugated (Invitrogen, REF. A11039-0.5 mL, Eugene, OR, USA, 1:200) as secondary antibody was used for labeling the cytoskeleton of non-neuronal cells. Then the procedure is completed as previously described in Section 2.8.3. Images were taken with a Leica confocal laser scanning microscope (Leica DMI8, Wetzlar, Germany), and five to eight areas were randomly captured per coverslip in three independent experiments.

### 2.8.5. Analysis of Apoptosis by Assessment of Nuclear Morphology

DRG non-neuronal cells were stained with the DNA dye DAPI to visualize nuclear morphology. The percentage of apoptosis (early and late apoptosis) was quantitated by scoring the percentage of apoptotic cells in the adherent cell population. Stained nuclei with a uniform and regular morphology were scored manually as healthy and viable cells. Cells with condensed, fragmented, or blubber nuclei were scored as apoptotic cells. The total number of nuclei in non-neuronal cells was counted automatically using Fiji software (<https://imagej.net/Fiji/Downloads>). After converting DAPI images into 8-bit gray scale images, the threshold of nuclei was adjusted manually, and the separation of attached nuclei was performed by applying a binary watershed. Finally, the analyzing particles option was applied, and the total number of nuclei was determined per image (Figure S2). Photomicrographs were captured using a Leica (DMI8, Wetzlar, Germany) confocal laser

scanning microscope, and five to eight areas were recorded per each coverslip randomly in three independent experiments.

### 2.8.6. Detection of Cell Death by Propidium Iodide Staining

For detection of degenerating non-neuronal nuclei of dead cells by late apoptosis or necrosis, cells ( $7 \times 10^3$  cells/well) were seeded on 12 mm sterile coverslips in a 24 well plate, cultured for 7 days, and then treated with various concentrations of paclitaxel at 24 h, 48 h, and 72 h after treatment. Then, 5  $\mu\text{g}/\text{mL}$  propidium iodide (PI, Merk, cat No. 537059-50 mg, Darmstadt, Germany) was added 2 h before fixation. Afterwards, cells were washed three times with PBS and then fixed with 4% PFA for 15 min (Figure 2e). Coverslips were washed three times with PBS/triton and incubated with DAPI. All stained slides were washed with aqua distilled water before being covered with a DAKO fluorescence mounting medium. Images were captured using a Leica (DMi8, Wetzlar, Germany) confocal laser scanning microscope, and five to eight areas were recorded per each coverslip randomly in three independent experiments. For the detection of PI-labeled dead cells, monochromatic light at 543 nm and an emission bandpass filter of 585–615 nm was used. PI-positive cells were counted manually using the multipoint tool of Image J software version v1.46r.

### 2.9. Statistical Analysis

GraphPad Prism 8.0.1 for Windows (GraphPad Software, La Jolla, CA, USA, [www.graphpad.com](http://www.graphpad.com), accessed on 22 May 2023) was used for data analysis and visualization. All the data were checked for normality using the Kolmogorov–Smirnov test. Statistics were performed using a one-way ANOVA (analysis of variance) followed by a Bonferroni post-test, with significance set at  $p < 0.05$ . All tests had an alpha level of 0.05.

## 3. Results

### 3.1. Characterization of Primary DRG Co-Culture

The growth of DRG co-culture was checked at different timelines (1, 3, 7, and 10 days) by a light microscope. DRG co-culture is a heterogeneous population of neuronal and non-neuronal cells. DRG neurons were characterized by refractile and bright cell bodies, and three different subpopulations were observed according to the size of their somata (small,  $\leq 599 \mu\text{m}^2$ ; medium, 600–1199  $\mu\text{m}^2$  and large, 1200–1300  $\mu\text{m}^2$ ), which represented 67%, 31%, and 2% of neurons in culture, respectively [37]. Additionally, three different subpopulations of DRG non-neuronal cells were observed in the culture (SCs, SGCs, and fibroblasts) (Figure 1a).

### 3.2. Effects of Paclitaxel on Viability of Primary DRG Co-Culture by MTT Assay

DRG co-cultures (neurons and non-neuronal cells) were treated with different concentrations of paclitaxel for 24 h, 48 h, and 72 h post-treatment. At 24 h post-treatment, the four different concentrations of paclitaxel showed no significant effects on the viability of DRG co-culture in comparison with the control group ( $p > 0.05$ ) (Figure 3a). However, all paclitaxel concentrations demonstrated a significant suppression in the viability of cells in DRG co-culture compared to the control group at 48 h and 72 h post-treatment ( $p < 0.0001$ ) (Figure 3b,c).

### 3.3. Characterization of Primary DRG Non-Neuronal Cells

DRG non-neuronal cells were examined under a light microscope at different time points (1, 2, 3, 4, 7, and 10 days) to analyze their growth and morphology. DRG non-neuronal cells are divided into three different subpopulations. The first population are SCs, which represent the majority of DRG non-neuronal cells [20,21]. They are distinguished by a single, small, spindle-shaped nucleus. These cells have a thin layer of cytoplasm surrounding the nucleus and bipolar cell bodies with long, thin projections or processes extending from each side. These long processes can either form a dense bundle of fibers or travel in a single thread of fibers away from the cell body (Figure 4). The population of

SGCs shows small, round, and flat cell bodies with wide cytoplasmic projections (Figure 4). These cells play a crucial role in the formation of an enveloping layer around DRG neurons for protection and metabolism. Lastly, fibroblasts are found under SCs with a large flat cell body and are pyramidal in shape with multipolar wide projections that are not associated with any other fibers. These cells are secretory active and form the connective tissue that supports cells in the culture (Figure 4).

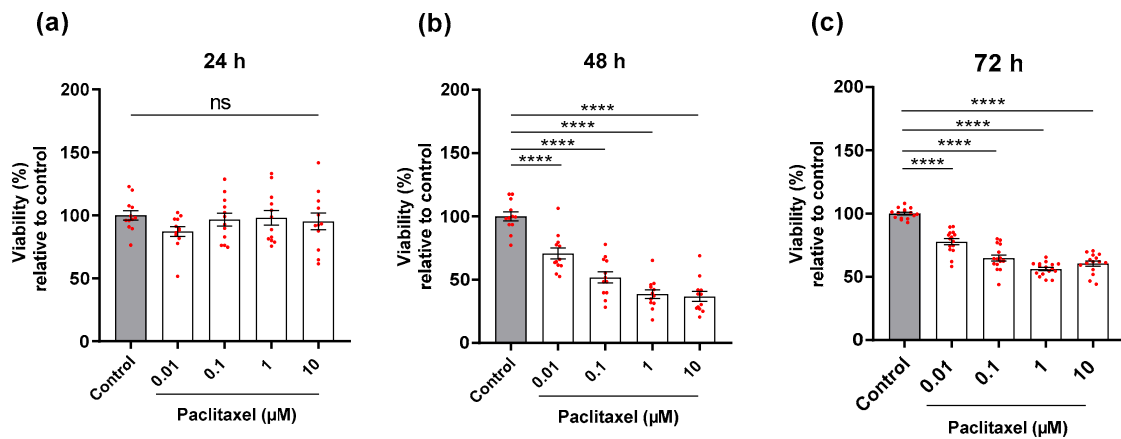


**Figure 3.** Effects of different paclitaxel concentrations on viability (%) of DRG co-culture at 24 h, 48 h, and 72 h post-treatment by MTT assay. (a) No significant effect on viability was found in co-cultures compared to controls at 24 h post-treatment ( $p > 0.05$ ). (b) 48 h, and (c) 72 h post-treatment, paclitaxel displayed a significant reduction in the viability of cells compared to the control (\*\*\*\*  $p < 0.0001$ ). The asterisks depict statistically significant results regarding the respective measurement indicated with the bar. Values are served as the mean  $\pm$  SEM of three independent experiments performed in triplicate. ns, non-significant.

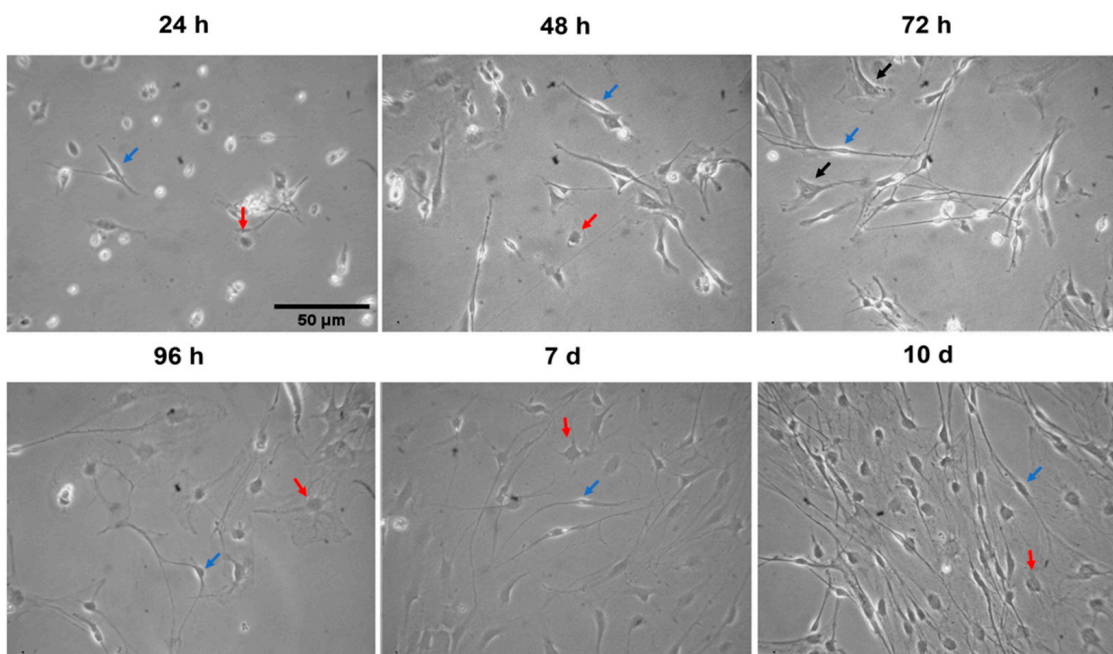


**Figure 4.** Representative phase contrast images show the morphology and growth of primary DRG non-neuronal cells at various time points. Blue arrows indicate Schwann cells, red arrows satellite glial cells, and black arrows represent fibroblasts, Scale bar = 50  $\mu$ m.

### 3.4. Effects of Paclitaxel on Primary DRG Non-Neuronal Cells

#### 3.4.1. Cell Viability (MTT Assay)

DRG non-neuronal cells were exposed to various concentrations of paclitaxel for 24 h, 48 h, and 72 h post-treatment. Only 10  $\mu\text{M}$  of paclitaxel showed a significant reduction in the viability of cells compared to the control group at 24 h post-treatment ( $p < 0.05$ ) (Figure 5a). While, at 48 h and 72 h post-treatment, different paclitaxel concentrations showed a significant reduction in the viability of non-neuronal cells compared to the untreated control group ( $p < 0.05$ ) (Figure 5b,c). At 72 h post-treatment, the effects of paclitaxel on the viability of non-neuronal cells were clearly concentration-dependent (Figure S3a). Notably, the effects of 10  $\mu\text{M}$  paclitaxel on the viability of non-neuronal cells were only time- but not concentration-dependent (Figure S3b).

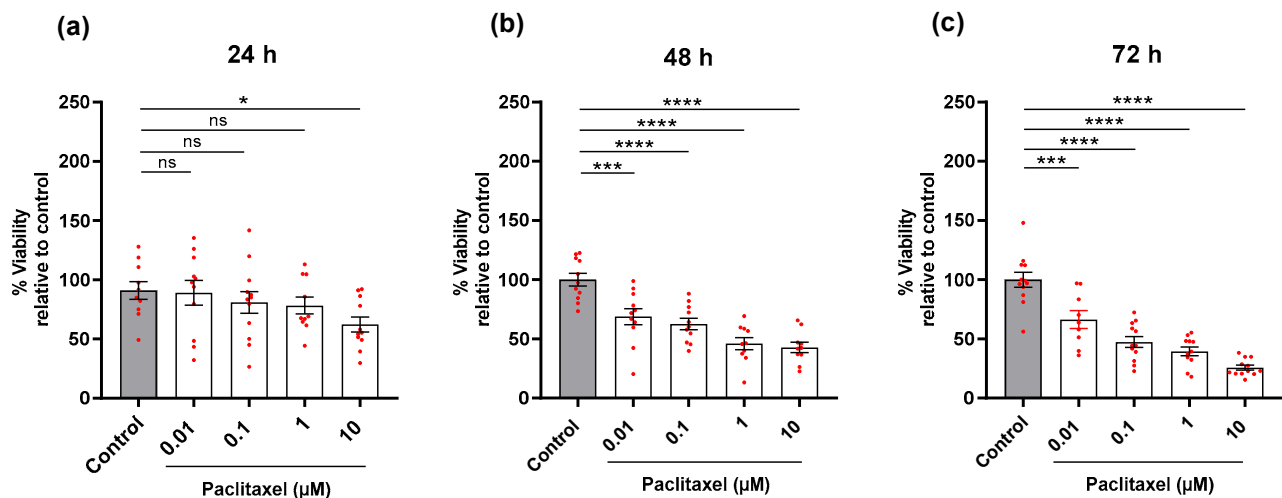


**Figure 5.** Effects of different concentrations of paclitaxel on the viability (%) of DRG non-neuronal cultures at 24 h, 48 h, and 72 h post-treatment by using MTT assay. (a) 10  $\mu\text{M}$  of paclitaxel was the only concentration that showed a significant effect on the viability of DRG non-neuronal cells compared to control at 24 h post-treatment (\*  $p < 0.05$ ). (b,c), Different concentrations of paclitaxel elucidated a significant reduction in the viability of cells compared to the control at 48 h and 72 h post-treatment (\*\*  $p < 0.01$ , \*\*\*\*  $p < 0.0001$ ). The asterisk denotes significant results regarding the respective measurement indicated with the bar. Values are served as mean  $\pm$  SEM of three independent experiments performed in triplicate, ns: non-significant.

#### 3.4.2. Determination of Cytotoxicity (LDH Assay)

The treatment of DRG non-neuronal cells with different paclitaxel concentrations (0.01  $\mu\text{M}$ , 0.1  $\mu\text{M}$ , 1  $\mu\text{M}$ , and 10  $\mu\text{M}$ ) resulted in a significant increase in the number of damaged or dead cells that was proportional to the amount of LDH released in the cell culture media compared to non-treated cells ( $p < 0.0001$ ) at 24 h after treatment (Figure 6a). After 48 h of treatment, the cytotoxicity of the four concentrations of paclitaxel increased remarkably compared to the control ( $p < 0.0001$ ) (Figure 6b). The increase in the number of dead cells in response to the exposure of non-neuronal cells to paclitaxel continued in comparison to the control group ( $p < 0.0001$ ) at 72 h post-treatment (Figure 6c). It was obvious that the effects of different paclitaxel concentrations on cytotoxicity were dose-dependent at only 72 h post-treatment (Figure S4a). Furthermore, a considerable difference was observed between different investigated time points for all applied concentrations, indicating time-dependent effects (Figure S4b).

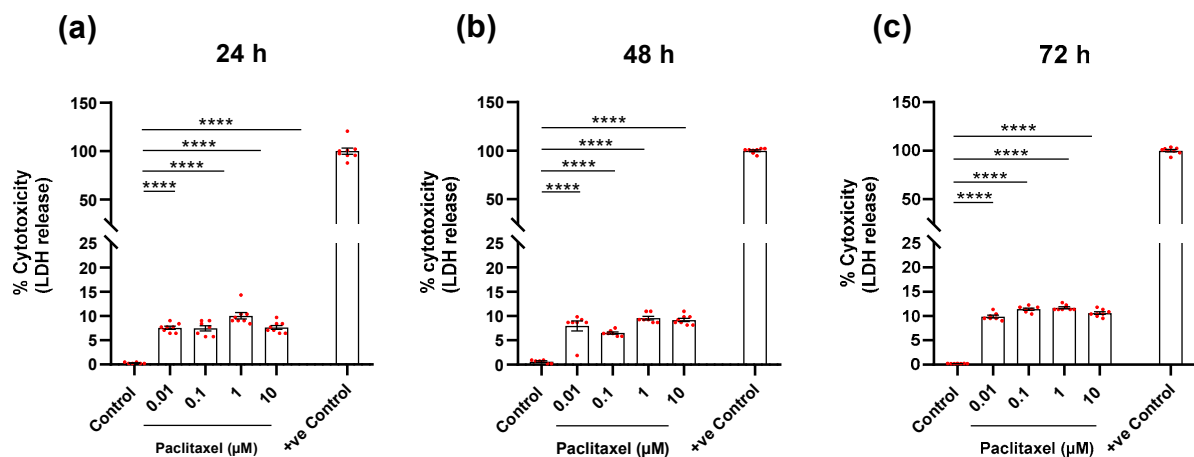


**Figure 6.** Effects of different concentrations of paclitaxel on cytotoxicity of DRG non-neuronal cultures using lactate dehydrogenase (LDH) assay. Levels of released LDH were quantified at (a) 24 h, (b) 48 h, and (c) 72 h post-treatment and showed a significant increase in LDH release that was proportional to the number of dead or damaged cells compared to the control group (\*\*\*\*  $p < 0.0001$ ). +ve Control represents the maximum release of LDH after 100% cell death. The asterisks denote significant results regarding the respective measurement indicated with the bar. Values are given as the mean  $\pm$  SEM of three independent experiments conducted in 15 replicates.

### 3.4.3. Cell Proliferation by BrdU Assay

The percentage of BrdU immunoreactive cells was determined in non-neuronal cells after exposure to various concentrations of paclitaxel at 24 h, 48 h, and 72 h post-treatment. At all investigated time points, a significantly lower number of BrdU-positive cells was found in treated cultures with different paclitaxel concentrations compared to the vehicle control group ( $p < 0.0001$ ) (Figure 7a–d). As no significant difference was detected between different paclitaxel concentrations, no concentration-dependent effect was assumed (Figure S5a). In contrast, a significant difference between different timelines for all applied concentrations of paclitaxel was found, revealing a time-dependency of anti-proliferative effects (Figure S5b).

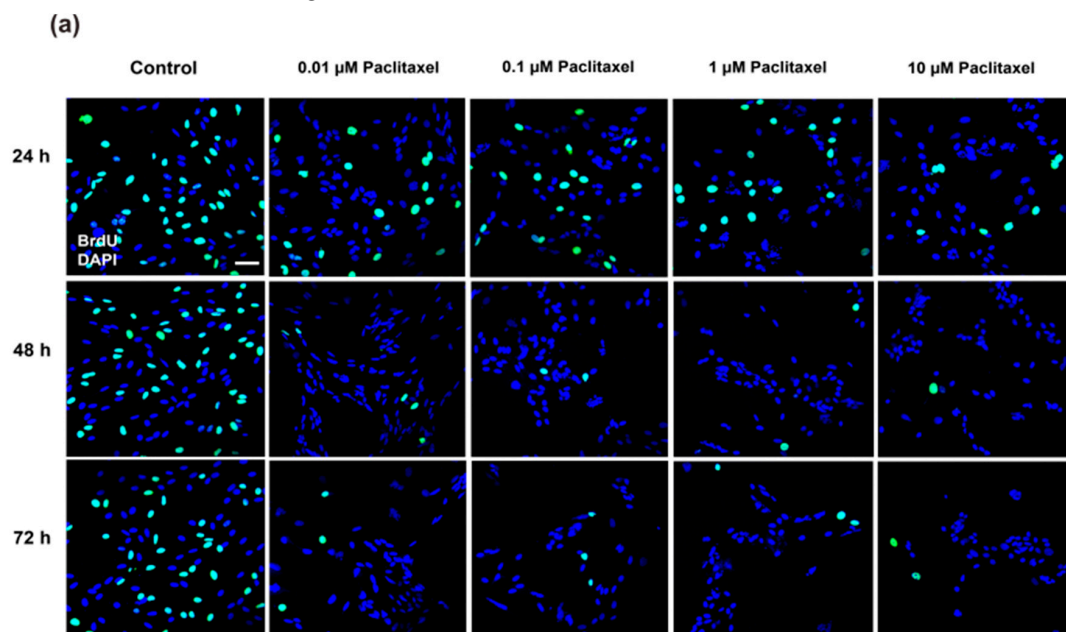


**Figure 7.** Cont.

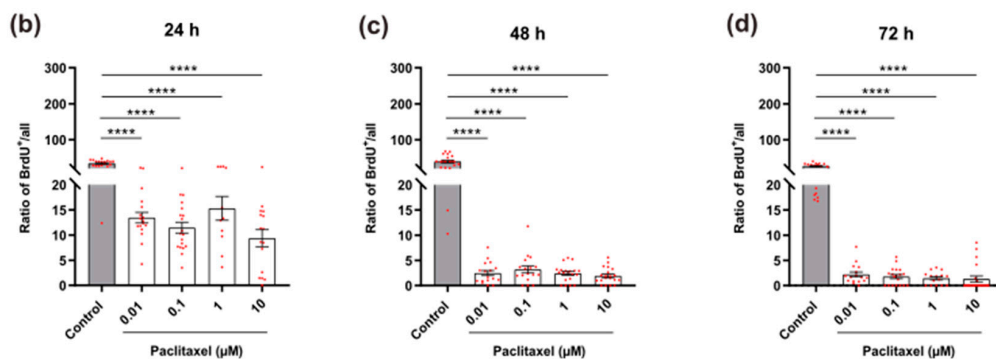


**Figure 7.** Effects of different concentrations of paclitaxel on cell proliferation of DRG non-neuronal cells using BrdU assay. (a) Representative immunofluorescence images of different non-neuronal cells treated with 0.01  $\mu\text{M}$ , 0.1  $\mu\text{M}$ , 1  $\mu\text{M}$ , and 10  $\mu\text{M}$  paclitaxel at 24 h, 48 h, and 72 h post-treatment show proliferating cells labeled with BrdU antibody (green) and all nuclei stained with DAPI (blue). 5–8 areas were recorded randomly per each coverslip; Scale bar = 75  $\mu\text{m}$ . Bar charts demonstrated a significant decrease in the rate of cell proliferation after treatment compared to the control group (\*\*\*\*  $p < 0.0001$ ) at (b) 24 h, (c) 48 h, and (d) 72 h post-treatment. The asterisks denote significant results regarding the respective measurement indicated with the bar. Values served as the mean  $\pm$  SEM of three independent experiments performed in 15 replicates.

#### 3.4.4. Cellular Morphological Changes

Except for 0.01  $\mu\text{M}$ , all applied paclitaxel concentrations showed hallmarks of cell death and a variety of toxic alterations to the morphology of non-neuronal cells, including cell shrinkage, swollen cell bodies, or reductions in the length of processes. Additionally, other morphologic changes were observed in nuclei, such as nuclear fragmentation and chromatin condensation (Figure 8). The number of viable DRG non-neuronal cells was significantly reduced ( $p < 0.05$ ) compared to the control group at all time windows (Figure 8).

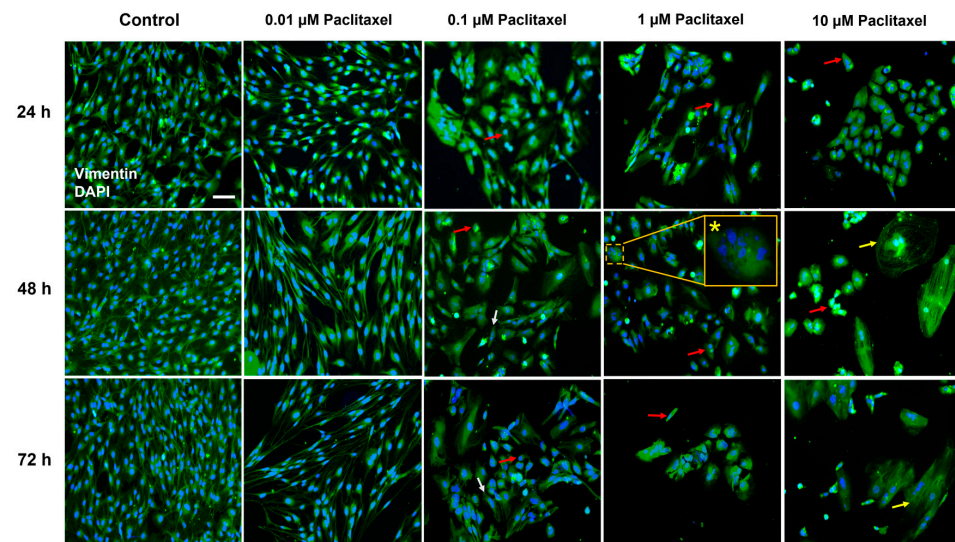


**Figure 8.** Effects of various paclitaxel concentrations on cellular morphology at different investigated time points using immunofluorescence staining. Representative microphotographs demonstrate cells stained with vimentin antibody (green) and nuclei counterstained with DAPI (blue). Paclitaxel (0.1  $\mu\text{M}$ , 1  $\mu\text{M}$ , and 10  $\mu\text{M}$ ) strongly affected the cell morphology of non-neuronal cells including shrinkage of cells' bodies (red arrows) and retraction of processes (white arrows). In addition, some cells treated with 10  $\mu\text{M}$  paclitaxel were swelling (yellow arrows). Additionally, nuclear changes were observed, such as nuclear fragmentation (indicated by an asterisk in the inlet) and condensation. Five to eight regions were recorded randomly per coverslip by fluorescence microscopy. Scale bar = 75  $\mu\text{m}$ .



### 3.4.5. Analysis of Changes in Nuclear Morphology

The effects of paclitaxel on nuclear morphology were investigated 24 h, 48 h, and 72 h after treatment. Paclitaxel induces nuclear fragmentation and condensation, which are hallmarks of apoptosis (Figure 9a). Different paclitaxel concentrations revealed a substantially increased number of apoptotic cells when compared to the control group ( $p < 0.05$ ) at all investigated time points (Figure 9b–d). There was a significant difference between paclitaxel concentrations, indicating concentration dependence at the various time points studied (Figure S6a). Moreover, there was a significant difference between different investigated time windows, particularly between 24 h and 48 h for all paclitaxel concentrations, indicating a time dependence for the effects of different paclitaxel concentrations (Figure S6b).

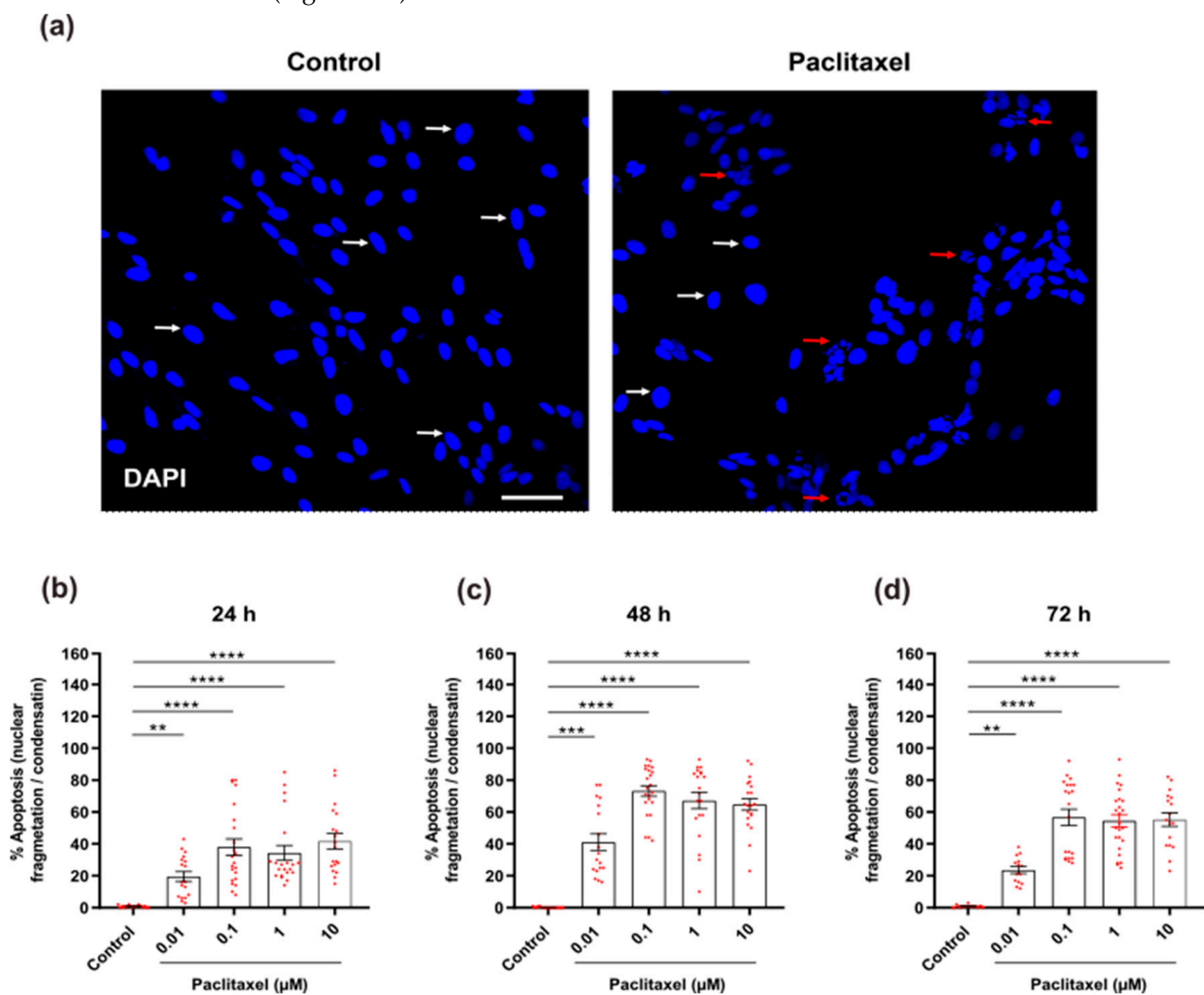


**Figure 9.** Effects of different concentrations of paclitaxel on nuclear morphology of DRG non-neuronal cells were analyzed by DAPI staining to detect % of apoptosis. (a) Representative images show DAPI-stained nuclei of non-neuronal cells of the control group (left) or 1 μM paclitaxel group (right) at 48 h post-treatment, Scale bar = 75 μm. White arrows indicate healthy and uniformly stained nuclei, whereas red arrows identify apoptotic nuclei. (b–d) A significant increase in % of apoptotic cells with fragmented or condensed nuclei was observed in different cultures treated with various paclitaxel concentrations (0.01 μM, 0.1 μM, 1 μM, and 10 μM) in comparison with the control group (\*\*  $p < 0.01$ , \*\*\*  $p < 0.001$ , \*\*\*\*  $p < 0.0001$ ). Data represented as mean  $\pm$  SEM. The experiments were performed at least three independent times with  $n = 15$  replicas. The asterisk denotes significant results regarding the respective measurement indicated with the bar graphs.

### 3.4.6. Detection of Cell Death by Propidium Iodide Staining

To detect degenerating non-neuronal cells with late apoptosis and necrosis, combined staining with PI and DAPI was performed. Dead cells showed pycnotic highly condensed or fragmented nuclei in bright pink, while live cells showed normal nuclei with homogeneously distributed chromatin and regular morphology (Figure 10a). Except for 0.01  $\mu\text{M}$  at 48 h post-treatment, all treated groups at all time points showed an apparent increase in the ratio of positive PI cells when compared to their corresponding untreated control group ( $p < 0.05$ ) (Figure 10b–d). The presence of dead cells also increased with increasing paclitaxel concentrations when compared to the control, confirming a concentration dependency at different investigated time points (Figure S7a). Furthermore, a time-dependent increase in the ratio of cell death to DRG non-neuronal cells was observed except for 0.01  $\mu\text{M}$  paclitaxel at 48 h (Figure S7a).

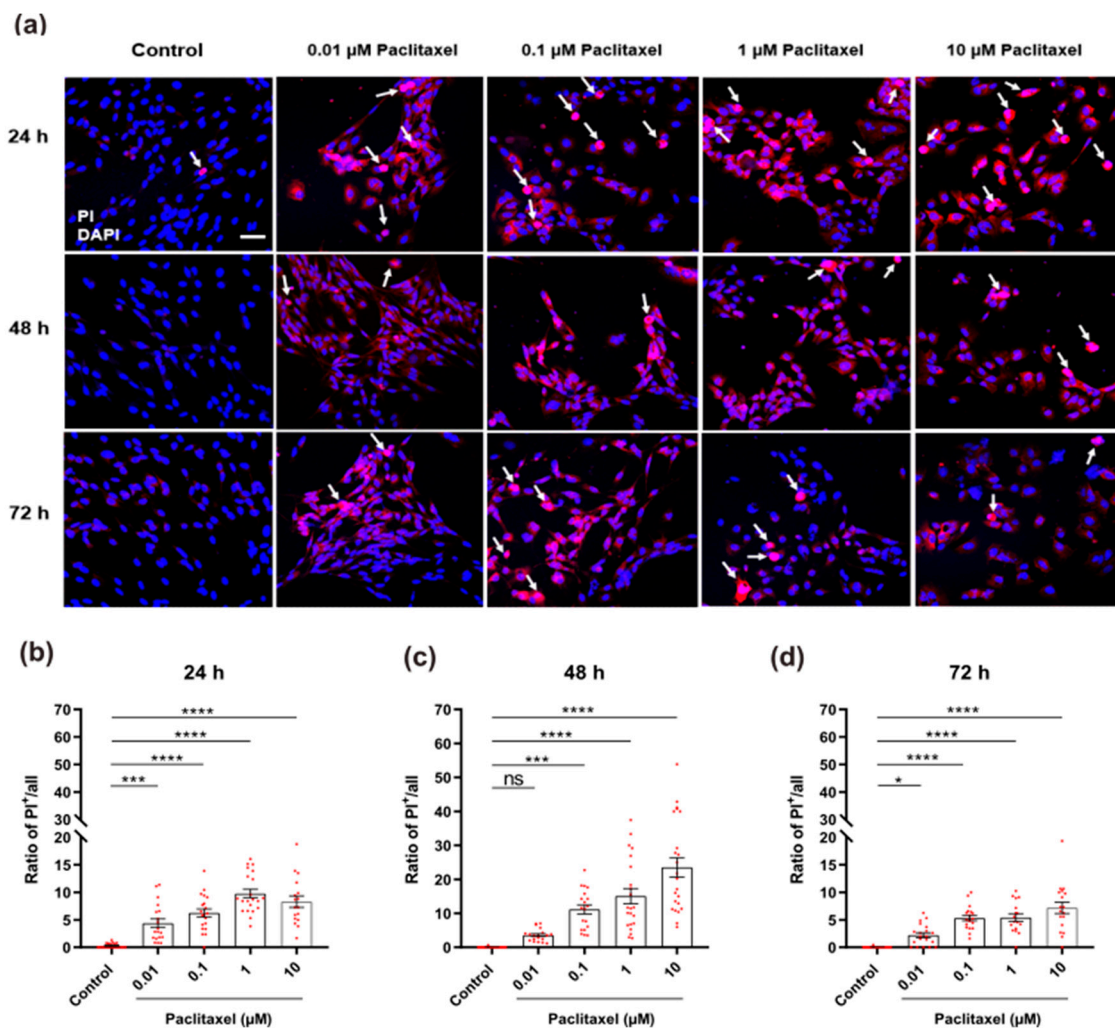


**Figure 10.** Effects of different paclitaxel concentrations on cell death of DRG non-neuronal cells by using PI assay. (a) Representative immunofluorescent fields show the amount of damaged non-neuronal cells (PI-positive) in treated groups compared to control fields. The white arrows represent degenerating cells (bright pink nuclei), Scale bar = 75  $\mu\text{m}$ . At 24 h (b), 48 h (c), and 72 h (d) post-treatment, all concentrations of paclitaxel led to a massive increase in the number of dead cells compared to the control group (\*  $p < 0.05$ , \*\*\*  $p < 0.001$ , \*\*\*\*  $p < 0.0001$ ), except for 0.01  $\mu\text{M}$  paclitaxel concentration at 48 h ( $p > 0.05$ ). Values served as mean  $\pm$  SEM, and the experiments were carried out three times independently with  $n = 15$  replicas. The asterisk denotes significant results regarding the respective measurement indicated with the bar graphs, ns: non-significant.

#### 4. Discussion

Primary DRG non-neuronal cells play a crucial role in supporting DRG neurons [22,31]. Previous studies investigated the toxic effects of paclitaxel on Primary DRG neurons, but little is known about the toxicity of paclitaxel on non-neuronal cells. Furthermore, the time course and concentration-dependency of paclitaxel's toxic effects on non-neuronal cells attracted little attention. To address these aspects, a more comprehensive approach using a variety of techniques, time points, and concentrations was chosen to demonstrate the effects of paclitaxel on DRG non-neuronal cell culture *in vitro*.

Paclitaxel exhibited several toxicological effects on primary DRG non-neuronal cells, including a decrease in cell viability, an increase in cell death, inhibition of cell proliferation, and cellular and nuclear changes, all of which were concentration- and time-dependent. Our findings on DRG SCs are consistent with previous research that studied paclitaxel effects on viability in a model of isolated SCs from the sciatic nerve [31]. These effects were attributed to paclitaxel's fast and strong mechanism of action on primary DRG non-neuronal cells, as these cells are non-transformed and proliferating cells. Therefore, paclitaxel selectively induces the death of transformed cells, possibly by arresting the cell cycle at G1 as well as G2/M phases [54–58].

Our results also revealed that paclitaxel significantly reduced the proliferation rate of DRG non-neuronal cells at various investigated timelines regardless of the applied concentration, but this suppression increased in a time-dependent manner. These findings expand the data of previous research, which reported a decrease in cell proliferation of SGCs of DRG after 24 h of treatment with 1  $\mu\text{M}$  and 5  $\mu\text{M}$  paclitaxel [14]. The authors postulated a paclitaxel stabilizing effect on microtubules by binding to beta-tubulin units, which disrupts microtubule dynamics [58]. As a result, mitosis was arrested between metaphase and anaphase (G2/M phase), suggesting a mitotic block and proliferation inhibition [57–59].

The majority of anticancer drugs have been shown to induce apoptosis in vulnerable cells [60–62]. Cellular and nuclear changes induced by anticancer drugs are very common and involve shrinkage of cell bodies, nuclear condensation, and chromatin fragmentation [54–56]. As shown here, the response to paclitaxel seems similar in primary DRG non-neuronal cells and affects all cellular subtypes.

Interestingly, we found that the percentage of apoptotic cells in DRG non-neuronal cell culture detected by DAPI staining at different investigated time points was higher when compared to the proportion of dead cells determined by the PI assay. This seeming discrepancy can be explained as DAPI staining detects cells in the early and late stages of apoptosis based on their nuclear morphology [63], but PI labels late apoptotic and dead cells with damaged cell membranes [64].

Furthermore, retraction and loss or shortening of processes increased strongly with the duration of treatment. These results add to the time- and concentration-dependency of paclitaxel effects and support previous research that reported a loss or shortening of processes in non-neuronal cells, however, in primary DRG co-culture after 24 h of exposure to paclitaxel [31,39]. These effects are comparable to those found in sensory neurons [17,37,65], implying the strong toxicity of paclitaxel on DRG non-neuronal cells, which might have adverse functional consequences for DRG sensory neurons.

Dose- and time-dependent pharmacokinetics have been reported more frequently for anticancer drugs than for other medications [66–70]. Our findings revealed that the effects of paclitaxel on Primary DRG non-neuronal cell culture are concentration- and time-dependent. Previous studies also reported similar findings on primary DRG neuronal and non-neuronal cells [14,17,39]. Low concentrations of paclitaxel (0.01–0.1  $\mu\text{M}$ ) were reported to suppress microtubule dynamics and inhibit mitotic spindle formation, resulting in a cell cycle arrest at the G2/M phase [55]. Considerably, low concentrations of paclitaxel showed no effect on the overall architecture of the microtubule cytoskeleton (Jordan et al., 1993), as noticed with 0.01  $\mu\text{M}$  paclitaxel in the current study. In contrast, higher doses of paclitaxel were found to cause massive microtubule damage [59,71,72] and activate kinase pathways such

as JNK/SAPK and p34 (cdc2) pathways [73–76], all of which are associated with paclitaxel-induced apoptosis [57]. It is important to note that apoptosis induced by these pathways is not dependent on mitotic arrest at higher concentrations, suggesting that it may occur in cells at any phase of the cell cycle [55]. This interpretation is consistent with our data that 0.01  $\mu\text{M}$  paclitaxel did not exhibit a significant toxic effect on the morphology of primary DRG non-neuronal cells, whereas the higher concentrations (1 and 10  $\mu\text{M}$ ) did.

In the current study, the effect of paclitaxel on the cell viability of primary DRG co-culture by MTT assay was time-dependent and modulated by the presence of neuronal and non-neuronal cells in primary DRG culture. For example, the toxic effects of paclitaxel on the viability of non-neuronal cells alone were apparent earlier, at 24 h post-treatment, while a significant reduction appeared at 72 h after treatment in DRG neuronal cells [17]. However, in primary DRG co-cultures containing neuronal and non-neuronal cells, the effect was present 48 h post-treatment. A possible explanation might be that non-neuronal cells are more susceptible and sensitive to paclitaxel treatment when compared to neurons. As a result, paclitaxel's effects on non-neuronal cells become more apparent because they are actively growing, whereas post mitotic neurons need longer to respond to cell death [77,78]. Importantly, the effects of paclitaxel on the viability of primary DRG co-culture appeared at 48 h, not 24 h post-treatment, implying that there are cell-cell interactions between neurons and non-neuronal cells and modulating signaling pathways that impact the paclitaxel toxicity in the co-culture. Furthermore, the fate of cells after paclitaxel treatment might be affected by both paclitaxel concentrations and exposure time [51,59].

Neuronal function studies showed that neurons are not the only cell type that contributes to neuronal signaling. In the CNS, non-neuronal cells such as astrocytes, oligodendrocytes, and microglia all play important roles in influencing neuronal activity via interactions between neuronal cells and both glial cells and SGCs [79–82]. Non-neuronal glial cells and macrophages were shown to play critical roles in neuronal excitability modulation as well as in nutrition, structural, and maintenance functions [83,84]. In addition, they become activated following peripheral nerve injury or chronic inflammation and are involved in controlling neuronal excitability [85]. An interesting structural feature of the sensory ganglia is that the somata of sensory neurons do not form synaptic contacts with one another [86]. Additionally, neuronal cell bodies are enwrapped by SGCs inside the ganglia to form a structural and functional unit [27]. This specific structural arrangement stands for the communication between neurons and SGCs and is a determinant of somatic activity, as recently reported [82]. Changes in communication after injury are critical for understanding the development of abnormal ectopic discharges in somata that influence afferent signaling [28]. As a result, interactions between DRG neurons and glia and the activation of signaling pathways are believed to play an important role in the management of peripheral neuropathy [82].

## 5. Conclusions

Paclitaxel showed a set of toxicological effects on primary DRG non-neuronal cells that included a reduction in cell viability, an increase in cell death, inhibition of cell proliferation, and morphological changes. The effects of paclitaxel on primary DRG non-neuronal cells are concentration- and time- dependent. Given the crucial role of primary DRG non-neuronal cells in supporting DRG neurons and in the development and maintenance of neuropathic pain, the described adverse effects of paclitaxel on DRG non-neuronal cells might have functional consequences for sensory neurons in the DRG and should be considered in the management of peripheral neuropathy. Future research should investigate the potential negative effects of paclitaxel on signaling pathways and interactions between DRG neuronal and non-neuronal cells.

**Supplementary Materials:** The following supporting information can be downloaded at: <https://www.mdpi.com/article/10.3390/toxics11070581/s1>, Figure S1: (a) DRG isolation from 6–8 weeks old Wister rats, and (b) extraction and purification of DRG non-neuronal cells by using the density gradient centrifugation method; Figure S2: Representative example of automatic counting of

nuclei of non-neuronal cells by the FIJI program for the control group; Figure S3: Effects of different concentrations of paclitaxel on the viability of DRG non-neuronal cells at different investigated time points using the MTT assay; Figure S4: Effects of different concentrations of paclitaxel on the percentage of cytotoxicity of DRG non-neuronal cells at different investigated time windows using the LDH assay; Figure S5: Effects of different concentrations of paclitaxel on the rate of cell proliferation of DRG non-neuronal cells at 24 h, 48 h, and 72 h post-treatment using BrdU assay; Figure S6: Effects of different concentrations of paclitaxel on nuclear morphology (% apoptosis) of DRG non-neuronal cells at 24 h, 48 h, and 72 h post-treatment by DAPI staining; Figure S7: Effects of different concentrations of paclitaxel on the ratio of PI<sup>+</sup> of DRG non-neuronal cells at 24 h, 48 h, and 72 h post-treatment by propidium iodide assay.

**Author Contributions:** Conceptualization, F.D., and A.E.; methodology, A.E.; formal analysis, A.E.; investigation, A.E.; resources, F.D.; data curation, A.E.; writing—original draft preparation, A.E. and F.D.; writing—review and editing, F.D. and A.E.; visualization, A.E.; supervision, F.D.; project administration, F.D. All authors have read and agreed to the published version of the manuscript.

**Funding:** This research received no external funding.

**Institutional Review Board Statement:** All animal experiments were carried out in accordance with the policy on ethics and the policy on the use of animals in neuroscience research, as specified in Directive 2010/63/EU of the European Parliament and of the Council of the European Union on the protection of animals used for scientific purposes, and were approved by local authorities for laboratory animal care and use (State of Saxony-Anhalt, Germany, permission number: I11M27).

**Informed Consent Statement:** Not applicable.

**Data Availability Statement:** All datasets generated for this study are included in the article/supplementary material.

**Acknowledgments:** We acknowledge the Katholischer Akademischer Ausländer-Dienst (KAAD) for the Ph.D. scholarship to A.E. The authors would like to thank Chalid Ghadban and Candy Rothgänger-Strube for excellent technical assistance. We acknowledge the financial support of the Open Access Publication Fund of Martin Luther University Halle-Wittenberg.

**Conflicts of Interest:** The authors declare no conflict of interest.

## References

1. Kim, E. Chemotherapy-Induced Peripheral Neuropathy: Bench to Clinical Practice. *Korean J. Pain* **2020**, *33*, 291–293. [[CrossRef](#)] [[PubMed](#)]
2. Seretny, M.; Currie, G.L.; Sena, E.S.; Ramnarine, S.; Grant, R.; MacLeod, M.R.; Colvin, L.A.; Fallon, M. Incidence, Prevalence, and Predictors of Chemotherapy-Induced Peripheral Neuropathy: A Systematic Review and Meta-Analysis. *Pain* **2014**, *155*, 2461–2470. [[CrossRef](#)] [[PubMed](#)]
3. Han, Y.; Smith, M.T. Pathobiology of Cancer Chemotherapy-Induced Peripheral Neuropathy (CIPN). *Front. Pharmacol.* **2013**, *4*, 156. [[CrossRef](#)] [[PubMed](#)]
4. Miltenburg, N.C.; Boogerd, W. Chemotherapy-Induced Neuropathy: A Comprehensive Survey. *Cancer Treat. Rev.* **2014**, *40*, 872–882. [[CrossRef](#)]
5. Argyriou, A.; Kyritsis, A.; Makatsoris, T.; Kalofonos, H. Chemotherapy-Induced Peripheral Neuropathy in Adults: A Comprehensive Update of the Literature. *Cancer Manag. Res.* **2014**, *6*, 135–147. [[CrossRef](#)] [[PubMed](#)]
6. Boyette-Davis, J.A.; Hou, S.; Abdi, S.; Dougherty, P.M. An Updated Understanding of the Mechanisms Involved in Chemotherapy-Induced Neuropathy. *Pain Manag.* **2018**, *8*, 363–375. [[CrossRef](#)]
7. Zajączkowska, R.; Kocot-Kępska, M.; Leppert, W.; Wrzosek, A.; Mika, J.; Wordliczek, J. Mechanisms of Chemotherapy-Induced Peripheral Neuropathy. *Int. J. Mol. Sci.* **2019**, *20*, 1451. [[CrossRef](#)]
8. Gießen-Jung, C.; von Baumgarten, L. Chemotherapie-Induzierte Periphere Neuropathie. *DMW—Dtsch. Med. Wochenschr.* **2018**, *113*, 970–978. [[CrossRef](#)]
9. Windebank, A.J.; Smith, A.G.; Russell, J.W. The Effect of Nerve Growth Factor, Ciliary Neurotrophic Factor, and ACTH Analogs on Cisplatin Neurotoxicity in Vitro. *Neurology* **1994**, *44 Pt 1*, 488–494. [[CrossRef](#)]
10. Melli, G.; Höke, A. Dorsal Root Ganglia Sensory Neuronal Cultures: A Tool for Drug Discovery for Peripheral Neuropathies. *Expert Opin. Drug Discov.* **2009**, *4*, 1035–1045. [[CrossRef](#)]
11. Li, Y.; Marri, T.; North, R.Y.; Rhodes, H.R.; Uhelski, M.L.; Tatsui, C.E.; Rhines, L.D.; Rao, G.; Corrales, G.; Abercrombie, T.J.; et al. Chemotherapy-Induced Peripheral Neuropathy in a Dish: Dorsal Root Ganglion Cells Treated in Vitro with Paclitaxel Show Biochemical and Physiological Responses Parallel to That Seen in Vivo. *Pain* **2021**, *162*, 84–96. [[CrossRef](#)]

12. Jimenez-Andrade, J.M.; Herrera, M.B.; Ghilardi, J.R.; Vardanyan, M.; Melemedjian, O.K.; Mantyh, P.W. Vascularization of the Dorsal Root Ganglia and Peripheral Nerve of the Mouse: Implications for Chemical-Induced Peripheral Sensory Neuropathies. *Mol. Pain* **2008**, *4*, 10. [[CrossRef](#)] [[PubMed](#)]
13. Cavaletti, G.; Cavalletti, E.; Oggioni, N.; Sottani, C.; Minoia, C.; D'Incalci, M.; Zucchetti, M.; Marmiroli, P.; Tredici, G. Distribution of Paclitaxel within the Nervous System of the Rat after Repeated Intravenous Administration. *Neurotoxicology* **2000**, *21*, 389–393. [[CrossRef](#)] [[PubMed](#)]
14. Klein, I.; Boenert, J.; Lange, F.; Christensen, B.; Wassermann, M.K.; Wiesen, M.H.J.; Olschewski, D.N.; Rabenstein, M.; Müller, C.; Lehmann, H.C.; et al. Glia from the Central and Peripheral Nervous System Are Differentially Affected by Paclitaxel Chemotherapy via Modulating Their Neuroinflammatory and Neuroregenerative Properties. *Front. Pharmacol.* **2022**, *13*, 1038285. [[CrossRef](#)] [[PubMed](#)]
15. Gill, J.S.; Windebank, A.J. Cisplatin-Induced Apoptosis in Rat Dorsal Root Ganglion Neurons Is Associated with Attempted Entry into the Cell Cycle. *J. Clin. Investig.* **1998**, *101*, 2842–2850. [[CrossRef](#)]
16. Fischer, S.J.; McDonald, E.S.; Gross, L.; Windebank, A.J. Alterations in Cell Cycle Regulation Underlie Cisplatin Induced Apoptosis of Dorsal Root Ganglion Neurons in Vivo. *Neurobiol. Dis.* **2001**, *8*, 1027–1035. [[CrossRef](#)] [[PubMed](#)]
17. Elfarnawany, A.; Dehghani, F. Palmitoylethanolamide Mitigates Paclitaxel Toxicity in Primary Dorsal Root Ganglion Neurons. *Biomolecules* **2022**, *12*, 1873. [[CrossRef](#)]
18. Delree, P.; Leprince, P.; Schoenen, J.; Moonen, G. Purification and Culture of Adult Rat Dorsal Root Ganglia Neurons. *J. Neurosci. Res.* **1989**, *23*, 198–206. [[CrossRef](#)] [[PubMed](#)]
19. Grothe, C.; Unsicker, K. Neuron-Enriched Cultures of Adult Rat Dorsal Root Ganglia: Establishment, Characterization, Survival, and Neuropeptide Expression in Response to Trophic Factors. *J. Neurosci. Res.* **1987**, *18*, 539–550. [[CrossRef](#)] [[PubMed](#)]
20. Li, R.; Sliwkowski, M.X.; Lo, J.; Mather, J.P. Establishment of Schwann Cell Lines from Normal Adult and Embryonic Rat Dorsal Root Ganglia. *J. Neurosci. Methods* **1996**, *67*, 57–69. [[CrossRef](#)]
21. Wrathall, J.R.; Rigamonti, D.D.; Braford, M.R.; Kao, C.C. Non-Neuronal Cell Cultures from Dorsal Root Ganglia of the Adult Cat: Production of Schwann-like Cell Lines. *Brain Res.* **1981**, *229*, 163–181. [[CrossRef](#)] [[PubMed](#)]
22. Ji, R.-R.; Berta, T.; Nedergaard, M. Glia and Pain: Is Chronic Pain a Gliopathy? *Pain* **2013**, *154* (Suppl. S1), S10–S28. [[CrossRef](#)] [[PubMed](#)]
23. Ji, R.-R.; Chamesian, A.; Zhang, Y.-Q. Pain Regulation by Non-Neuronal Cells and Inflammation. *Science* **2016**, *354*, 572–577. [[CrossRef](#)]
24. Nascimento, R.S.; Santiago, M.F.; Marques, S.A.; Allodi, S.; Martinez, A.M.B. Diversity among Satellite Glial Cells in Dorsal Root Ganglia of the Rat. *Brazilian J. Med. Biol. Res.* **2008**, *41*, 1011–1017. [[CrossRef](#)]
25. Hanani, M.; Spray, D.C. Emerging Importance of Satellite Glia in Nervous System Function and Dysfunction. *Nat. Rev. Neurosci.* **2020**, *21*, 485–498. [[CrossRef](#)] [[PubMed](#)]
26. Avraham, O.; Deng, P.-Y.; Jones, S.; Kuruvilla, R.; Semenkovich, C.F.; Klyachko, V.A.; Cavalli, V. Satellite Glial Cells Promote Regenerative Growth in Sensory Neurons. *Nat. Commun.* **2020**, *11*, 4891. [[CrossRef](#)] [[PubMed](#)]
27. Pannese, E. The Structure of the Perineuronal Sheath of Satellite Glial Cells (SGCs) in Sensory Ganglia. *Neuron Glia Biol.* **2010**, *6*, 3–10. [[CrossRef](#)] [[PubMed](#)]
28. Huang, L.-Y.M.; Gu, Y.; Chen, Y. Communication between Neuronal Somata and Satellite Glial Cells in Sensory Ganglia. *Glia* **2013**, *61*, 1571–1581. [[CrossRef](#)]
29. Jasmin, L.; Vit, J.-P.; Bhargava, A.; Ohara, P.T. Can Satellite Glial Cells Be Therapeutic Targets for Pain Control? *Neuron Glia Biol.* **2010**, *6*, 63–71. [[CrossRef](#)]
30. Bhatheja, K.; Field, J. Schwann Cells: Origins and Role in Axonal Maintenance and Regeneration. *Int. J. Biochem. Cell Biol.* **2006**, *38*, 1995–1999. [[CrossRef](#)]
31. Imai, S.; Koyanagi, M.; Azimi, Z.; Nakazato, Y.; Matsumoto, M.; Ogihara, T.; Yonezawa, A.; Omura, T.; Nakagawa, S.; Wakatsuki, S.; et al. Taxanes and Platinum Derivatives Impair Schwann Cells via Distinct Mechanisms. *Sci. Rep.* **2017**, *7*, 5947. [[CrossRef](#)] [[PubMed](#)]
32. Chen, G.; Zhang, Z.; Wei, Z.; Cheng, Q.; Li, X.; Li, W.; Duan, S.; Gu, X. Lysosomal Exocytosis in Schwann Cells Contributes to Axon Remyelination. *Glia* **2012**, *60*, 295–305. [[CrossRef](#)] [[PubMed](#)]
33. Kidd, G.J.; Ohno, N.; Trapp, B.D. Biology of Schwann Cells. In *Handbook of Clinical Neurology*; Elsevier: Amsterdam, The Netherlands, 2013; Volume 115, pp. 55–79. [[CrossRef](#)]
34. Su, W.; Gu, Y.; Wei, Z.; Shen, Y.; Jin, Z.; Yuan, Y.; Gu, X.; Chen, G. Rab27a/Slp2-a Complex Is Involved in Schwann Cell Myelination. *Neural Regen. Res.* **2016**, *11*, 1830. [[CrossRef](#)]
35. Flatters, S.J.L.; Dougherty, P.M.; Colvin, L.A. Clinical and Preclinical Perspectives on Chemotherapy-Induced Peripheral Neuropathy (CIPN): A Narrative Review. *Br. J. Anaesth.* **2017**, *119*, 737–749. [[CrossRef](#)] [[PubMed](#)]
36. Cirrincione, A.M.; Pellegrini, A.D.; Dominy, J.R.; Benjamin, M.E.; Utkina-Sosunova, I.; Lotti, F.; Jergova, S.; Sagen, J.; Rieger, S. Paclitaxel-Induced Peripheral Neuropathy Is Caused by Epidermal ROS and Mitochondrial Damage through Conserved MMP-13 Activation. *Sci. Rep.* **2020**, *10*, 3970. [[CrossRef](#)] [[PubMed](#)]
37. Park, S.H.; Eber, M.R.; Fonseca, M.M.; Patel, C.M.; Cunnane, K.A.; Ding, H.; Hsu, F.-C.; Peters, C.M.; Ko, M.-C.; Strowd, R.E.; et al. Usefulness of the Measurement of Neurite Outgrowth of Primary Sensory Neurons to Study Cancer-Related Painful Complications. *Biochem. Pharmacol.* **2021**, *188*, 114520. [[CrossRef](#)] [[PubMed](#)]

38. Scuteri, A.; Nicolini, G.; Miloso, M.; Bossi, M.; Cavaletti, G.; Windebank, A.J.; Tredici, G. Paclitaxel Toxicity in Post-Mitotic Dorsal Root Ganglion (DRG) Cells. *Anticancer Res.* **2006**, *26*, 1065–1070.
39. Guo, L.; Hamre, J.; Eldridge, S.; Behrsing, H.P.; Cutuli, F.M.; Mussio, J.; Davis, M. Multiparametric Image Analysis of Rat Dorsal Root Ganglion Cultures to Evaluate Peripheral Neuropathy-Inducing Chemotherapeutics. *Toxicol. Sci.* **2017**, *156*, 275–288. [[CrossRef](#)]
40. Hansen, J.; Bross, P. A Cellular Viability Assay to Monitor Drug Toxicity. In *Protein Misfolding and Cellular Stress in Disease and Aging: Concepts and Protocols*; Springer: Berlin/Heidelberg, Germany, 2010; pp. 303–311. [[CrossRef](#)]
41. Kumar, P.; Nagarajan, A.; Uchil, P.D. Analysis of Cell Viability by the Lactate Dehydrogenase Assay. *Cold Spring Harb. Protoc.* **2018**, *2018*, pdb.prot095497. [[CrossRef](#)]
42. Brana, C.; Benham, C.; Sundstrom, L. A Method for Characterising Cell Death in Vitro by Combining Propidium Iodide Staining with Immunohistochemistry. *Brain Res. Protoc.* **2002**, *10*, 109–114. [[CrossRef](#)]
43. Liu, R.; Lin, G.; Xu, H. An Efficient Method for Dorsal Root Ganglia Neurons Purification with a One-Time Anti-Mitotic Reagent Treatment. *PLoS ONE* **2013**, *8*, e60558. [[CrossRef](#)] [[PubMed](#)]
44. Gao, W.; Zan, Y.; Wang, Z.J.; Hu, X.; Huang, F. Quercetin Ameliorates Paclitaxel-Induced Neuropathic Pain by Stabilizing Mast Cells, and Subsequently Blocking PKC $\epsilon$ -Dependent Activation of TRPV1. *Acta Pharmacol. Sin.* **2016**, *37*, 1166–1177. [[CrossRef](#)]
45. Jang, H.J.; Hwang, S.; Cho, K.Y.; Kim, D.K.; Chay, K.-O.; Kim, J.-K. Taxol Induces Oxidative Neuronal Cell Death by Enhancing the Activity of NADPH Oxidase in Mouse Cortical Cultures. *Neurosci. Lett.* **2008**, *443*, 17–22. [[CrossRef](#)] [[PubMed](#)]
46. Pittman, S.K.; Gracias, N.G.; Vasko, M.R.; Fehrenbacher, J.C. Paclitaxel Alters the Evoked Release of Calcitonin Gene-Related Peptide from Rat Sensory Neurons in Culture. *Exp. Neurol.* **2014**, *253*, 146–153. [[CrossRef](#)] [[PubMed](#)]
47. Malin, S.A.; Davis, B.M.; Molliver, D.C. Production of Dissociated Sensory Neuron Cultures and Considerations for Their Use in Studying Neuronal Function and Plasticity. *Nat. Protoc.* **2007**, *2*, 152–160. [[CrossRef](#)] [[PubMed](#)]
48. Akin, E.J.; Alsaloum, M.; Higerd, G.P.; Liu, S.; Zhao, P.; Dib-Hajj, F.B.; Waxman, S.G.; Dib-Hajj, S.D. Paclitaxel Increases Axonal Localization and Vesicular Trafficking of Nav1.7. *Brain* **2021**, *144*, 1727–1737. [[CrossRef](#)]
49. Shin, G.J.; Pero, M.E.; Hammond, L.A.; Burgos, A.; Kumar, A.; Galindo, S.E.; Lucas, T.; Bartolini, F.; Grueber, W.B. Integrins Protect Sensory Neurons in Models of Paclitaxel-Induced Peripheral Sensory Neuropathy. *Proc. Natl. Acad. Sci. USA* **2021**, *118*, e2006050118. [[CrossRef](#)]
50. Liebmans, J.; Cook, J.; Lipschultz, C.; Teague, D.; Fisher, J.; Mitchell, J. Cytotoxic Studies of Paclitaxel (Taxol<sup>®</sup>) in Human Tumour Cell Lines. *Br. J. Cancer* **1993**, *68*, 1104–1109. [[CrossRef](#)]
51. Zasadil, L.M.; Andersen, K.A.; Yeum, D.; Rocque, G.B.; Wilke, L.G.; Tevaarwerk, A.J.; Raines, R.T.; Burkard, M.E.; Weaver, B.A. Cytotoxicity of Paclitaxel in Breast Cancer Is Due to Chromosome Missegregation on Multipolar Spindles. *Sci. Transl. Med.* **2014**, *6*, 229ra43. [[CrossRef](#)]
52. Tolkovsky, A.M.; Brelstaff, J. Sensory Neurons from Tau Transgenic Mice and Their Utility in Drug Screening. *Methods Mol. Biol.* **2018**, *1727*, 93–105. [[CrossRef](#)]
53. Aras, M.A.; Hartnett, K.A.; Aizenman, E. Assessment of Cell Viability in Primary Neuronal Cultures. *Curr. Protoc. Neurosci.* **2008**, *44*, 7.18.1–7.18.15. [[CrossRef](#)] [[PubMed](#)]
54. Trielli, M.O.; Andreassen, P.R.; Lacroix, F.B.; Margolis, R.L. Differential Taxol-Dependent Arrest of Transformed and Nontransformed Cells in the G1 Phase of the Cell Cycle, and Specific-Related Mortality of Transformed Cells. *J. Cell Biol.* **1996**, *135*, 689–700. [[CrossRef](#)]
55. Wang, T.-H.; Wang, H.-S.; Soong, Y.-K. Paclitaxel-Induced Cell Death. *Cancer* **2000**, *88*, 2619–2628. [[CrossRef](#)] [[PubMed](#)]
56. Weaver, B.A. How Taxol/Paclitaxel Kills Cancer Cells. *Mol. Biol. Cell* **2014**, *25*, 2677–2681. [[CrossRef](#)] [[PubMed](#)]
57. Hammad, A.; Mohamed M, S.A.; Khalifa, M.; El-Daly, M. Mechanisms of Paclitaxel-Induced Peripheral Neuropathy. *J. Adv. Biomed. Pharm. Sci.* **2023**, *6*, 25–35. [[CrossRef](#)]
58. Klein, I.; Lehmann, H. Pathomechanisms of Paclitaxel-Induced Peripheral Neuropathy. *Toxics* **2021**, *9*, 229. [[CrossRef](#)]
59. Jordan, M.A.; Toso, R.J.; Thrower, D.; Wilson, L. Mechanism of Mitotic Block and Inhibition of Cell Proliferation by Taxol at Low Concentrations. *Proc. Natl. Acad. Sci. USA* **1993**, *90*, 9552–9556. [[CrossRef](#)]
60. Hickman, J.A. Apoptosis Induced by Anticancer Drugs. *Cancer Metastasis Rev.* **1992**, *11*, 121–139. [[CrossRef](#)]
61. Pistrutto, G.; Trisciuglio, D.; Ceci, C.; Garufi, A.; D’Orazi, G. Apoptosis as Anticancer Mechanism: Function and Dysfunction of Its Modulators and Targeted Therapeutic Strategies. *Aging* **2016**, *8*, 603–619. [[CrossRef](#)]
62. Fischer, U.; Schulze-Osthoff, K. Apoptosis-Based Therapies and Drug Targets. *Cell Death Differ.* **2005**, *12*, 942–961. [[CrossRef](#)]
63. Figueroa-Masot, X.A.; Hetman, M.; Higgins, M.J.; Kokot, N.; Xia, Z. Taxol Induces Apoptosis in Cortical Neurons by a Mechanism Independent of Bcl-2 Phosphorylation. *J. Neurosci.* **2001**, *21*, 4657–4667. [[CrossRef](#)] [[PubMed](#)]
64. Rieger, A.M.; Nelson, K.L.; Konowalchuk, J.D.; Barreda, D.R. Modified Annexin V/Propidium Iodide Apoptosis Assay for Accurate Assessment of Cell Death. *J. Vis. Exp.* **2011**, *50*, e2597. [[CrossRef](#)]
65. Yang, I.H.; Siddique, R.; Hosmane, S.; Thakor, N.; Höke, A. Compartmentalized Microfluidic Culture Platform to Study Mechanism of Paclitaxel-Induced Axonal Degeneration. *Exp. Neurol.* **2009**, *218*, 124–128. [[CrossRef](#)] [[PubMed](#)]
66. Li, J.; Chen, R.; Yao, Q.; Liu, S.; Tian, X.; Hao, C.; Lu, W.; Zhou, T. Time-Dependent Pharmacokinetics of Dexamethasone and Its Efficacy in Human Breast Cancer Xenograft Mice: A Semi-Mechanism-Based Pharmacokinetic/Pharmacodynamic Model. *Acta Pharmacol. Sin.* **2018**, *39*, 472–481. [[CrossRef](#)] [[PubMed](#)]

67. Madeddu, C.; Deidda, M.; Piras, A.; Cadeddu, C.; Demurtas, L.; Puzzone, M.; Piscopo, G.; Scartozzi, M.; Mercurio, G. Pathophysiology of Cardiotoxicity Induced by Nonanthracycline Chemotherapy. *J. Cardiovasc. Med.* **2016**, *17*, e12–e18. [[CrossRef](#)]
68. Lennernäs, B.; Albertsson, P.; Lennernäs, H.; Norrby, K. Chemotherapy and Antiangiogenesis. *Acta Oncol.* **2003**, *42*, 294–303. [[CrossRef](#)]
69. Powis, G.; Ames, M.; Kovach, J. Dose-Dependent Pharmacokinetics and Cancer Chemotherapy. *Cancer Chemother. Pharmacol.* **1981**, *6*, 1–9. [[CrossRef](#)]
70. WANG, P.; SONG, J.; SONG, D.; ZHANG, J.; HAO, C. Role of Death Receptor and Mitochondrial Pathways in Conventional Chemotherapy Drug Induction of Apoptosis. *Cell. Signal.* **2006**, *18*, 1528–1535. [[CrossRef](#)]
71. Jordan, M.A.; Wilson, L. Microtubules as a Target for Anticancer Drugs. *Nat. Rev. Cancer* **2004**, *4*, 253–265. [[CrossRef](#)]
72. Jordan, M.A.; Wendell, K.; Gardiner, S.; Derry, W.B.; Copp, H.; Wilson, L. Mitotic Block Induced in HeLa Cells by Low Concentrations of Paclitaxel (Taxol) Results in Abnormal Mitotic Exit and Apoptotic Cell Death. *Cancer Res.* **1996**, *56*, 816–825.
73. Wang, T.-H.; Popp, D.M.; Wang, H.-S.; Saitoh, M.; Mural, J.G.; Henley, D.C.; Ichijo, H.; Wimalasena, J. Microtubule Dysfunction Induced by Paclitaxel Initiates Apoptosis through Both C-Jun N-Terminal Kinase (JNK)-Dependent and -Independent Pathways in Ovarian Cancer Cells. *J. Biol. Chem.* **1999**, *274*, 8208–8216. [[CrossRef](#)]
74. Lee, L.-F.; Li, G.; Templeton, D.J.; Ting, J.P.-Y. Paclitaxel (Taxol)-Induced Gene Expression and Cell Death Are Both Mediated by the Activation of c-Jun NH2-Terminal Kinase (JNK/SAPK). *J. Biol. Chem.* **1998**, *273*, 28253–28260. [[CrossRef](#)] [[PubMed](#)]
75. Wang, T.-H.; Wang, H.-S.; Ichijo, H.; Giannakakou, P.; Foster, J.S.; Fojo, T.; Wimalasena, J. Microtubule-Interfering Agents Activate c-Jun N-Terminal Kinase/Stress-Activated Protein Kinase through Both Ras and Apoptosis Signal-Regulating Kinase Pathways. *J. Biol. Chem.* **1998**, *273*, 4928–4936. [[CrossRef](#)] [[PubMed](#)]
76. Scatena, C.D.; Stewart, Z.A.; Mays, D.; Tang, L.J.; Keefer, C.J.; Leach, S.D.; Pietsenpol, J.A. Mitotic Phosphorylation of Bcl-2 during Normal Cell Cycle Progression and Taxol-Induced Growth Arrest. *J. Biol. Chem.* **1998**, *273*, 30777–30784. [[CrossRef](#)] [[PubMed](#)]
77. Leung, J.C.; Cassimeris, L. Reorganization of Paclitaxel-Stabilized Microtubule Arrays at Mitotic Entry: Roles of Depolymerizing Kinesins and Severing Proteins. *Cancer Biol. Ther.* **2019**, *20*, 1337–1347. [[CrossRef](#)]
78. Lieu, C.-H.; Chang, Y.-N.; Lai, Y.-K. Dual Cytotoxic Mechanisms of Submicromolar Taxol on Human Leukemia HL-60 Cells. *Biochem. Pharmacol.* **1997**, *53*, 1587–1596. [[CrossRef](#)] [[PubMed](#)]
79. Chiang, C.-Y.; Dostrovsky, J.O.; Iwata, K.; Sessle, B.J. Role of Glia in Orofacial Pain. *Neurosci.* **2011**, *17*, 303–320. [[CrossRef](#)]
80. Hanani, M.; Huang, T.Y.; Cherkas, P.S.; Ledda, M.; Pannese, E. Glial Cell Plasticity in Sensory Ganglia Induced by Nerve Damage. *Neuroscience* **2002**, *114*, 279–283. [[CrossRef](#)]
81. Kettenmann, H.; Hanisch, U.-K.; Noda, M.; Verkhratsky, A. Physiology of Microglia. *Physiol. Rev.* **2011**, *91*, 461–553. [[CrossRef](#)]
82. Pozzi, E.; Ballarini, E.; Rodriguez-Menendez, V.; Canta, A.; Chiorazzi, A.; Monza, L.; Bossi, M.; Alberti, P.; Malacrida, A.; Meregalli, C.; et al. Paclitaxel, but Not Cisplatin, Affects Satellite Glial Cells in Dorsal Root Ganglia of Rats with Chemotherapy-Induced Peripheral Neurotoxicity. *Toxics* **2023**, *11*, 93. [[CrossRef](#)]
83. Zhang, Z.-J.; Jiang, B.-C.; Gao, Y.-J. Chemokines in Neuron–Glial Cell Interaction and Pathogenesis of Neuropathic Pain. *Cell. Mol. Life Sci.* **2017**, *74*, 3275–3291. [[CrossRef](#)] [[PubMed](#)]
84. Herculano-Houzel, S. The Glia/Neuron Ratio: How It Varies Uniformly across Brain Structures and Species and What That Means for Brain Physiology and Evolution. *Glia* **2014**, *62*, 1377–1391. [[CrossRef](#)] [[PubMed](#)]
85. Tsuboi, Y.; Takeda, M.; Tanimoto, T.; Ikeda, M.; Matsumoto, S.; Kitagawa, J.; Teramoto, K.; Simizu, K.; Yamazaki, Y.; Shima, A.; et al. Alteration of the Second Branch of the Trigeminal Nerve Activity Following Inferior Alveolar Nerve Transection in Rats. *Pain* **2004**, *111*, 323–334. [[CrossRef](#)] [[PubMed](#)]
86. Pannese, E. Advances in Anatomy Embryology and Cell Biology. In *The Satellite Cells of the Sensory Ganglia*; Springer: Berlin/Heidelberg, Germany, 1981; Volume 65. [[CrossRef](#)]

**Disclaimer/Publisher’s Note:** The statements, opinions and data contained in all publications are solely those of the individual author(s) and contributor(s) and not of MDPI and/or the editor(s). MDPI and/or the editor(s) disclaim responsibility for any injury to people or property resulting from any ideas, methods, instructions or products referred to in the content.



# **Declarations of independence**

(1) I declare that I have not completed or initiated a doctorate procedure at any other universities.

(2) I declare that all information given is accurate and complete. The thesis has not been used previously at this or any other university to achieve an academic degree.

(3) I declare under oath that this thesis is my work entirely and has been written without any help from other people. I complied with all regulations of good scientific practice, and I used only the sources mentioned and included all the citations correctly both in words and content.

Halle (Saale),

Amira Elfarnawany

## **Declarations of previous dissertation attempt**

I declare that this work is my first attempt of writing a dissertation. Also, I declare that this work is exclusively submitted as a dissertation for the Medical Faculty of Martin Luther University Halle-Wittenberg.

Halle (Saale),

Amira Elfarnawany

## Acknowledgments

- I want to express my gratitude to Prof. Dr. Faramarz Dehghani for giving me the opportunity to work in his group. Thank you for all the fruitful discussions, the freedom I had in pursuing new ideas and methods, and your in-depth feedback on all parts of my work. Also, great thanks for his guidance, supervision, ongoing support in hard times, insightful criticism, and allocating time for hours to respond to all my questions. Furthermore, I'd like to thank Prof. FD's working group for their insightful discussions and valuable feedback on my work during the weekly lab meetings.
- I want to thank Chalid Ghadban and Candy Rothgänger-Strube for their great technical support and assistance.
- I thank the Katholischer Akademischer Ausländer-Dienst (KAAD) for the Ph.D. scholarship.
- I am grateful to my home university (Zoology Department, Faculty of Science, Tanta University, Egypt), which allowed me to pursue my doctoral studies abroad, provided ongoing support, and streamlined all administrative processes.
- I would especially like to thank my father, sister, and brother for their encouragement and support. My husband deserves appreciation for his patience, continuous encouragement, and taking care of the children, as well as for making time for me to finish my Ph.D. project.

## Appendix

---

### Supplementary Material

#### Publication 1:

#### Palmitoylethanolamide Mitigates Neurotoxicity of Paclitaxel in Primary Dorsal Root Ganglion Neurons

Amira Elfarnawany<sup>1,2</sup> and Faramarz Dehghani<sup>1\*</sup>

<sup>1</sup>Department of Anatomy and Cell Biology, Medical Faculty, Martin Luther University Halle-Wittenberg, Halle (Saale), Germany.

<sup>2</sup> Zoology Department, Faculty of Science, Tanta University 31527, Tanta, Egypt.

\*Corresponding author: [faramarz.dehghani@medizin.uni-halle.de](mailto:faramarz.dehghani@medizin.uni-halle.de) (FD)

Supplementary data associated with this article can be found, in the online version, at: <https://www.mdpi.com/article/10.3390/biom12121873/s1>.

**Figure S1:** Representative example for tracing neurites by ImageJ program.

**Figure S2:** Effects of different PEA concentrations on neuronal cell viability (%) (mean  $\pm$  SEM) at 72 h post-treatment.

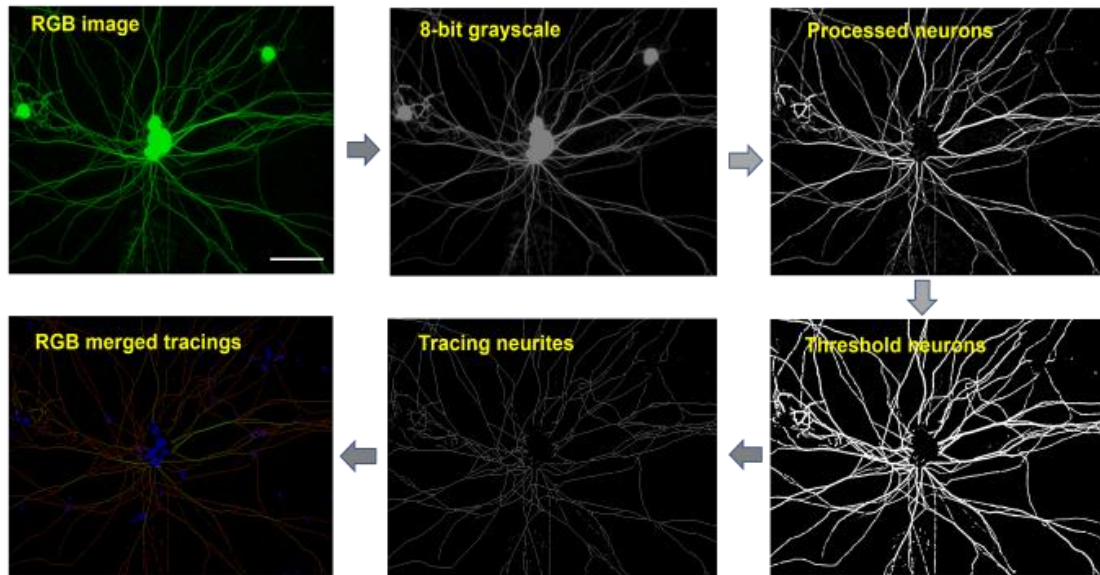
**Figure S3:** Effects of different concentrations of PEA on neurite lengths and soma sizes (mean  $\pm$  SEM) of DRG neurons at 24, 48, and 72-h posttreatment.

**Figure S4:** Effects of different PEA concentrations (0.1, 1, and 10  $\mu$ M) combined with 0.01  $\mu$ M Paclitaxel on neurite length of DRG neurons at 24, 48, and 72-h post-treatment.

**Figure S5:** Effects of different PEA concentrations (0.1, 1, and 10  $\mu$ M) combined with 0.1  $\mu$ M Paclitaxel at 24, 48, and 72-h post-treatment.

**Figure S6:** The effects of different PEA concentrations (0.1, 1, and 10  $\mu$ M) co-applied with 0.01  $\mu$ M Paclitaxel on soma sizes of DRG neurons at 24, 48, and 72-h post-treatment.

a)



b)

A	B	C	D	E	F
	Label	Length(pixels)	Length( $\mu\text{m}$ )	Nu.cells	Length/cell
1	Neuronal-1.tif	11703.555	44.27	1	44.27
2	Neuronal-2.tif	18245.877	69.01	1	69.01
3	Neuronal-3.tif	27843.286	105.32	2	52.66
4	Neuronal-4.tif	21344.411	80.73	2	40.365
	average	24022.18	90.86		51.58

**Figure S1.** Representative example for tracing neurites by ImageJ program for the control group **a)** Step-by-step Demonstration of neurite tracing and measurement of their length by automatic neurite tracer (ImageJ). Scale bars =  $75\mu\text{m}$ . **b)** Results of different neurite length measurements of sensory neurons for four different images for the same control group. Total neurite length in pixels converted to micrometers in the unit and normalized to the number of neurons per photo resulted in neurite length/cell.

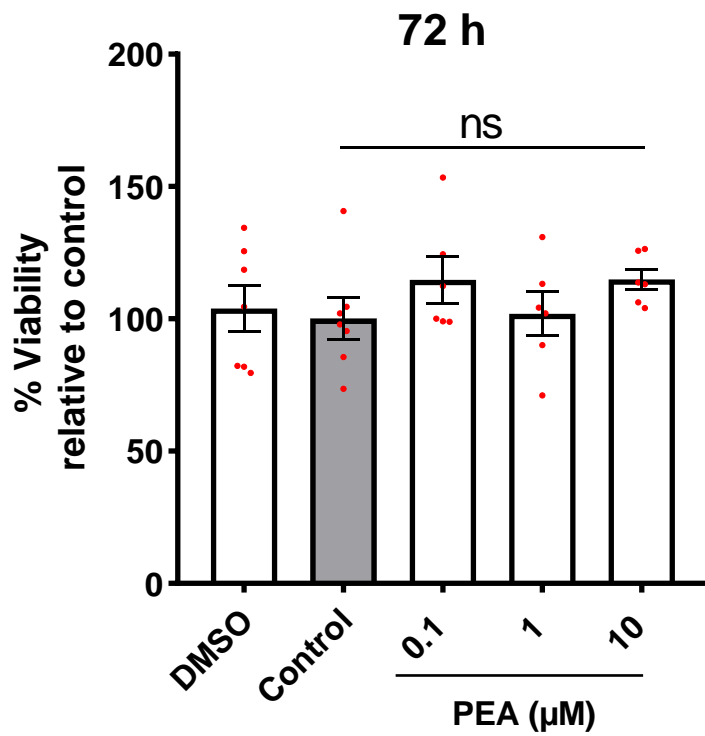


**Figure S2.** Effects of different PEA concentrations on neuronal cell viability (%) (mean  $\pm$  SEM) at 72h post-treatment. PEA showed no significant effect on the viability of cells compared to the control ( $P > 0.05$ ). Experiments were performed 3 times independently of (6-9) technical replicates. SEM: standard error mean.

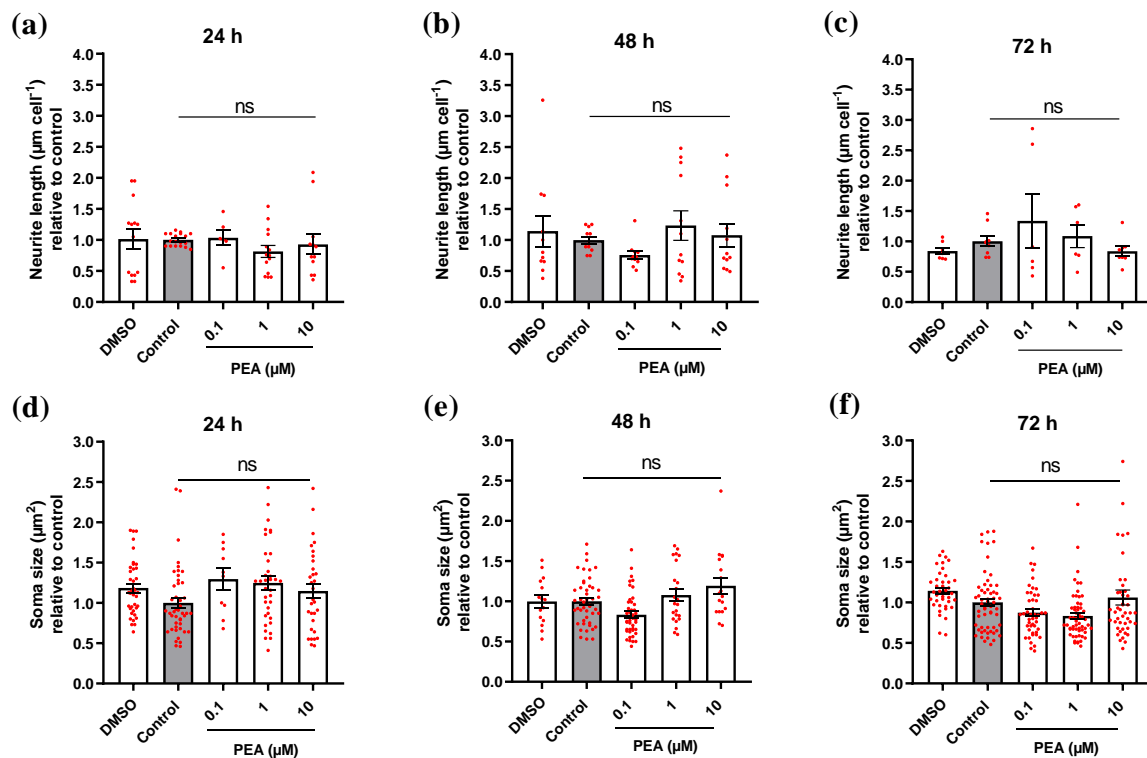


**Figure S3.** Effects of different concentrations of PEA on neurite lengths and soma sizes (mean  $\pm$  SEM) of DRG neurons at 24, 48, and 72-h post-treatment. **a), b), and c)** No significant effect of PEA was found on the neurite lengths ( $n= 10-15$  replicates) and **(d, e, and f)** soma sizes ( $n= 30-45$  replicates) compared to control ( $P > 0.05$ ). experiments were performed 3 times independently. SEM: standard error mean.

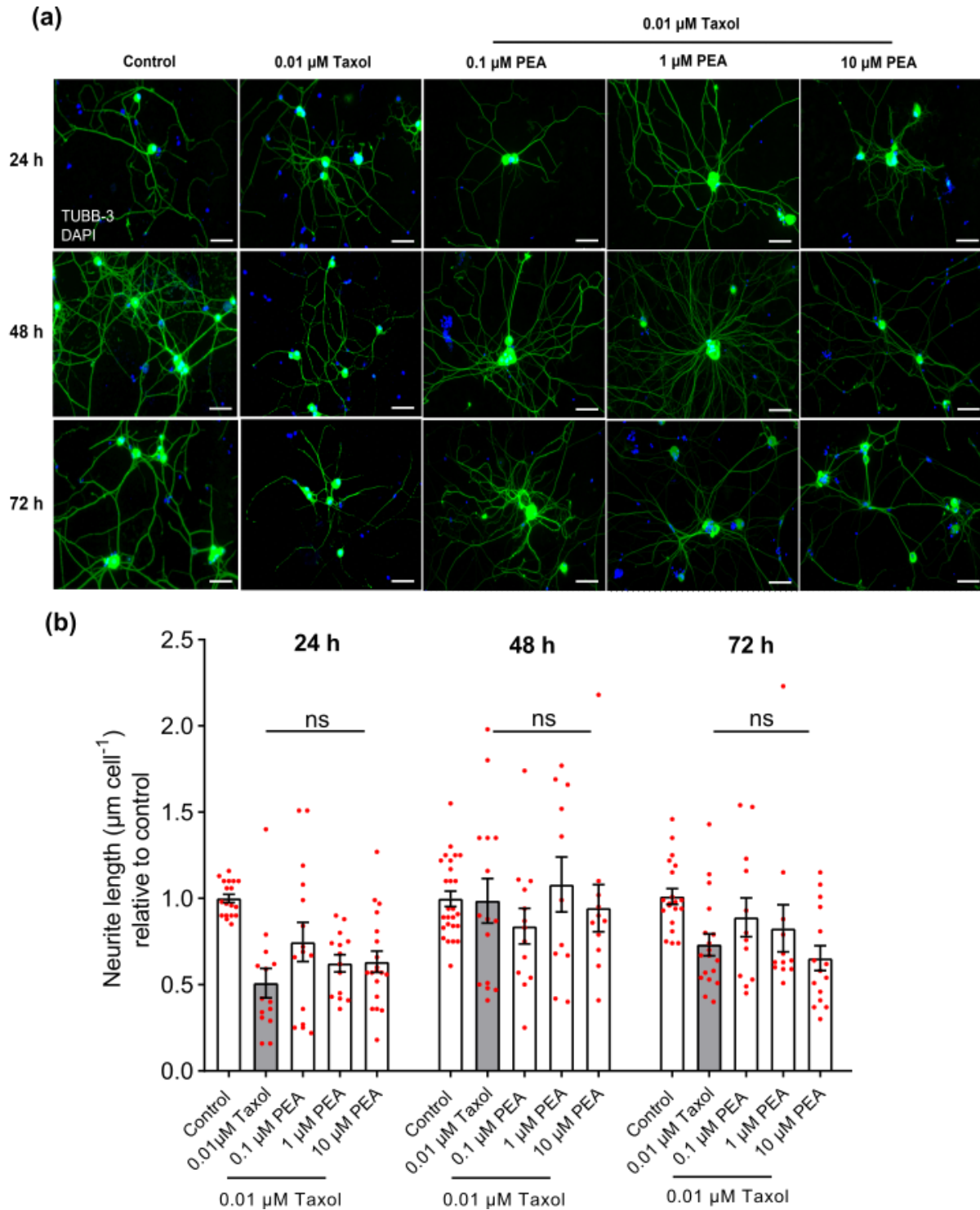


**Figure S4.** Effects of different PEA concentrations (0.1, 1, and 10  $\mu\text{M}$ ) combined with 0.01  $\mu\text{M}$  Paclitaxel on neurite length of DRG neurons at 24, 48, and 72-h post-treatment **a)** representative images of DRG neurons labeled with beta III Tubulin antibody (green) and DAPI for nuclear staining (blue). Scale bars = 75 $\mu\text{m}$ . **b)** No significant effects on neurite lengths were observed in DRG neurons treated with different concentrations of PEA at 24, 48, and 72h post-treatment compared to cells treated with only 0.01 $\mu\text{M}$  Paclitaxel ( $P > 0.05$ ). Data represented (mean  $\pm$  SEM) of N=3 independent experiments, n=10-15 replica.



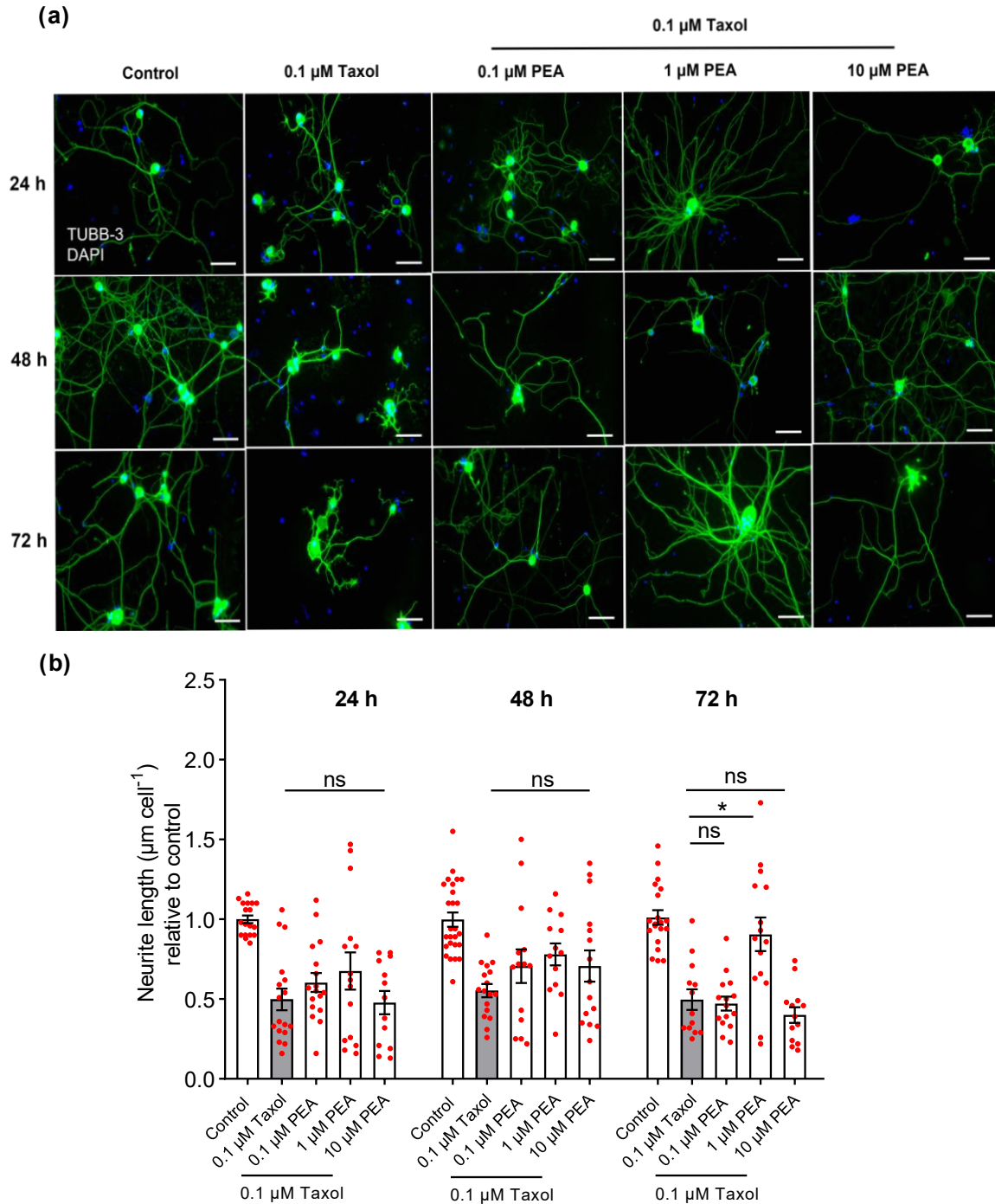


**Figure S5.** Effects of different PEA concentrations (0.1, 1, and 10  $\mu\text{M}$ ) combined with 0.1  $\mu\text{M}$  Paclitaxel at 24, 48, and 72-h post-treatment **a)** representative images showed sensory neurons labeled with beta III Tubulin antibody (green) and DAPI for nuclear staining (blue). Scale bars = 75 $\mu\text{m}$ . **b)** Bar graphs showed no significant effects on neurite lengths of DRGs neurons treated with different concentrations of PEA at 24, and 48-h of treatment compared to cells treated with only 0.01 $\mu\text{M}$  Paclitaxel ( $P > 0.05$ ). 1  $\mu\text{M}$  of PEA plus 0.1  $\mu\text{M}$  Paclitaxel showed an apparent increase in neurite length of neurons against 0.1  $\mu\text{M}$  Paclitaxel at only 72 h post-treatment ( $*P < 0.05$ ). Data represented as (mean  $\pm$  SEM), and the experiments were performed at least 3 independent times and 10-15 replicas. The asterisk denotes significant results regarding the respective measurement indicated with the bar graphs.

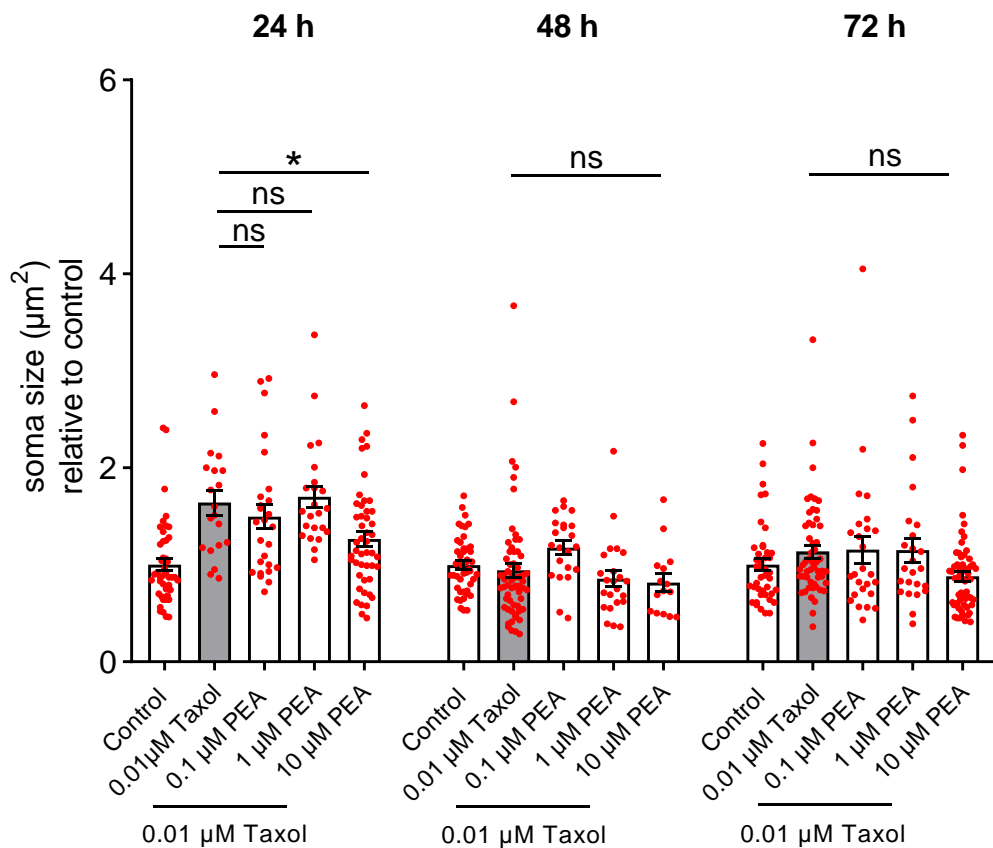


**Figure S6.** The effects of different PEA concentrations (0.1, 1, and 10  $\mu\text{M}$ ) co-applied with 0.01  $\mu\text{M}$  Paclitaxel on soma sizes of DRG neurons at 24, 48, and 72-h post-treatment. At 24h, only 10  $\mu\text{M}$  PEA showed a significant decrease in soma size against 0.01  $\mu\text{M}$  Paclitaxel alone ( $*P < 0.05$ ), while there were no significant effects on soma sizes of DRG neurons treated with different concentrations of PEA at 48 and 72h post-treatment compared to cells treated with 0.01  $\mu\text{M}$  Paclitaxel ( $P > 0.05$ ). Data represented as (mean  $\pm$  SEM), and the experiments were performed at least 3 independent times and 30-45 replicas. The asterisk denotes significant results regarding the respective measurement indicated with the bar graphs.

## Supplementary Material

### Publication 2:

#### Time- and Concentration-Dependent Adverse Effects of Paclitaxel on Non-Neuronal Cells in Rat Primary Dorsal Root Ganglia

Amira Elfarnawany<sup>1,2</sup> and Faramarz Dehghani<sup>1\*</sup>

<sup>1</sup>Department of Anatomy and Cell Biology, Medical Faculty, Martin Luther University Halle-Wittenberg, Grosse Steinstrasse 52, 06108 Halle (Saale), Germany

([faramarz.dehghani@medizin.uni-halle.de](mailto:faramarz.dehghani@medizin.uni-halle.de))

<sup>2</sup> Zoology Department, Faculty of Science, Tanta University 31527, Tanta, Egypt

([amira.elfarnawany@science.tanta.edu.eg](mailto:amira.elfarnawany@science.tanta.edu.eg))

#### \*Corresponding at:

Faramarz Dehghani ([faramarz.dehghani@medizin.uni-halle.de](mailto:faramarz.dehghani@medizin.uni-halle.de))

Supplementary data associated with this article can be found, in the online version, at:

<https://www.mdpi.com/article/10.3390/toxics11070581/s1>

**Figure S1:** (a) DRG isolation from 6–8 weeks old Wister rats, and (b) extraction and purification of DRG non-neuronal cells by using the density gradient centrifugation method.

**Figure S2:** Representative example of automatic counting of nuclei of non-neuronal cells by the FIJI program for the control group; **Figure S3:** Effects of different concentrations of paclitaxel on the viability of DRG non-neuronal cells at different investigated time points using the MTT assay.

**Figure S4:** Effects of different concentrations of paclitaxel on the percentage of cytotoxicity of DRG non-neuronal cells at different investigated time windows using the LDH assay.

**Figure S5:** Effects of different concentrations of paclitaxel on the rate of cell proliferation of DRG non-neuronal cells at 24 h, 48 h, and 72 h post-treatment using BrdU assay.

**Figure S6:** Effects of different concentrations of paclitaxel on nuclear morphology (% apoptosis) of DRG non-neuronal cells at 24 h, 48 h, and 72 h post-treatment by DAPI staining.

**Figure S7:** Effects of different concentrations of paclitaxel on the ratio of PI+ of DRG non-neuronal cells at 24 h, 48 h, and 72 h post-treatment by propidium iodide assay.

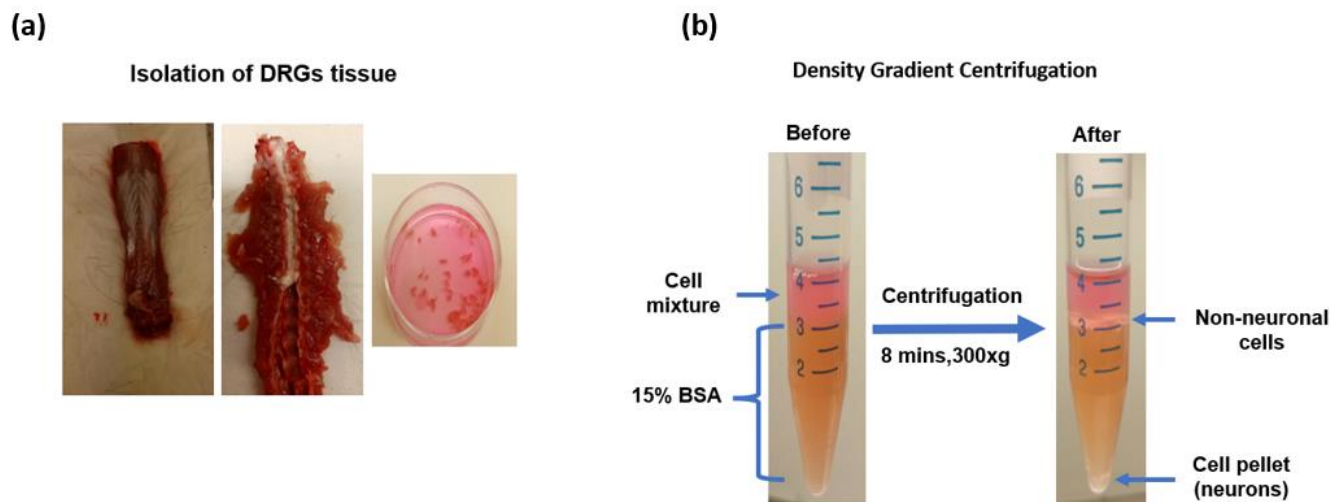
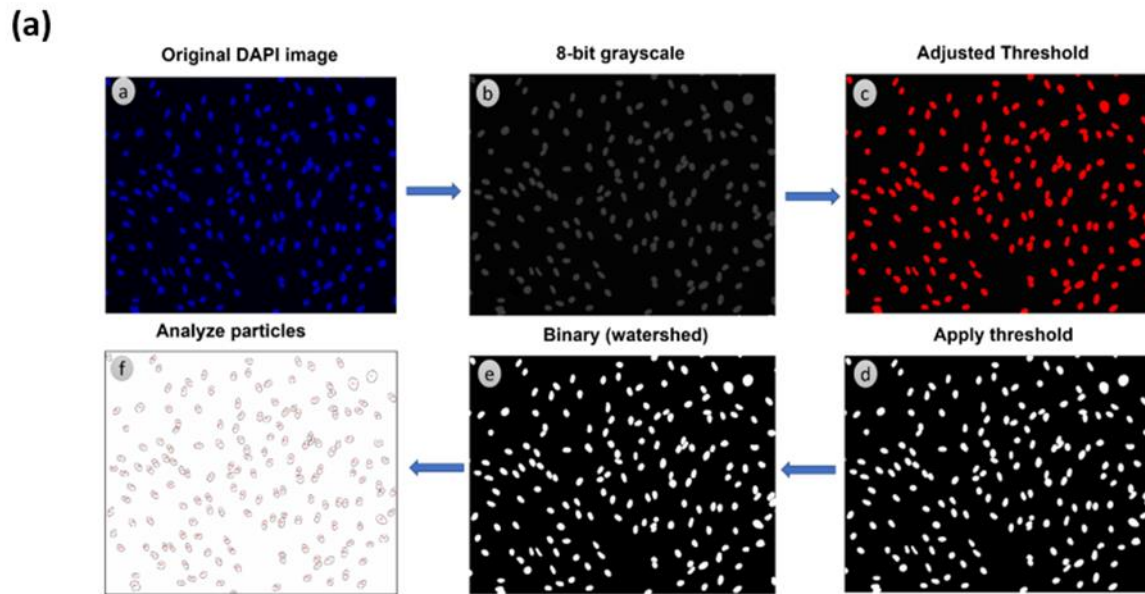


**Figure S1.** (a) DRGs isolation from 6–8 weeks old Wister rats, and (b) extraction and purification of DRG non-neuronal cells by using the density gradient centrifugation method.



(b)

	A	B	C	D	E	F
Slice	Count	Total Area	Average Size	%Area	Mean	
100 nM PEA_rep_ch01.tif	173	13087252281	75648857.12	8.554	255	
100 nM PEA_Series002_ch01.tif	213	15721611087	73810380.69	10.276	255	
100 nM PEA_Series006_ch01.tif	150	10700915261	71339435.07	6.994	255	
100 nM PEA_Series009_ch01.tif	108	7826254297	72465317.57	5.115	255	
100 nM PEA_Series011_ch01.tif	177	14087432142	79590012.1	9.208	255	
100 nM PEA_Series013_ch01.tif	186	15059099381	80962899.9	9.843	255	

**Figure S2.** Representative example for automatic counting of nuclei of non-neuronal cells by FIJI program for the control group. (a) Step-by-step demonstration of automatic counting of nuclei (ImageJ). (b) Results of the different counts of nuclei of non-neuronal cells for six different images for the same control group.

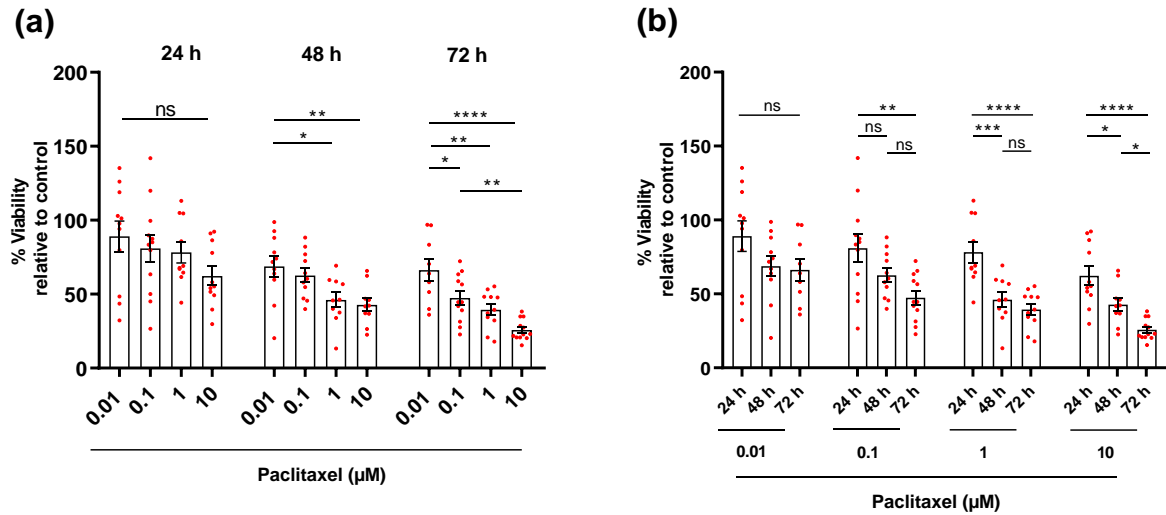


**Figure S3.** Effects of different concentrations of paclitaxel on the viability of DRG non-neuronal cells at different investigated time points using MTT assay. **(a)** A significant difference was found between different paclitaxel concentrations with a concentration dependency at 48 h and 72 h post-treatment. **(b)** Time-dependent significant differences were observed for 1 μM, and 10 μM paclitaxel concentrations. Values served as the mean ± SEM of three independent experiments performed in triplicates. The asterisks denote significant results regarding the respective measurement indicated with the bar. The data were analyzed using one-way ANOVA, followed by the Bonferroni post-hoc test ( $p < 0.05$ ). \*  $p < 0.05$ , \*\*  $p < 0.01$ , \*\*\*  $p < 0.001$ , \*\*\*\*  $p < 0.0001$ , ns (non-significant).

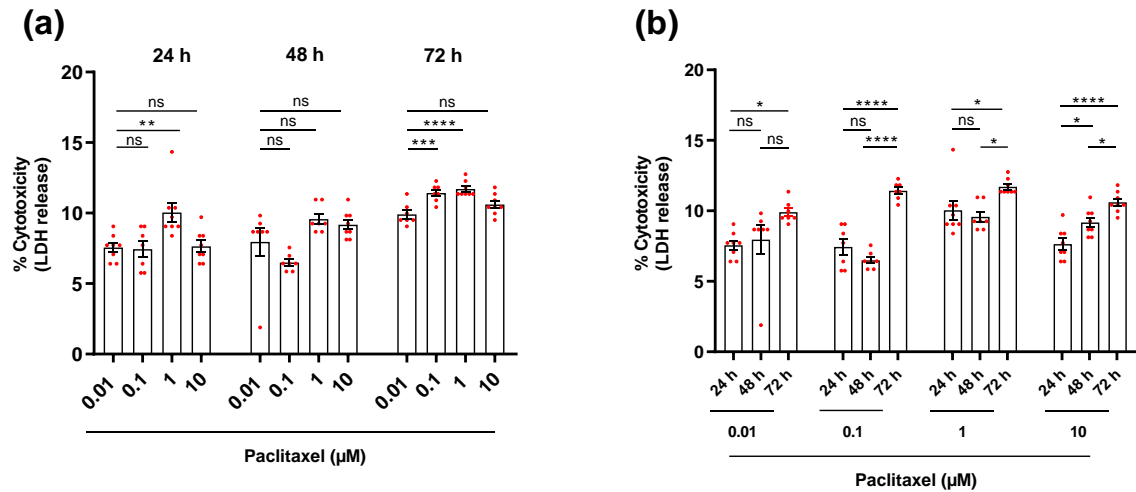


**Figure S4.** Effects of different concentrations of paclitaxel on the percentage of cytotoxicity of DRG non-neuronal cells at different investigated time windows using LDH assay. **(a)** A significant difference was presented between different paclitaxel concentrations, indicating concentration-dependent effects on cell death at 72 h post-treatment. **(b)** for all applied concentrations, time-dependent effects were observed for various concentrations of paclitaxel on the cytotoxicity of DRG non-neuronal cells. Values served as the mean  $\pm$  SEM of three independent experiments and  $n = 15$  replicates. The asterisks denote significant results regarding the respective measurement indicated with the bar. The data were analyzed using one-way ANOVA, followed by the Bonferroni post-hoc test ( $p < 0.05$ ). \*\*  $p < 0.01$ , \*\*\*  $p < 0.001$ , \*\*\*\*  $p < 0.0001$ , ns (non-significant).

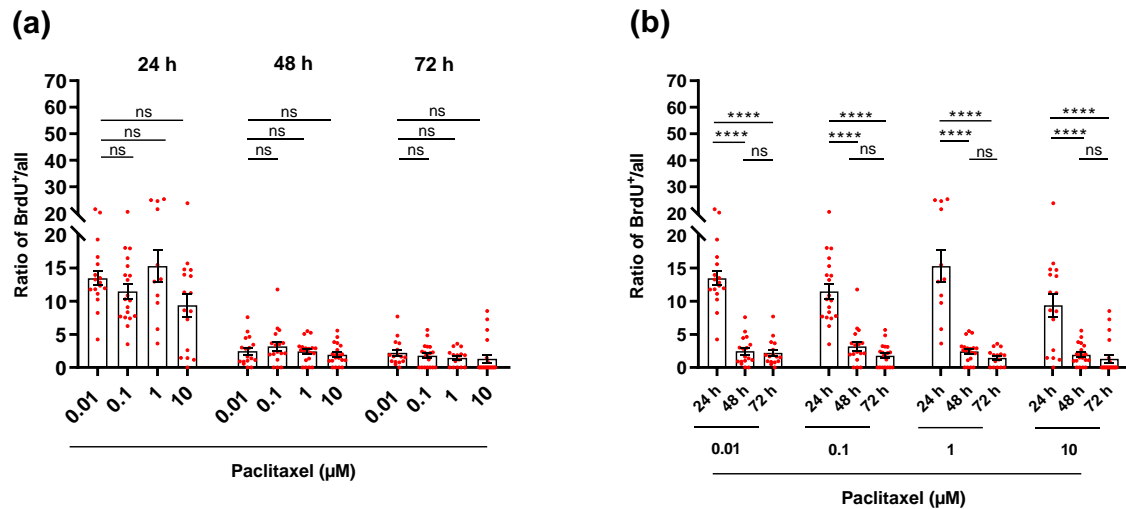


**Figure S5.** Effects of different concentrations of paclitaxel on the rate of cell proliferation of DRG non-neuronal cells at 24 h, 48 h, and 72 h post-treatment using BrdU assay. **(a)** The bar charts revealed no significant difference between different paclitaxel concentrations, implying that the effects of paclitaxel on cell proliferation are not concentration-dependent at different time points. **(b)** The graph revealed a significant difference between different timelines for all applied concentrations of paclitaxel, indicating that the effects of various concentrations of paclitaxel on the cell proliferation of DRG non-neuronal cells are time-dependent. Values served as the mean  $\pm$  SEM of three independent experiments and  $n=15$  replicates. The asterisk denotes statistically significant results for the measurement indicated by the bar. The data were analyzed using one-way ANOVA, followed by the Bonferroni post-hoc test ( $p < 0.05$ ). \*\*\*\*  $p < 0.0001$ , ns (non-significant).



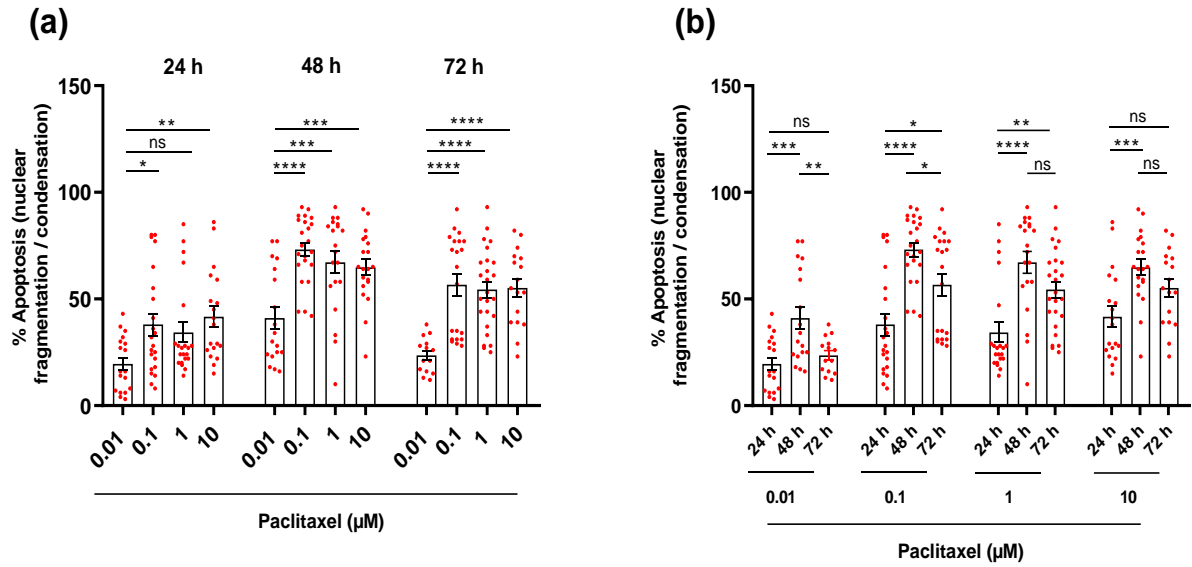


**Figure S6.** Effects of different concentrations of paclitaxel on nuclear morphology (% apoptosis) of DRG non-neuronal cells at 24 h, 48 h, and 72 h post-treatment by DAPI staining. **(a)** The chart demonstrated a significant difference between different paclitaxel concentrations, implying that the effects of paclitaxel on % of apoptosis are concentration-dependent at different investigated time points. **(b)** The graph showed a significant difference between different timelines specifically between 24 h and 48 h of treatment for all concentrations of paclitaxel, indicating that the effects of various concentrations of paclitaxel on the % of apoptosis of DRG non-neuronal cells are time-dependent. Values served as the mean  $\pm$  SEM of three independent experiments and  $n = 15$  replicates. The asterisk denotes statistically significant results for the measurement indicated by the bar. The data were analyzed using one-way ANOVA, followed by the Bonferroni post-hoc test ( $p < 0.05$ ). \*  $p < 0.05$ , \*\*  $p < 0.01$ , \*\*\*  $p < 0.001$ , \*\*\*\*  $p < 0.0001$ , ns (non-significant).

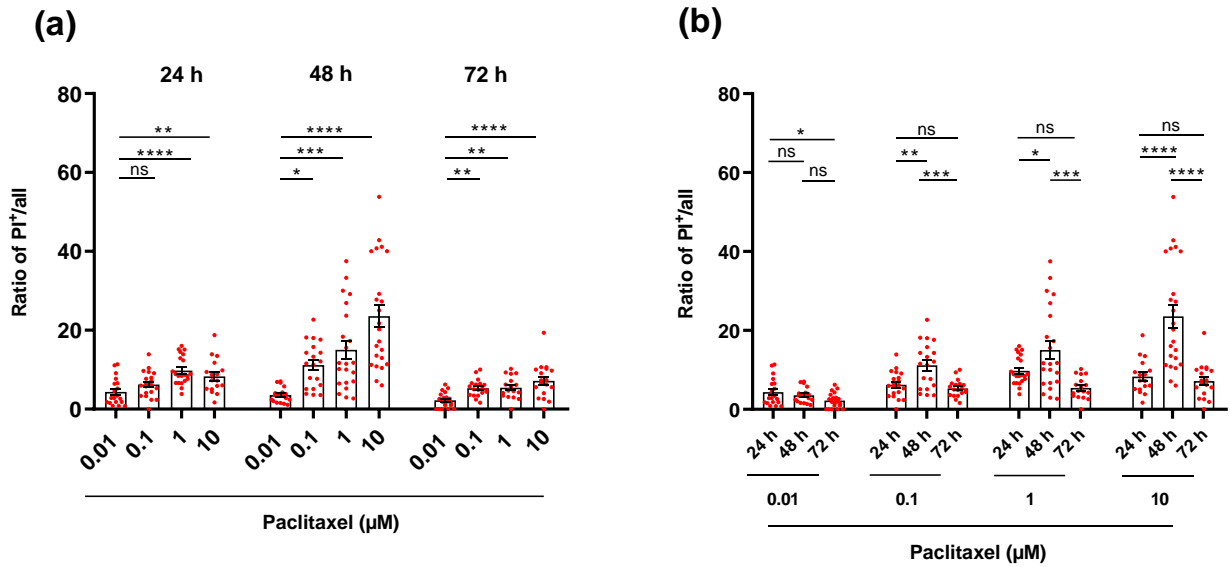


**Figure S7.** Effects of different concentrations of paclitaxel on the ratio of PI<sup>+</sup> of DRG non-neuronal cells at 24 h, 48 h, and 72 h post-treatment by propidium iodide assay. **(a)** The Bar chart showed a significant difference between different paclitaxel concentrations, implying that the effects of paclitaxel on cell death are concentration-dependent at different investigated time points. **(b)** The graph showed a significant difference between different timelines for all concentrations of paclitaxel except only 0.01 μM paclitaxel, indicating that the effects of various concentrations of paclitaxel on the % of cell death of DRG non-neuronal cells are time-dependent. Values served as the mean ± SEM of three independent experiments and n= 15 replicates. The asterisk denotes statistically significant results for the measurement indicated by the bar. The data were analyzed using one-way ANOVA, followed by the Bonferroni post-hoc test ( $p < 0.05$ ). \*  $p < 0.05$ , \*\*  $p < 0.01$ , \*\*\*  $p < 0.001$ , \*\*\*\*  $p < 0.0001$ , ns (non-significant).

## Supplementary Videos

**Video S1:** A phase contrast live imaging microscope was used to show normal cell division of DRG non-neuronal cells in the control group for up to 72 hours when a single cell divided into two daughter cells.

**Video S2:** Effects of 0.1  $\mu\text{M}$  PEA on cell proliferation of DRG non-neuronal cells using a phase contrast live imaging microscope showed that cells normally divided such as the control group.

**Video S3:** Effects of 10  $\mu\text{M}$  paclitaxel on the cell division of DRG non-neuronal cells for up to 72 h using a phase contrast live imaging microscope.

**Video S4:** Effects of 0.1  $\mu\text{M}$  PEA on the toxic effect of 10  $\mu\text{M}$  paclitaxel on DRG non-neuronal cells for up to 72 h using a phase contrast live imaging microscope.

These videos can be accessed via this link:

[https://sciencetantaedu-my.sharepoint.com/:f:/g/personal/amira\\_elfarnawany\\_science\\_tanta\\_edu\\_eg/Erd-KLmYcOZMi0t0DJbM\\_sYB82FqfFgHpKSOy0Zq\\_jssXA?e=MPJHO4](https://sciencetantaedu-my.sharepoint.com/:f:/g/personal/amira_elfarnawany_science_tanta_edu_eg/Erd-KLmYcOZMi0t0DJbM_sYB82FqfFgHpKSOy0Zq_jssXA?e=MPJHO4)

## Copyright Permission

---

**Figures 1, 2, and 4** were used with permission from Open Access - Creative Commons **CC BY 4.0** (<http://creativecommons.org/licenses/by/4.0/>), and **Figure 3** was used with permission from **CC BY-NC-SA** <https://creativecommons.org/licenses/by-nc-sa/4.0/>.

**Figure 1.** Sketch-map of the mechanism of chemotherapy-induced peripheral neuropathy (CIPN).

Yang, Y., Zhao, B., Gao, X., Sun, J., Ye, J., Li, J., & Cao, P. (2021). Targeting strategies for oxaliplatin-induced peripheral neuropathy: clinical syndrome, molecular basis, and drug development. *Journal of Experimental & Clinical Cancer Research*, 40(1), 1-25. DOI: [10.1186/s13046-021-02141-z](https://doi.org/10.1186/s13046-021-02141-z)

**Figure 2.** Mechanism of action of paclitaxel.

Abu Samaan, T. M., Samec, M., Liskova, A., Kubatka, P., & Büsselberg, D. (2019). Paclitaxel's mechanistic and clinical effects on breast cancer. *Biomolecules*, 9(12), 789. *Biomolecules* 2019, 9, 789. <https://doi.org/10.3390/biom9120789>

**Figure 3.** Schematic diagram of DRG structure and cell types of composition

Martin, S. L., Reid, A. J., Verkhatsky, A., Magnaghi, V., & Faroni, A. (2019). Gene expression changes in dorsal root ganglia following peripheral nerve injury: roles in inflammation, cell death and nociception. *Neural regeneration research*, 14(6), 939. <https://doi.org/10.4103/1673-5374.250566>

**Figure 4.** Metabolic pathways and mechanisms of action of PEA.

Petrosino, S., & Schiano Moriello, A. (2020). Palmitoylethanolamide: A Nutritional Approach to Keep Neuroinflammation within Physiological Boundaries—A Systematic Review. *International Journal of Molecular Sciences*, 21(24), 9526. DOI: [10.3390/ijms21249526](https://doi.org/10.3390/ijms21249526)

**CC BY:** This license allows reusers to distribute, remix, adapt, and build upon the material in any medium or format, so long as attribution is given to the creator. The license allows for commercial use. The licensor cannot revoke these freedoms as long as you follow the license terms.

**CC BY-NC-SA:** This license allows reusers to distribute, remix, adapt, and build upon the material in any medium or format for noncommercial purposes only, and only so long as attribution is given to the creator. If you remix, adapt, or build upon the material, you must license the modified material under identical terms.